

**Association of a high fat diet, gut microbiota and host
interactions with enteric neuropathy and dysmotility in a mouse
model of type two diabetes**

A Dissertation

Presented in Partial Fulfillment of the Requirements for the

Degree of Doctor of Philosophy

with a

Major in Neuroscience

in the

College of Graduate Studies

University of Idaho

by

Yvonne Elikplim Akua Nyavor

Major Professor: Onesmo Balemba, Ph.D.

Committee Members: Larry Forney, Ph.D.; Lee Fortunato, Ph.D.; Steve Simasko, Ph.D.

Department Administrator: James Nagler, Ph.D.

August 2019

Authorization to Submit Dissertation

This dissertation of Yvonne E.A Nyavor, submitted for the degree of Doctor of Philosophy with a Major in Neuroscience and titled “Association of a high fat diet, gut microbiota and host interactions with enteric neuropathy and dysmotility in a mouse model of type two diabetes ” has been reviewed in final form. Permission, as indicated by the signatures and dates below, is now granted to submit final copies to the College of Graduate Studies for approval.

Major Professor: _____ Date: _____
 Onesmo Balemba, Ph.D.

Committee Members: _____ Date: _____
 Larry Forney, Ph.D.

_____ Date: _____
 Lee Fortunato, Ph.D.

_____ Date: _____
 Steve Simasko, Ph.D.

Department Administrator: _____ Date: _____
 Douglas Cole, Ph.D.

Abstract

Type 2 diabetes is associated with gut microbiota alterations and debilitating gastrointestinal illnesses caused by neuropathy of the enteric nervous system and smooth muscle dysfunction. However, the specific triggers of enteric neuropathy and muscle dysfunction, and the role of gut microbiota alterations are not fully understood. We studied the specific roles played by gut microbiota alterations in the development of enteric neuropathy using germ free and conventionally raised high fat mouse models. We then studied gut microbiota, myenteric inhibitory neurons and intestinal dysmotility in these mice using next generation sequencing, tissue culture, immunohistochemistry, transmission electron microscopy, *ex vivo* gastrointestinal motility assays and intracellular microelectrode recording in smooth muscle cells. Conventionally raised male mice became obese, and had impaired glucose tolerance and insulin resistance after 4 weeks of high fat diet (HFD) ingestion.

Conventionally raised female mice were however resistant to the weight gain, impaired glucose tolerance, and insulin resistance induced by HFD ingestion even after 8 weeks. Despite these differences, after 8 weeks, conventionally raised male and female mice fed a HFD had slower intestinal propulsive motility. These mice had microbiota alterations marked by increased gram-positive Firmicutes and lower Gram-negative Bacteroidetes. In addition, they had fewer numbers of neurons per ganglion, lower numbers of myenteric inhibitory neurons, and axonal damage including swelling and loss of cytoskeletal filaments. HFD ingestion also impaired inhibitory neuromuscular transmission in both genders.

To determine the role of HFD-microbiota-host interactions in HFD-induced enteric neuropathy and dysmotility, filtrates of luminal contents from the ileum and cecum (hereafter, ileocecal supernatants) of both conventionally raised male and female HFD fed mice were superfused into the lumen of isolated intestinal segments or applied on cultured duodenal or distal colon muscularis preparations. Ileocecal supernatants inhibited intestinal propulsive motility and muscularis contractions. We then used solid phase extraction to separate ileocecal supernatants into water-soluble and methanol (20%, 50% and 100%) soluble fractions and tested them in motility assays. Like the ileocecal supernatants, the water fraction from HFD mice inhibited intestinal propulsive motility and blocked muscularis contractions. HFD Supernatants and water fractions also caused loss of myenteric nitrergic neurons and inflammation. They damaged smooth muscle and impaired neuromuscular transmission in cultured muscularis preparations. Supernatants and water fractions blocked the discharge of spontaneous slow waves and action potentials, the electrical activities underlying contractions of smooth muscle cells. These effects matched the effect of HFD ingestion on the excitability of smooth muscle cells in distal colon.

To determine the role of an intact gut microbiota in the development of enteric neuropathy, we used a germ free HFD mouse model. We found that compared to conventionally raised mice, HFD ingestion did not reduce the number of myenteric inhibitory neurons in the duodenum of germ free mice. HFD also induced alterations in the cecum of conventionally raised mice, which led to increased gram-positive bacteria. Subsequent studies revealed that lipoteichoic acid from gram-positive bacteria induced a loss of myenteric nitroergic neurons associated with oxidative stress and inflammation. Taken together, these studies provide new evidence to support the hypothesis that diet-microbiota-host interactions play a crucial role in the development of enteric neuropathy and dysmotility in a high fat diet mouse model of type 2 diabetes.

Acknowledgements

"It takes a village to raise a child." –African Proverb

I am first and foremost grateful to God for making it possible for me to pursue and complete my doctoral education. I arrived at the UI as a 'child' in scientific matters, and have been raised to this point by the relentless encouragement and support of my major professor, Dr. Balemba. His advice, scientific knowledge, wisdom and hard work have been things I knew I could count on. During the hardest times, such as when we had a complete loss of lab data, his calmness and optimism helped me to keep going when I would otherwise have given up. None of the work in this dissertation would be possible without him. I am deeply indebted to him, and to his wife and son, Dorah and Jeremiah, for opening their home to my husband and I. I also want to thank my committee members: Dr. Larry Forney, Dr Lee Fortunato and Dr. Steve Simasko. Their support and belief in me were invaluable in times when I doubted both my ability and intelligence and encouraged me to complete this PhD. Their critique of my experiments and suggestions improved the quality of my work, and enabled me to pursue directions I would otherwise not have considered. I would also like to thank Dr. James Nagler and Dr. Doug Cole for the departmental fellowship and financial support that made my education possible. I was also financially supported by the Howard Hughes Medical Institute through a grant received by Drs. Trish Hartzell and Martina Ederer, and also by President Chuck Staben of the University of Idaho, Dr. Jerry McMurtry of the College of Graduate Studies, the College of Science, INBRE, PEO, and the National Society of Black Engineers (NSBE). I next want to thank the professors in the department of Biological Sciences who permitted me to use their lab resources and personnel: Dr. Forney, Dr. Fortunato, Dr. Tanya Miura, Dr. Holly Wichman, Dr. Peter Fuerst and Dr. Deb Stenkamp. I also want to thank Dr. Ben Ridenhour, Dr. Celeste Brown, Dr. Lena Mendes-Soares, LuAnn Scott, Maria Schneider, Sanqing Yuan, Kenetta Nunn and Dan New for assistance in learning new methods related to next generation sequencing and data analysis. I next want to thank LARF Staff for caring for mice, Audrey Harris, Ann Norton, Gina Tingley, Kristi Accola, Jean Norris, and Dr. David Pfeiffer, for their support and help in times of need. I also want to thank my collaborators: Dr. Timo Stark, Dr. Heino Heyman, Dr. Yogesh Bhattarai, Dr. Purna Kashyap, Dr. David Linden, Dr. Martin Gericke, and Dr. Thomas Metz. I next want to thank all the undergraduates I have worked with: especially Catherine, Kortni, Jessica, Sydney, George, Rachel, Kiefer, Abigail, Allysha and Lance for also becoming friends. I thank my college professors, especially: Dr. John Larbi, Dr. Terlabi, Dr. Tay, Dr. Belford, Mr. Ofori, and Dr. Karen Duca who first helped me to come to study in the United States, Dr. Joan Mecsas, Dr. Tena Rolan and Dr. Honorine Ward of Tufts University and my Boston Family: Emmanuel, Philip, Charles, ICGC and LCI for housing me while I was there.

Dedication

I dedicate this dissertation to my husband Joel, whose unwavering love and support I am privileged to have and to our families: my mom Vida Agyabga who believed that a woman could be whoever and accomplish whatever she wanted, my sisters Jemima, Alberta, Faakor, and Irene, my brothers Prince and Desire, my nephews and nieces and my in-laws: Professor and mummy Oduro-Afriyie, Alice, Kate, Nana, Angie, Adjoa, Emmanuel, Makafui, Daddy Mike, and Dr. Ken Barnes. Finally, I want to thank the many friends and church family that have supported me throughout my education: Amma, Roberta, Collins, Tenzin, Farjahan, Brian, Labib, Sadeed, Irene, Freda, Ezekiel and family, Cheryl and Bob Mitchell, the Andersons, Pastors Phil and Kari of LFF Pullman, LFF worship team, Mia, Danna, Jesse, CJ and Jenny, and the numerous families that took care of me when I was recovering from surgery. My final thank you goes to my friends that have become family in the US: Bridget (Awo) and Dr. Isaiah Gyan and their boys PK and NK, without whom I would be just another grad school drop out. Thank you for always leaving me room in your home, no questions asked.

I also dedicate this dissertation to those who left before seeing me finish: my aunt and second mom Comfort, my grandmother Mercy, and my dad CB who first cultivated the love for Biology in me.

To Rebecca. I still don't understand, but this is for you. I hope you've found peace now, my dear.

I will always miss you.

Table of Contents

Authorization to Submit Dissertation	ii
Abstract.....	iii
Acknowledgements	v
Dedication.....	vi
Table of Contents	vii
List of Tables	ix
List of Figures.....	x
Statement of Contribution	xii
Chapter 1: Introduction and Literature Review	1
Literature Cited.....	5
Chapter 2: Intestinal nerve cell injury occurs prior to insulin resistance in female mice ingesting a high fat diet.....	12
Abstract.....	12
Introduction	12
Methods and Materials	14
Results	19
Discussion.....	29
Literature Cited.....	32
Chapter 3: Intestinal luminal contents from mice fed high fat diet impair intestinal motility by injuring enteric neurons and smooth muscle cells.....	37
Abstract.....	37
Introduction	37
Methods and Materials	39
Results	43
Discussion.....	59
Literature Cited.....	64

Chapter 4: High fat diet-induced alterations to gut microbiota and gut-derived lipoteichoic acid contributes to the development of enteric neuropathy	69
Abstract.....	69
Introduction	69
Methods and Materials	71
Results	73
Discussion.....	86
Literature Cited.....	89
Chapter 5: Conclusion	94
Appendix A- Supplementary Table 2-1	96
Appendix B- Supplementary Table 2-2.....	97
Appendix C- Supplementary Table 2-3.....	99
Appendix D- Supplementary Table 2-4	101
Appendix E- Supplementary Table 2-5	103
Appendix F- Supplementary Table 2-6	105
Appendix G- Supplementary Table 2-7	106
Appendix H- Copyright Release for Chapter 2	108
Appendix I- IACUC Approvals to conduct animal experiments	111

List of Tables

Table 2-1 Bacterial genera that show significant correlations with intestinal motility, neuropathy or both in duodenum and colon.	28
--	----

List of Figures

Figure 2-1 HFD has a greater metabolic effect on male mice than on female mice.	22
Figure 2-2 HFD results in intestinal dysmotility and disrupts inhibitory intestinal neuromuscular transmission in both male and female mice.	23
Figure 2-3 HFD reduces intestinal nitrergic myenteric neurons in both male and female mice.	24
Figure 2-4 HFD reduces myenteric VIP immunoreactive varicosities in the myenteric plexus in both male and female mice intestines.	25
Figure 2-5 HFD reduces the total number of myenteric neurons, and causes axonal swelling and loss of cytoskeletal filaments in the myenteric plexus in both male and female mice.	26
Figure 2-6 HFD is the primary determinant of gut bacterial community composition. Hierarchical clustering revealed samples grouped together by diet and not by sex (a).	27
Figure 3-1 HFD-ICS induces dysmotility in both duodenum and colon <i>ex vivo</i>	48
Figure 3-2 HFD-ICS reduces contractions of small and large intestine muscularis preparations and damages smooth muscle cells (SMCs).	49
Figure 3-3 HFD-ICS reduces the percentage of nNOS neurons in the myenteric plexus in duodenum.	50
Figure 3-4 HFD-ICS impairs intestinal inhibitory neuromuscular transmission to circular smooth muscle in distal colon.	51
Figure 3-5 HFD ICS inhibits the excitability of smooth muscle cells.	52
Figure 3-6 Aqueous SPE fractions of HFD-ICS (HFD-SPE1) block muscularis contractions by damaging smooth muscle cells and nNOS neurons, and inhibiting the excitability of SMCs.	54
Figure 3-7 HFD-ICS does not induce oxidative stress in myenteric neurons.	56
Figure 3-8 HFD-ICS treatment induces the production of TNF α but does not cause nitrosative stress.	58
Figure 4-1. The gut microbiota is required for HFD-induced injury to nitrergic myenteric neurons. .	77
Figure 4-2 The microbiota is necessary for HFD-induced injury to myenteric VIP neurons in mouse duodenum.	78
Figure 4-3 HFD ingestion caused microbial alterations in the cecum, which was marked by increased gram-positive bacteria.	80
Figure 4-4 Bacterially derived cellular components, LTA and LPS damage nitrergic myenteric neurons without affecting intestinal muscle contractions in culture.	81
Figure 4-5 Bacterially derived SCFAs do not affect contractions or injure nNOS neurons in cultured duodenojejunal muscularis.	82
Figure 4-6 LTA induces oxidative stress in myenteric neurons.	84

Figure 4-7 LTA treatment caused nitrosative stress and induced the production of TNF α 85

Statement of Contribution

I hereby declare that all the research in this dissertation is my own and that I am the first author on all data chapters 2-4 of this dissertation. The specific contributions of other authors are elaborated upon below:

Complete list of authors for Chapter 2: Yvonne Nyavor (YN), Rachel Estill (RE), Hannah Edwards (HE), Hailey Ogden (HO), Kaila Heideman (KH), Kiefer Starks (KS), Christopher Miller (CM), George May (GM), Lance Flesch (LF), John McMillan (JM), Martin Gericke (GM), Larry J. Forney (LJF), Onesmo B. Balemba (OBB).

Author Contributions for Chapter 2: Conception and design: **YN**, LF and OBB. Development of methodology: **YN**, MG and OBB. Acquisition of data: **YN**, RE, KS, CM, HE, KH, HO, JM, GM, MG and OBB. Analysis and interpretation of data: **YN**, MG and OBB. Writing, review and/or revision of the manuscript: **YN**, LF, MG and OBB. Study supervision: OBB.

Complete list of authors for Chapter 3: Yvonne Nyavor (YN), Catherine R. Brands (CB), Sydney Kuther (SK), Jessica Nicholson (JN), Kortni K. Cox (KKC), George May (GM), Christopher Miller (CM), Allysha Yasuda (AY), Joshua Cady (JC), Heino Heyman (HH), Thomas O. Metz (TOM), Timo D. Stark (TDS), Thomas Hofmann (TH), Onesmo B. Balemba (OBB).

Author Contributions for Chapter 3: Conception and design: **YN** and OB. Development of methodology: **YN**, HH, TOM, TDS and OBB. Acquisition of data: **YN**, CB, SK, JN, KKC, GM, CM, AY, JC, HH, TOM, TDS and OBB. Analysis and interpretation of data: **YN** and OBB. Writing, review and/or revision of the manuscript: **YN**, TDS, TM, HH and OBB. Study supervision: TDS, TOM, TH and OBB.

Complete list of authors for Chapter 4: Yvonne Nyavor (YN), Catherine R. Brands (CB), George May (GM), Sydney Kuther (SK), Jessica Nicholson (JN), Kathryn Tiger (KT), Allysha Yasuda (AY), Kiefer Starks (KS), Diana Litvinenko (DL), Abigail Teslonidek (AT), Yogesh Bhattarai (YB), Purna C. Kashyap (PCK), David R. Linden (DRL), Larry J. Forney (LJF), Onesmo B Balemba (OBB).

Author Contributions for Chapter 4: Conception and design: **YN**, LJF and OBB. Development of methodology: **YN**, YB, PK, DRL, and OBB. Acquisition of data: **YN**, CRB, GM, CM, SK, JN, KT, AY, KS, DL, AT, YB, PK and OBB. Analysis and interpretation of data: **YN** and OBB. Writing, review and/or revision of the manuscript: **YN**, YB, LJF and OBB. Study supervision: OBB, YB, PK

Chapter 1: Introduction and Literature Review

Type 2 Diabetes (T2D) is a global health problem affecting over 382 million people¹. In the USA, T2D affects over 30 million people, and accounts for \$245 billion in costs related to its diagnosis, treatment and management of associated disease complications². One of the most debilitating complications of diabetes is damage and dysfunction (neuropathy) of the peripheral and autonomic nervous systems, which affects over 60% of diabetic patients³⁻⁵. Autonomic neuropathy of the enteric nervous system (ENS) and smooth muscle dysfunction^{6,7} cause gastrointestinal (GI) illnesses in diabetic patients⁸⁻¹⁰. Such GI illnesses include dysphagia, gastro-esophageal reflux disease, gastroparesis (nausea, vomiting, bloating, pain), and enteropathy (constipation and diarrhea, incontinence and bowel pain)⁸⁻¹². These illnesses reduce the quality of life of up to 75% of T2D patients and pose a significant socioeconomic burden^{8,10}. In addition, dysmotility ensuing from dysfunction of the ENS and GI smooth muscle may increase the rate of progression and severity of diabetic symptoms, since nutrient breakdown and absorption by the body is partially regulated by the ENS and influenced by GI movements¹³. It is therefore important to understand the specific causes of ENS neuropathy and GI dysfunction in type 2 Diabetes.

The ENS is the third division of the autonomic nervous system, which controls gut functions: motility, secretion, absorption and immunity¹⁴⁻¹⁶. It innervates the entire GI tract and is composed of millions of motor, sensory and inter-neurons^{17,18}. The ENS consists of interconnected networks or plexuses of intrinsic neurons, glial cells and extrinsic parasympathetic, sympathetic and sensory nerve fibers¹⁸. Neurons and supporting glial cells are grouped into clusters called enteric ganglia, connected by nerve fiber bundles¹⁸. There are two ganglionated plexuses—the submucosal plexus and myenteric plexus¹⁹. The submucosal plexus neurons, found between the muscularis mucosae and the circular muscle, mainly regulate GI mucosal function (absorption and secretion), mucosal-submucosal blood flow and immune system functions¹⁹. The myenteric plexus neurons, which are located between the circular muscle and the longitudinal muscle layers, regulate the contraction and relaxation of muscle^{16,19}.

Diabetic GI illnesses are indicative of GI dysmotility, which is associated with damage to the myenteric plexus and other cells in the muscularis propria including smooth muscle cells, interstitial cells of Cajal and resident macrophages^{7,10}. Diabetic injuries of the myenteric plexus include altered neurochemical expression, swelling and loss of neuronal cell bodies as well as axonal swelling and loss of cytoskeletal filaments^{20,21}. Diabetic damage mainly leads to loss of nitrergic inhibitory myenteric neurons, which co-express neuronal nitric oxide synthase (nNOS) and vasoactive intestinal peptide (VIP)^{10,20,22,23}. Diabetic ENS injuries are commonly thought to be caused by hyperglycemia

or inflammation-induced oxidative-nitrosative stress, microRNAs, fatty acids such as palmitate, dyslipidemia, growth factor deficiencies, advanced glycation end products and sorbitol accumulation in neurons^{4,10,22,24–27}. Diabetic GI motility disorders and ENS neuropathy have therefore long been considered complications of diabetes, initially triggered by high levels of circulating systemic factors like glucose, fatty acids and vascular damage, and inflammation^{10,28}. However, recent studies have demonstrated that GI dysmotility and associated ENS neuropathy develop before hyperglycemia and insulin resistance^{29–31}, suggesting that there are other initial triggers. Saturated fatty acids (palmitate in particular) and bacterially derived lipopolysaccharide (LPS) are thought to act synergistically in triggering GI dysmotility and ENS neuropathy in diabetic patients^{25,29,32,33}. This suggests that interactions between the diet, gut bacteria and the host could produce molecules in the gut that have a crucial role in the pathophysiology of GI diabetic motility disorders and neuropathy^{29,30}.

The gut bacteria are major components of the gut microbiota, which is a complex community composed of trillions of bacteria, fungi, archaea and viruses^{34,35}. Several phyla of bacteria are represented in the gut, but the two most abundant phyla are Firmicutes, composed mostly of gram-positive bacteria and Bacteroidetes, composed of gram-negative bacteria³⁶. In most cases the gut microbiota is a symbiont, providing several advantages to the host while receiving food and shelter³⁷. This community of microorganisms aids in host immunity, the development of intestinal microvilli, fermentation of otherwise undigested molecules (starch, oligosaccharides, inulin and protein), defense against pathogens, production of essential vitamins, and increase vascularization and blood flow within the mucosa, facilitating nutrient absorption^{37–41}. Furthermore, the microbiota modulates ENS development and function^{42–45} and helps maintain normal GI motility pattern^{44,46–49}.

Diet is an important determinant of gut microbiota composition, and HFD ingestion is thought to be involved in the pathophysiology of obesity and T2D by causing alterations of the gut microbiota^{46,50–53}. Studies in humans have found an increase in the ratio of gram positive Firmicutes to gram negative Bacteroidetes in T2D patients^{53–55}. Similarly, studies in HFD mice mouse models of T2D have shown increases in Firmicutes and a reduction of Bacteroidetes^{56–58}. Gram-positive bacteria are distinguished from gram-negative bacteria by the absence of an outer cell membrane⁵⁹, and an inner cell membrane which is composed of lipoteichoic acid (LTA) and peptidoglycan instead of LPS⁵⁹. T2D dysbiosis correlates with the increased presence of gram-positive gut bacteria in the blood of T2D patients⁶⁰. Likely, this is associated with an increase of the intestinal and circulating levels of LTA. However, the majority of previous studies linking gut microbiota alterations to enteric neuropathy have focused on LPS^{29,61}. It is not known whether alterations of the gut microbiota and LTA play a role in the development of the enteric neuropathy associated with T2D.

Gut microbiota alterations also impairs the production of short chain fatty acids (SCFAs), which are produced as end products of bacterial fermentation^{62,63}. The three most abundant SCFAs in the gut are acetate, propionate and butyrate^{64,65}. Bacteria belonging to the Bacteroidetes phylum predominantly produce acetate and propionate, whereas butyrate is primarily produced by the Firmicutes phylum⁶⁶. In previous studies, treatment with higher concentrations of propionate and butyrate prevented hyperglycemia and improved insulin sensitivity^{65,67,68}. HFD induced microbiota alterations results in lower proportions of fermentative bacteria, resulting in lower concentrations of SCFAs^{52,69}. However, it is not known if these lowered concentrations of SCFAs contribute to the development of enteric neuropathy and dysmotility.

Studies focused on elucidating the role of gut microbiota, diabetic GI dysmotility and enteric neuropathy typically use HFD, conventionally raised mice and in some cases germ free (GF) mouse models. HFD ingestion in conventionally raised mice results in gut microbiota alterations, T2D symptoms, enteric neuropathy and intestinal dysmotility, which are similar to that observed in diabetic patients^{20,58,70,71}. However, GF mice fed HFD are resistant to the development of obesity, hyperlipidemia, hyperglycemia and insulin resistance^{72,73}. It is not known if germ free mice develop enteric neuropathy after HFD ingestion. HFD mouse models also have impaired gut mucosal barrier function, which increases permeability and can allow lumenally-derived molecules, such as those produced from a HFD dysbiotic microbiota, to interact with cell types such as inflammatory cells and enteric neurons⁷⁴. Recent studies have shown that unknown substances in gut contents from irritable bowel and colicky infants initiate inflammation and dysmotility in these other GI motility illnesses^{75,76}. It is not known whether molecules other than LPS and palmitate are involved in triggering neuropathy and dysmotility observed on obese and T2D patients. All together, there is a critical need to better understand the role of the interactions between diet-, an intact gut microbiota and the host in the pathophysiology of GI neuropathy and dysmotility. HFD mouse models of T2D are therefore the most appropriate to address these knowledge gaps.

In summary, despite increasing evidence that the gut microbiota is able to modulate GI motility and enteric sensory neurons^{43,44,48} and is implicated in the development of T2D and obesity, it is not known what role gut microbiota alterations play in the pathogenesis of diabetic enteric neuropathy and subsequent GI dysmotility. We do not fully know how bacterial products, cellular constituents or other molecules derived from host-diet-microbiota interactions in the gut lumen of obese, pre-diabetic and diabetic patients affect the development of enteric neuropathy and GI dysmotility. These are important gaps of knowledge because enteric neuropathy and dysmotility are implicated in the early stages of the development of T2D before the manifestation of the debilitating GI illnesses that reduce

the quality of life of diabetic patients. **The Aim of this dissertation** is to use HFD germ free and conventional mouse models to determine how interactions between a HFD, the gut microbiota and the host are involved in the development of HFD-induced diabetic enteric neuropathy and dysmotility illnesses.

The studies within this dissertation will focus on four main questions derived from the central Aim. The **first question** is: does HFD ingestion impact gut microbiota, myenteric neurons and intestinal motility in male and female mice differently (Chapter 2)? The **second question** is: Does gut microbiota alteration, neuropathy and dysmotility precede diabetic conditions in HFD mice, and do microbiota alterations correlate with enteric neuropathy and GI dysmotility (Chapter 2)? Once gut microbiota alterations have been determined to be present and the correlation with neuropathy and dysmotility established, **our third question** will be: what specific molecules in the gut contents are involved/responsible for triggering diabetic enteric neuropathy and dysmotility (Chapter 3) and are these molecules derived from the gut microbiota (Chapter 4)? Our **fourth and final question** is: what role do LTA and SCFAs play in the pathophysiology of enteric neuropathy and dysmotility (Chapter 4)?

Overall, answering these questions is essential because it is the first step towards a better understanding of the role diet-gut microbiota-host interactions plays in the pathophysiology of neuropathy, dysmotility and T2D. Therefore, the outcomes of this research are significant because enteric neuropathy and dysmotility underlie the prevalent negative GI symptoms that reduce the quality of life of diabetic patients. Importantly, neuropathy and dysmotility contribute to early T2D progression. The outcomes of this research could reveal new treatments targets and early biomarkers of neuropathy and dysmotility. Our findings will form a foundation for future studies aimed at identifying specific triggers of ENS damage and dysmotility and their mechanisms of action. These studies will likely also contribute towards meeting the growing need to identify the unknown toxic molecules in the gut which are associated with the development of neurodegenerative disorders such as Alzheimer's and Parkinson's disease⁷⁷⁻⁷⁹.

Literature Cited

1. Guariguata, L. *et al.* Global estimates of diabetes prevalence for 2013 and projections for 2035. *Diabetes Res. Clin. Pract.* **103**, 137–149 (2014).
2. National Center for Chronic Disease Prevention and Health Promotion. National Diabetes Statistics Report, 2017. Estimates of Diabetes and Its Burden in the United States. *Centers Dis. Control Prev.* (2017).
3. Singh, R., Kishore, L. & Kaur, N. Diabetic peripheral neuropathy: Current perspective and future directions. *Pharmacological Research* **80**, 21–35 (2014).
4. Zochodne, D. W. Diabetes mellitus and the peripheral nervous system: manifestations and mechanisms. *Muscle Nerve* **36**, 144–66 (2007).
5. Vinik, A. I., Maser, R. E., Mitchell, B. D. & Freeman, R. Diabetic autonomic neuropathy. *Diabetes Care* **26**, 1553–79 (2003).
6. Krishnan, B., Babu, S., Walker, J., Walker, A. B. & Pappachan, J. M. Gastrointestinal complications of diabetes mellitus. *World J. Diabetes* **4**, 51 (2013).
7. Bhattarai, Y. *et al.* High-fat diet-induced obesity alters nitric oxide-mediated neuromuscular transmission and smooth muscle excitability in the mouse distal colon. *Am. J. Physiol. Liver Physiol.* **311**, G210–G220 (2016).
8. Feldman, M. & Schiller, L. R. Disorders of gastrointestinal motility associated with diabetes mellitus. *Ann. Intern. Med.* **98**, 378–84 (1983).
9. Abrahamsson, H. Gastrointestinal motility disorders in patients with diabetes mellitus. *J. Intern. Med.* **237**, 403–9 (1995).
10. Yarandi, S. S. & Srinivasan, S. Diabetic gastrointestinal motility disorders and the role of enteric nervous system: current status and future directions. *Neurogastroenterol. Motil.* **26**, 611–24 (2014).
11. Ohlsson, B. *et al.* Oesophageal dysmotility, delayed gastric emptying and autonomic neuropathy correlate to disturbed glucose homeostasis. *Diabetologia* **49**, 2010–2014 (2006).
12. Gotfried, J., Priest, S. & Schey, R. Diabetes and the Small Intestine. *Curr. Treat. Options Gastroenterol.* **15**, 490–507 (2017).

13. Horváth, V. J. *et al.* Diabetes-Related Dysfunction of the Small Intestine and the Colon: Focus on Motility. *Curr. Diab. Rep.* **15**, 94 (2015).
14. Furness, J. B. The enteric nervous system: normal functions and enteric neuropathies. *Neurogastroenterol. Motil.* **20 Suppl 1**, 32–8 (2008).
15. Hansen, M. B. The Enteric Nervous System II: Gastrointestinal Functions. *Pharmacol. Toxicol.* **92**, 249–257 (2003).
16. Kunze, W. A. & Furness, J. B. The enteric nervous system and regulation of intestinal motility. *Annu. Rev. Physiol.* **61**, 117–42 (1999).
17. Furness, J. . Types of neurons in the enteric nervous system. *J. Auton. Nerv. Syst.* **81**, 87–96 (2000).
18. Hansen, M. B. The Enteric Nervous System I: Organisation and Classification. *Pharmacol. Toxicol.* **92**, 105–113 (2003).
19. Furness, J. B. The enteric nervous system and neurogastroenterology. *Nat. Rev. Gastroenterol. Hepatol.* **9**, 286–94 (2012).
20. Stenkamp-Strahm, C. M., Kappmeyer, A. J., Schmalz, J. T., Gericke, M. & Balemba, O. High-fat diet ingestion correlates with neuropathy in the duodenum myenteric plexus of obese mice with symptoms of type 2 diabetes. *Cell Tissue Res.* **354**, 381–94 (2013).
21. Schmidt, H., Riemann, J. F., Schmid, A. & Sailer, D. [Ultrastructure of diabetic autonomic neuropathy of the gastrointestinal tract]. *Klin. Wochenschr.* **62**, 399–405 (1984).
22. Anitha, M. *et al.* GDNF rescues hyperglycemia-induced diabetic enteric neuropathy through activation of the PI3K/Akt pathway. *J. Clin. Invest.* **116**, 344–356 (2006).
23. Sang, Q. & Young, H. M. Chemical coding of neurons in the myenteric plexus and external muscle of the small and large intestine of the mouse. *Cell Tissue Res.* **284**, 39–53 (1996).
24. Vincent, A. M., Russell, J. W., Low, P. & Feldman, E. L. Oxidative stress in the pathogenesis of diabetic neuropathy. *Endocr. Rev.* **25**, 612–28 (2004).
25. Voss, U., Sand, E., Olde, B. & Ekblad, E. Enteric Neuropathy Can Be Induced by High Fat Diet In Vivo and Palmitic Acid Exposure In Vitro. *PLoS One* **8**, e81413 (2013).
26. Chandrasekharan, B. & Srinivasan, S. Diabetes and the enteric nervous system. *Neurogastroenterol. Motil.* **19**, 951–60 (2007).

27. Yamagishi, S. & Imaizumi, T. Diabetic vascular complications: pathophysiology, biochemical basis and potential therapeutic strategy. *Curr. Pharm. Des.* **11**, 2279–99 (2005).
28. Bagyánszki, M. & Bódi, N. Diabetes-related alterations in the enteric nervous system and its microenvironment. *World J. Diabetes* **3**, 80–93 (2012).
29. Reichardt, F. *et al.* Western diet induces colonic nitrenergic myenteric neuropathy and dysmotility in mice via saturated fatty acid- and lipopolysaccharide-induced TLR4 signalling. *J. Physiol.* **595**, 1831–1846 (2017).
30. Nyavor, Y. E. A. & Balemba, O. B. Diet-induced dysmotility and neuropathy in the gut precedes endotoxaemia and metabolic syndrome: the chicken and the egg revisited. *J. Physiol.* **595**, 1441–1442 (2017).
31. Rivera, L. R. *et al.* Damage to enteric neurons occurs in mice that develop fatty liver disease but not diabetes in response to a high-fat diet. *Neurogastroenterol. Motil.* **26**, 1188–99 (2014).
32. Cani, P. D. *et al.* Metabolic endotoxemia initiates obesity and insulin resistance. *Diabetes* **56**, 1761–72 (2007).
33. Aziz, Q., Doré, J., Emmanuel, A., Guarner, F. & Quigley, E. M. M. Gut microbiota and gastrointestinal health: current concepts and future directions. *Neurogastroenterol. Motil.* **25**, 4–15 (2013).
34. Sekirov, I., Russell, S. L., Antunes, L. C. M. & Finlay, B. B. Gut Microbiota in Health and Disease. *Physiol. Rev.* **90**, 859–904 (2010).
35. Reigstad, C. S. & Kashyap, P. C. Beyond phylotyping: understanding the impact of gut microbiota on host biology. *Neurogastroenterol. Motil.* **25**, 358–72 (2013).
36. Schwartz, A. *et al.* Microbiota and SCFA in lean and overweight healthy subjects. *Obesity (Silver Spring)*. **18**, 190–5 (2010).
37. Ray, K. Gut microbiota: Married to our gut microbiota. *Nat. Rev. Gastroenterol. Hepatol.* **9**, 555 (2012).
38. Vrieze, A. *et al.* The environment within: how gut microbiota may influence metabolism and body composition. *Diabetologia* **53**, 606–13 (2010).
39. Bäckhed, F. Programming of host metabolism by the gut microbiota. *Ann. Nutr. Metab.* **58 Suppl 2**, 44–52 (2011).

40. Cani, P. D. Crosstalk between the gut microbiota and the endocannabinoid system: impact on the gut barrier function and the adipose tissue. *Clin. Microbiol. Infect.* **18 Suppl 4**, 50–3 (2012).
41. Stappenbeck, T. S., Hooper, L. V & Gordon, J. I. Nonlinear partial differential equations and applications: Developmental regulation of intestinal angiogenesis by indigenous microbes via Paneth cells. *Proc. Natl. Acad. Sci.* **99**, 15451–15455 (2002).
42. De Vadder, F. *et al.* Gut microbiota regulates maturation of the adult enteric nervous system via enteric serotonin networks. *Proc. Natl. Acad. Sci.* **115**, 6458–6463 (2018).
43. Khoshdel, A. *et al.* Bifidobacterium longum NCC3001 inhibits AH neuron excitability. *Neurogastroenterol. Motil.* **25**, e478–e484 (2013).
44. Mao, Y.-K. *et al.* Bacteroides fragilis polysaccharide A is necessary and sufficient for acute activation of intestinal sensory neurons. *Nat. Commun.* **4**, 1465 (2013).
45. Perez-Burgos, A. *et al.* Psychoactive bacteria Lactobacillus rhamnosus (JB-1) elicits rapid frequency facilitation in vagal afferents. *Am. J. Physiol. Liver Physiol.* **304**, G211–G220 (2013).
46. Kashyap, P. C. *et al.* Complex interactions among diet, gastrointestinal transit, and gut microbiota in humanized mice. *Gastroenterology* **144**, 967–77 (2013).
47. Collins, J., Borojevic, R., Verdu, E. F., Huizinga, J. D. & Ratcliffe, E. M. Intestinal microbiota influence the early postnatal development of the enteric nervous system. *Neurogastroenterol. Motil.* **26**, 98–107 (2014).
48. Wu, R. Y. *et al.* Spatiotemporal maps reveal regional differences in the effects on gut motility for Lactobacillus reuteri and rhamnosus strains. *Neurogastroenterol. Motil.* **25**, e205–e214 (2013).
49. Wang, B. *et al.* Luminal administration ex vivo of a live Lactobacillus species moderates mouse jejunal motility within minutes. *FASEB J.* **24**, 4078–88 (2010).
50. Nicholson, J. K. *et al.* Host-gut microbiota metabolic interactions. *Science* **336**, 1262–7 (2012).
51. Shen, W., Gaskins, H. R. & McIntosh, M. K. Influence of dietary fat on intestinal microbes, inflammation, barrier function and metabolic outcomes. *J. Nutr. Biochem.* **25**, 270–80 (2014).
52. Amar, J. *et al.* Energy intake is associated with endotoxemia in apparently healthy men. *Am. J. Clin. Nutr.* **87**, 1219–1223 (2008).

53. Tilg, H. & Moschen, A. R. Microbiota and diabetes: an evolving relationship. *Gut* **63**, 1513–21 (2014).
54. Qin, J. *et al.* A metagenome-wide association study of gut microbiota in type 2 diabetes. *Nature* **490**, 55–60 (2012).
55. Larsen, N. *et al.* Gut Microbiota in Human Adults with Type 2 Diabetes Differs from Non-Diabetic Adults. *PLoS One* **5**, e9085 (2010).
56. Anhê, F. F. *et al.* A polyphenol-rich cranberry extract protects from diet-induced obesity, insulin resistance and intestinal inflammation in association with increased *Akkermansia* spp. population in the gut microbiota of mice. *Gut* **64**, 872–883 (2015).
57. Everard, A. *et al.* Cross-talk between *Akkermansia muciniphila* and intestinal epithelium controls diet-induced obesity. *Proc. Natl. Acad. Sci. U. S. A.* **110**, 9066–71 (2013).
58. Van Hul, M. *et al.* Reduced obesity, diabetes, and steatosis upon cinnamon and grape pomace are associated with changes in gut microbiota and markers of gut barrier. *Am. J. Physiol. Metab.* **314**, E334–E352 (2018).
59. Silhavy, T. J., Kahne, D. & Walker, S. The Bacterial Cell Envelope. *Cold Spring Harb. Perspect. Biol.* **2**, a000414–a000414 (2010).
60. Sato, J. *et al.* Gut Dysbiosis and Detection of “Live Gut Bacteria” in Blood of Japanese Patients With Type 2 Diabetes. *Diabetes Care* **37**, 2343–2350 (2014).
61. Anitha, M. *et al.* Intestinal Dysbiosis Contributes to the Delayed Gastrointestinal Transit in High-Fat Diet Fed Mice. *Cell. Mol. Gastroenterol. Hepatol.* **2**, 328–339 (2016).
62. Gong, J. *et al.* Lack of short-chain fatty acids and overgrowth of opportunistic pathogens define dysbiosis of neuromyelitis optica spectrum disorders: A Chinese pilot study. *Mult. Scler. J.* 135245851879039 (2018).
63. Rodríguez-Carrío, J. *et al.* Intestinal Dysbiosis Is Associated with Altered Short-Chain Fatty Acids and Serum-Free Fatty Acids in Systemic Lupus Erythematosus. *Front. Immunol.* **8**, (2017).
64. Binder, H. J. Role of Colonic Short-Chain Fatty Acid Transport in Diarrhea. *Annu. Rev. Physiol.* **72**, 297–313 (2010).

65. Puddu, A., Sanguineti, R., Montecucco, F. & Viviani, G. L. Evidence for the Gut Microbiota Short-Chain Fatty Acids as Key Pathophysiological Molecules Improving Diabetes. *Mediators Inflamm.* **2014**, 1–9 (2014).
66. Walker, A. W., Duncan, S. H., McWilliam Leitch, E. C., Child, M. W. & Flint, H. J. pH and Peptide Supply Can Radically Alter Bacterial Populations and Short-Chain Fatty Acid Ratios within Microbial Communities from the Human Colon. *Appl. Environ. Microbiol.* **71**, 3692–3700 (2005).
67. Kimura, I. *et al.* The gut microbiota suppresses insulin-mediated fat accumulation via the short-chain fatty acid receptor GPR43. *Nat. Commun.* **4**, 1829 (2013).
68. Lin, H. V *et al.* Butyrate and propionate protect against diet-induced obesity and regulate gut hormones via free fatty acid receptor 3-independent mechanisms. *PLoS One* **7**, e35240 (2012).
69. Fernandes, J., Su, W., Rahat-Rozenbloom, S., Wolever, T. M. S. & Comelli, E. M. Adiposity, gut microbiota and faecal short chain fatty acids are linked in adult humans. *Nutr. Diabetes* **4**, e121 (2014).
70. Everard, A. *et al.* Microbiome of prebiotic-treated mice reveals novel targets involved in host response during obesity. *ISME J.* **8**, 2116–2130 (2014).
71. Winzell, M. S. & Ahren, B. The High-Fat Diet-Fed Mouse: A Model for Studying Mechanisms and Treatment of Impaired Glucose Tolerance and Type 2 Diabetes. *Diabetes* **53**, S215–S219 (2004).
72. Rabot, S. *et al.* Germ-free C57BL/6J mice are resistant to high-fat-diet-induced insulin resistance and have altered cholesterol metabolism. *FASEB J.* **24**, 4948–4959 (2010).
73. Bäckhed, F., Manchester, J. K., Semenkovich, C. F. & Gordon, J. I. Mechanisms underlying the resistance to diet-induced obesity in germ-free mice. *Proc. Natl. Acad. Sci.* **104**, 979–984 (2007).
74. de Kort, S., Keszthelyi, D. & Masclee, A. A. M. Leaky gut and diabetes mellitus: what is the link? *Obes. Rev.* **12**, 449–458 (2011).
75. Eutamène, H. *et al.* Luminal contents from the gut of colicky infants induce visceral hypersensitivity in mice. *Neurogastroenterol. Motil.* **29**, e12994 (2017).
76. Guarino, M. P. *et al.* Supernatants of irritable bowel syndrome mucosal biopsies impair human colonic smooth muscle contractility. *Neurogastroenterol. Motil.* **29**, 1–9 (2017).

77. Chalazonitis, A. & Rao, M. Enteric nervous system manifestations of neurodegenerative disease. *Brain Research* **1693**, 207–213 (2018).
78. Roy Sarkar, S. & Banerjee, S. Gut microbiota in neurodegenerative disorders. *Journal of Neuroimmunology* **328**, 98–104 (2019).
79. Idiaquez, J. & Roman, G. C. Autonomic dysfunction in neurodegenerative dementias. *J. Neurol. Sci.* **305**, 22–27 (2011).

Chapter 2: Intestinal nerve cell injury occurs prior to insulin resistance in female mice ingesting a high fat diet

Abstract

Diabetic patients suffer from gastrointestinal disorders associated with dysmotility, enteric neuropathy and dysbiosis of gut microbiota, however gender differences are not fully known. Previous studies show that high-fat diet (HFD) causes type two diabetes (T2D) in male mice after 4-8 weeks, but only does so in female mice after 16 weeks. This study sought to determine whether sex influences the development of intestinal dysmotility, enteric neuropathy and dysbiosis in mice fed HFD. We fed 8-week old C57BL6 male and female mice a standard chow diet (SCD) or a 72% Kcal HFD for 8 weeks. We analyzed the associations between sex and intestinal dysmotility, neuropathy and dysbiosis using motility assays, immunohistochemistry and next generation sequencing.

HFD ingestion caused obesity, glucose intolerance and insulin resistance in male but not female mice. However, HFD ingestion slowed intestinal propulsive motility in both male and female mice. This was associated with decreased inhibitory neuromuscular transmission, loss of myenteric inhibitory motor neurons, and axonal swelling and loss of cytoskeletal filaments. HFD induced dysbiosis and changed the abundance of specific bacteria, especially *Allobaculum*, *Bifidobacterium* and *Lactobacillus*, which correlated with dysmotility and neuropathy. Female mice had higher immunoreactivity and numbers of myenteric inhibitory motor neurons, matching larger amplitudes of inhibitory junction potentials.

This study suggests that sex influences the development of HFD-induced metabolic syndrome, but dysmotility, neuropathy and dysbiosis occur independent of sex, and prior to T2D conditions. Gastrointestinal dysmotility, neuropathy and dysbiosis might play a crucial role in the pathophysiology of T2D in humans irrespective of sex.

Introduction

Of the 422 million adults living with diabetes globally, 85% are overweight and 90-95% have type 2 Diabetes (T2D)¹. These individuals are at great risk of life-threatening complications autonomic nerve cell damage- (neuropathy-) related conditions including: cardiovascular disease, and gastrointestinal (GI) motility disorders². In fact, up to 70% of T2D patients suffer from symptoms of GI dysmotility including dysphagia, gastroparesis, constipation, diarrhea and fecal incontinence, and pain as a result of neuropathy of the enteric nervous system (ENS)^{3,4}.

Damage to the myenteric plexus causing axonal swelling and loss of cytoskeletal filaments, disorganization of the neuropil, and loss of myenteric inhibitory motor (VIP/nNOS) neurons due to apoptosis or necrosis^{5,6} is associated with dysmotility. This is because myenteric neurons play a crucial role in regulating gastrointestinal motility mainly by signaling contraction and relaxation of smooth muscle, and coordinating propulsive movements^{7,8}.

High fat diet (HFD) animal models are commonly used to study T2D, diabetic ENS neuropathy and accompanying dysmotility because T2D is commonly associated with consuming a high fat western diets⁹. In addition, HFD-induces diabetic ENS injuries in both laboratory mice and rats^{5,10,11} that correlate with ENS injuries in diabetic (T2D) humans¹²⁻¹⁴. In both animal models and humans, ENS injuries are attributed to oxidative stress induced by hyperglycemia and inflammation^{15,16}. However, new studies link ENS injuries elicited by HFD ingestion and T2D with dysbiosis of bacterial communities in the gut through synergist actions of LPS and the saturated fatty acid, palmitate¹⁷⁻¹⁹. Increasing evidence also suggests that molecules such as saturated fatty acids (palmitate), microbial metabolites, and lipopolysaccharide (LPS) have a fundamental role in the pathophysiology of T2D, obesity, and the accompanying GI neuropathy and dysmotility^{11,19-21}. Additionally, it is believed that disruption of GI motility and neuropathy occurs before overt symptoms of obesity and T2D^{19,22}. This suggests a need for a better understanding of the relationship between diet, gut microbiota, GI neuropathy and dysmotility in T2D.

The gut microbiota play a role in the development of the ENS, and establishing a healthy ENS and maintaining normal GI motility^{21,23,24}. Dysbiosis of the gut microbial community has been linked to several motility disorders^{25,26} but the association between gut microbial composition, intestinal dysmotility and nerve cell damage in T2D is not known. The composition of the gut microbiome is shaped by diet, gender and body mass index^{26,27}. Previous studies suggest that gender (sex) also plays a role in the incidence and disease severity of obesity and T2D, resultant complications including GI motility disorders and deaths attributed to T2D in humans²⁸⁻³⁰. Additionally, in mouse models of HFD obesity and T2D, female mice fed HFD for eight weeks do not develop hyperglycemia, hyperinsulinemia and low-grade inflammation³¹⁻³³. In contrast, male mice become obese and exhibit hyperglycemia, hyperinsulinemia and inflammation. Collectively, these observations suggest that dysbiosis of the gut microbial community and gender could influence the incidence of GI neuropathy and dysmotility in both diabetic animal models and humans.

The aims of this study were to: a) determine whether 8 week HFD ingestion in male and female C57BL6 mice disrupts duodenal and colon motility by injuring myenteric inhibitory motor neurons, and reducing inhibitory neuromuscular transmission prior to overt diabetes; b) determine if altered

intestinal propulsive motility, neuropathy and gut dysbiosis are correlated; and c) determine whether there gender differences.

Methods and Materials

Mice

The University of Idaho Animal Care and Use Committee approved all study procedures. Seven week-old male and female C57Bl/6J mice were purchased from Jackson Laboratories (Bar Harbor, ME), and housed in the Laboratory Research Animal Facility. Mice were split into two groups and fed either a standard chow diet (SCD) composed of 6.2% fat (Teklad Global 2018, Teklad Diets, Madison WI) or a HFD containing 45% fat (70% kcal from lard plus 2% kcal from corn oil, TestDiet, Richmond, IN) *ad libitum* for 8 weeks (Appendix A, Supplementary Table S1). Mice were euthanized by exsanguination under deep isoflurane anesthesia.

Obesity and T2D Assessment

Weights of mice were monitored weekly throughout the study. Hyperglycemia was assessed every two weeks using an Abbott AlphaTrak glucometer (Abbott Park, IL). Glucose intolerance was assessed by intra-peritoneal glucose tolerance test at 8 weeks as previously described⁵. Briefly, after fasting mice for 6 hours during the onset of light cycle, blood was drawn from a tail vein and blood glucose (BG) values were obtained using an Abbott AlphaTrak glucometer. Each mouse received an intra-peritoneal injection of glucose solution (1 g/kg-1) and BG values were measured at 30, 60, 90 and 120 minutes after by tail vein blood draw. Homeostatic model (HOMA) values were generated to measure insulin resistance in mice as previously described³⁴. To measure insulin, on the day of euthanasia, mice were fasted for 4 hours during the light cycle and blood was collected from a submandibular vein. BG values were measured and serum was collected and stored at -80°C. Serum insulin values were measured using a Milliplex kit (Billerica, MA).

Measuring intestinal motility (motility assays)

All motility assays were conducted using the Gastrointestinal Motility Monitoring system (GIMM, Med-Associates Inc., Saint Albans, VT) for filming duodenal contractions triggered by intraluminal superfusion of Krebs, and pellet propulsion in colon as previously described^{35,36}. Briefly, approximately 6 cm long duodenum segments and the whole large intestine from cecum to the anus were immediately removed from euthanized animals and placed in ice-chilled Krebs solution. Each sample was pinned on either end in a Sylgard-lined 50 mL organ bath, continuously perfused with oxygenated Krebs solution (mmol L⁻¹: NaCl, 121; KCl, 5.9; CaCl₂, 2.5; MgCl₂, 1.2; NaHCO₃, 25;

NaH₂PO₄, 1.2; and glucose, 8; all from Sigma, St. Louis, MO, USA; aerated with 95% O₂/5% CO₂) at a rate of 10 mL per minute and maintained at temperatures between 35 and 36 °C. Duodenal segments were cannulated and intraluminally superfused with Krebs (kept at room temperature) at a flow rate of 1 mL min⁻¹ to trigger propagating contractile rings. Contraction velocities were determined by recording videos of contractions migrating from the oral to aboral end of the segment after a thirty-minute equilibration, and constructing spatiotemporal maps as previously described³⁷. Contraction frequency was determined as the number of contractions per second in spatiotemporal maps. Colon motility was performed using mouse fecal pellets coated with nail polish. The whole colon was pinned loosely in the tissue bath, and after 20 minutes of equilibration, nail polish coated pellets were inserted in the oral end and videos of the pellet moving through the intestine were recorded. We then used GIMM to determine the pellet propulsion velocity by calculating the time taken by the pellet to travel over a minimum distance of 4 cm in the aboral direction of the colon.

Measurement of inhibitory junction potentials (IJPs)

One cm long segment of oral distal colon was pinned in Krebs solution in a Sylgard-lined petri dish and opened along the mesenteric border. The sample was transferred into a recording chamber, pinned-stretched mucosal surface up and mucosal and submucosal layers were teased off with sharp forceps and mounted in a recording chamber. Roughly, 1.3 cm long × 1.0 cm wide samples of colon muscularis externa were pinned stretched between two parallel stainless steel stimulating electrodes (# 571000; A-M Systems, Sequim, WA) in Sylgard-lined 3.5 mL recording chambers, mucosal surface up. They were pinned between two electrodes for triggering electrical field stimulation. One electrode was placed at near the oral and another electrode was placed at close to the aboral ends. Samples were then mounted on an inverted Nikon Ti-S microscope and visualized using ×20 objective. IJPs were evoked by single electrical field stimulation (train duration, 500 ms; frequency, 10 Hz; pulse duration, 0.8 ms; and voltage, 100 V) using established procedures^{38,39}. IJPs were measured in the circular muscle by using glass microelectrodes (80–120 MΩ tip resistance). Recording was done at 0.5–0.8 cm from the aboral end of each sample.

Immunohistochemical Staining

Immunohistochemistry staining for nitric oxide synthase (nNOS, Abcam, Cambridge, MA) and vasoactive intestinal peptide (VIP, Abcam, Cambridge, MA) to localize myenteric inhibitory motor neurons was performed as previously described⁵. LMMPs were washed 6 x 20 minutes each in 1X phosphate buffered solution with 0.5% Triton X. Tissues were then incubated in 5% Normal Donkey serum overnight, and then in primary antibody solutions for 48 hours. After 6 x 20 minutes washes, tissues were incubated in secondary antibody solution for 3 hours, washed 3 x 20 minutes each and

mounted. Total neuron population analysis was completed using an antibody for anti-neuronal nuclear antibody 1 (ANNA1 positive human serum, kind gift from Dr. Vanda A. Lennon, Mayo Clinic).

ANNA1 positive serum was pre-adsorbed for 2 hours in beef liver powder and used at 1:20,000 to co-label tissues stained with nNOS and VIP. We used Donkey anti-rabbit 594 and donkey anti-human 488 secondary antibodies (Jackson ImmunoResearch, West Grove, PA), both at 1:300, to stain for nNOS/VIP and ANNA1, respectively. Tissues were mounted on objective slides using VectaShield Mounting Medium (Vector Labs, Burlingame, CA).

Measuring the packing density and density indices in myenteric ganglia

Myenteric ganglia were visualized with both TRITC and FITC filters and photographed using a wide field camera on a Nikon/Andor Spinning disk microscope with a 40x objective lens (Nikon, Melville, NY). Images were analyzed with Nikon NIS Elements software using the approach we previously described⁵. Briefly, at least 60 fields of view were uniformly randomly selected per tissue and marker. Ganglionic areas were measured and recorded as described previously¹⁰. Then, nNOS and ANNA1 positive neurons per ganglia were counted and used to generate neuronal densities (number of neurons/ganglionic area; packing density). For both nNOS and VIP stained LMMPs, images were manually thresholded to allow software to detect only stained neurons and nerve fibers (immunoreactive varicosities) within the ganglia, and this area was measured to compute density index (stained area/ganglionic area). To determine changes in ganglionic size, average ganglionic sizes were calculated using ganglionic areas measured from all images. Images for qualitative demonstration of nNOS, VIP and ANNA1 staining were acquired with a 60x objective lens with the Nikon Spinning disk laser confocal microscope and Nikon NIS elements acquisition software.

Analysis of Nerve Cell Injury by transmission electron microscopy (TEM)

Approximately 0.5 cm long, oral duodenal segments were cut along the mesenteric border, pinned flat and fixed in 2.5% glutaraldehyde with 4% paraformaldehyde (Electron Microscopy Sciences, Hatfield, PA) for 24 hours at 4 °C. Tissues were washed three times in 1X PBS, sectioned, stained and mounted as we previously described⁵. Image acquisition and analysis were done using a Zeiss SIGMA electron microscope (Zeiss, Germany). After washing tissues three times in 1X PBS, they were dehydrated in graded ethanol and stained with OsO₄ and uranyl acetate. Tissues were then embedded in Durcupan Fluka resin and polymerization for 48 hours at 56 °C. Tissue blocks were trimmed and cut into ultrathin 55 nm sections on an ultra-microtome. After collection on Formvar-coated single-slot grids, sections were incubated in lead citrate. Imaging was conducted on a Zeiss Sigma electron Microscope (Zeiss, Germany).

Analysis of the gut microbiota by 16S rRNA sequencing and taxonomic assignment of reads.

Genomic DNA was extracted from fecal pellets using enzymatic and mechanical lysis as previously described⁴⁰. Fecal pellets from individual mice were collected in sterile containers and stored at -80°C. All pellets were then thawed on ice and one pellet (~38mg) per mouse transferred into a sterile 2.0 mL glass tube with cell lysis buffer composed of 50 µL lysozyme (10 mg/ml, Sigma-Aldrich, St. Louis, MO, USA), 6 µL mutanolysin (25 KU/ml; Sigma-Aldrich, St. Louis, MO, USA), and 3 µL lysostaphin (4000 U/ml, Sigma-Aldrich, St. Louis, MO, USA) and 41 µL of TE50 buffer (10 mM Tris·HCl and 50 mM EDTA, pH 8.0). After incubating at 37°C for 1 hour, pellets were mechanically disrupted by vortexing at high speed. 600 mg of 0.1-mm-diameter zirconia/silica beads (BioSpec, Bartlesville, OK, USA) were added to the mixture to lyse bacterial cells by using Mini-BeadBeater-96 (BioSpec) at 2100 rpm for 1 minute. Further isolation and purification of the total genomic DNA from crude lysates were processed using QIAamp DNA Mini Kit (Qiagen, Hilden, GER) according to the manufacturer's handbook except that DNA was eluted into two separate tubes using two 100 µL aliquots. A Nanodrop 2000 was used to quantify genomic DNA in each sample according to manufacturer's instructions (Thermo Fisher Scientific, Waltham, MA, USA). Thereafter, DNA was purified on the Qiagen fecal DNA kit (Qiagen, Venlo, Netherlands). Bacterial 16S rRNA genes were amplified by PCR using barcoded primers flanking hypervariable regions V1 to V3 (*Escherichia coli* positions 27F to 534R). The variable V1-V3 regions of 16S rRNA genes in each sample were amplified in two rounds of PCR with dual barcode indexing prior to analysis on an Illumina MiSeq platform (Illumina, San Diego, CA, USA). The first PCR round amplified the target specific regions in 16S rRNA genes (*E. coli* positions 27F-534R), while the second attached sample specific barcodes and Illumina sequencing adapters. The V1-V3 regions of 16S rRNA genes were amplified in 96-well microtiter plates using the HotStar HiFidelity PCR kit (Qiagen) and 100 ng of template DNA in a total reaction volume of 50µl with the universal 16S rRNA primers 27F and 534R. The first round of PCR was run in a PTC-100 thermal controller (MJ Research, St. Bruno, Quebec, CAN) using the following cycling parameters: 2 min of denaturation at 95°C, followed by 20 cycles of 1 min at 95°C (denaturing), 1 min at 51 °C (annealing), and 1 min at 72 °C (elongation), with a final extension at 72°C for 10 min. The presence of amplicons was confirmed by agarose gel electrophoresis and staining with Gel Red. The second PCR was run in a total reaction volume of 20µl using the following cycling parameters: 10 min of denaturation at 95°C, followed by 10 cycles of 15 s at 95°C (denaturing), 30 s at 51 °C (annealing), and 1 min at 72 °C (elongation), with a final extension at 72 °C for 3 min. Negative controls without a template were included for each primer pair. The following procedure was performed by the Genomics Resources Core of the Institute for Bioinformatics and Evolutionary Studies (IBEST) at the University of Idaho: Amplicon concentrations were quantified

by fluorometry (GeminiXPS, Molecular Devices, Sunnyvale, CA, USA) using PicoGreen, then equimolar amounts of the PCR amplicons were pooled in a single tube. Short DNA fragments and amplification primers were removed from the pool amplicons using AMPure beads (Beckman-Coulter, Indianapolis, IN, USA), and then the purified amplicons were qualified on an Advanced Analytical Fragment Analyzer (Ankeny, IA). This cleaned amplicon pool was then quantified using the KAPA Illumina library quantification kit (KAPA Biosciences, Wilmington, MA, USA) on the Applied Biosystems StepOnePlus real-time PCR system. This concentration was used as a starting point to normalize the pool to 10nM. Amplicons were sequenced using an Illumina MiSeq platform and a 300bp paired-end protocol (Illumina, Inc., San Diego, CA) with custom sequencing primers. dbcAmplicons were used to demultiplex all amplicons from other reads in the run after identifying the dual-barcoded pair, and further by using the locus-specific primers as an additional “barcode. The final amplicons were sequenced using the Illumina MiSeq platform (Illumina, San Diego, CA, USA) at the University of Idaho. Sequence reads were cleaned, filtered, and taxonomically assigned using the Ribosomal Database Project (RDP) (<http://rdp.cme.msu.edu>) Naive Bayesian Classifier to the first RDP level with a bootstrap score of ≥ 50 for phylum to genus classification. Data were then processed using R scripts to calculate taxon relative abundance based on the total number of sequences within each sample. To simplify community composition analysis, we only included taxa constituting: a) at least 1% of the community in two or more samples or b) 5% of the community in at least one sample. Taxonomically assigned reads that did not meet this threshold were combined into an “Other Bacteria” category, along with reads that could not be taxonomically assigned beyond the level of bacteria. Qualitative assessments of changes in genus-level community richness and diversity were performed by calculating Shannon’s and Simpson’s indices⁴¹. Hierarchical clustering and principal components analysis (PCoA)⁴² were used to assess similarities and differences in bacterial community composition across HFD male and female mice.

Statistical analysis

Statistical analyses were performed using GraphPad Prism 5 software (GraphPad Software Inc, La Jolla, CA) unless otherwise indicated. A two-tailed unpaired Student’s t-test was used to compare means of SCD and HFD mice. A repeated measure ANOVA with Bonferroni post-hoc test was used to correct for multiple comparisons. Correlations were performed with a Spearman’s correlation matrix on average data for each group of test animals. Statistical significance was determined at $P < 0.05$. Similarities in gut bacterial communities’ composition were assessed with Ward’s linkage and Hellinger distance and hierarchical clustering using R. Principal Coordinates analysis (PCoA) was used to assign the variability of samples in the dataset to a reduced set of variables termed principal coordinates (PCs). Gut microbial communities in male and female mice fed SCD and HFD were

compared by PCoA utilizing computed Euclidean distances. The first two PCs were used to map each sample in a two dimensional space. Data in bar graphs are expressed as mean \pm SEM and analyzed by one-way analysis of variance followed by Tukey's post-tests. In addition, we performed correlation analysis between average relative abundance of bacteria and duodenal contraction velocity, number of nNOS neurons per ganglionic area in duodenum, colonic pellet propulsion velocity and number of nNOS neurons per ganglionic area in the colon. A correlation matrix generated by computing Pearson's coefficient was used to determine r and p values. Data is presented in tables.

Results

HFD ingestion for 8 weeks caused obesity and type 2 diabetes in male but not female mice.

To determine if HFD induced conditions associated with type two diabetes in both male and female mice in a similar manner after 8 weeks, we monitored weight gain, glucose intolerance, insulin sensitivity and levels of leptin, resistin and plasminogen activator inhibitor 1 (PAI1) in both SCD and HFD mice. The mean weight gained by male mice on HFD was statistically higher than that of male mice fed SCD after 8 weeks (Fig. 2-1a). Female mice fed HFD gained similar amounts of weight as those fed SCD. Immediately after euthanasia, epididymal fat pads were collected, weighed, and computed as a fraction of total mouse body weight. Compared to SCD mice, fat pad weights were found to be higher only in HFD male mice (Fig. 2-1b). Compared to the SCD group, after 8 weeks on HFD, male mice had impaired glucose tolerance and had higher HOMA values, indicating insulin resistance (Fig. 2-1c-d). In contrast, female mice on HFD had identical glucose tolerance and HOMA values to that of SCD female mice, suggesting HFD did not cause impaired glucose tolerance and insulin resistance in female mice. Taken together, these findings suggest that HFD caused obesity, impaired glucose tolerance, insulin resistance and inflammation in male, but not female, mice after 8 weeks.

HFD ingestion slowed intestinal propulsion in male and female mice.

To determine if HFD consumption affected intestinal motility in both male and female mice, we measured duodenal and colon motility *ex vivo*. Contraction velocities were significantly reduced in the small intestine of both HFD male and female mice (Fig. 2-2a). Colonic pellet propulsion velocities were significantly reduced in both HFD male and female mice (Fig. 2-2b). These results suggest that HFD ingestion reduces intestinal propulsion in male and female mice. Slowed intestinal propulsion occurred before the development of obesity, impaired glucose tolerance, and insulin resistance in female mice.

HFD ingestion diminished inhibitory neuromuscular transmission in male and female mice.

Previous studies suggest that diabetes and HFD dysmotility is caused by diminished inhibitory neuromuscular transmission as a result of damage to myenteric inhibitory motor, which release the inhibitory neurotransmitters NO and VIP to signal smooth muscle relaxation³⁸. NO and VIP act by triggering smooth muscle membrane hyperpolarizations termed inhibitory junction potentials (IJPs)^{38,39}. To analyze whether HFD disrupted relaxation by reducing IJPs, intracellular microelectrode recordings was used to measure IJPs in circular smooth muscle cells of the distal colon. We observed that the amplitudes and durations of IJPs were significantly reduced in both HFD male and female mice (Fig. 2-2c-f). Noteworthy, IJPs amplitudes were significantly larger in SCD female mice than SCD male mice (Fig. 2-2c-e). These results suggest that colonic IJPs were affected similarly by HFD ingestion regardless of gender and the absence of obesity and T2D conditions in female mice. Interestingly, female mice appear to have greater inhibitory neuromuscular transmission to colon circular muscle than male mice.

HFD ingestion damages inhibitory motor neurons in the intestine of male and female mice.

To further analyze the effect of HFD on myenteric inhibitory motor neurons, we determined if HFD damaged and reduced the number of myenteric inhibitory motor neurons in both male and female mice. This was achieved by analyzing the effect of HFD on nNOS, VIP and total number of neurons (ANNA-1 positive neurons) in LMMPs from duodenum and colon. The numbers of nNOS positive neurons, and the area of nNOS immunoreactive neurons and varicosities (nNOS density index), were significantly reduced in the duodenum and colon of both HFD male and female mice (Fig. 2-3a-h). Additionally, the VIP density index of HFD male and female mice was significantly lower than that of SCD mice in both duodenum and colon (Fig. 2-4a-f). HFD also reduced ANNA-1 positive cells per ganglionic area in the duodenum and colon of male and female mice (Fig. 2-5a-b). Of note, female mice had greater nNOS density indices compared to male mice in the duodenum and colon (Fig. 2-3b, d), greater VIP density index in colon (Fig. 4b) and number of neurons per ganglionic area in colon (Fig. 2-5b). To compare HFD effects on myenteric neurons further, we analyzed the ultrastructure of duodenal myenteric ganglia by TEM (Fig. 2-5g-j). We observed regular morphology of nerve fibers in SCD male and female mice (Fig. 2-5g, 2-5i). The myenteric plexus of HFD male and female mice exhibited axonal swelling as well as loss of neurofilaments and microtubules. These ultra-structural alterations in HFD-fed mice were more noticeable in males than females (Fig. 2-5h, 2-5j). Collectively, these findings show that damage to the ENS precedes development of obesity and T2D conditions in female mice.

HFD alters the composition of gut microbial community of both male and female mice in a similar manner.

The dysbiosis of the gut microbiota is associated with diabetes and intestinal^{26,43} dysmotility. We studied the differences in the composition of the fecal microbiota of both male and female mice by classifying bacteria based on 16S rRNA sequences. Clustering analysis revealed that the microbial communities of mice grouped together by diet (SCD vs. HFD clusters), but not by gender (Fig. 2-6a). PCoA using Euclidean distances confirmed that diet influenced community composition. Samples in the HFD cluster were defined by a higher observed relative abundance of *Firmicutes*, and lower relative abundances of *Bacteroidetes* and *Actinobacteria*, compared to samples in the SCD cluster (Fig. 2-6b). At the genus level, HFD ingestion caused a tremendous increase in the relative abundance of *Allobaculum*, and a reduction of the abundance of *Lactobacillus*, *Bifidobacterium*, and *Clostridium sensu stricto* (Fig. 2-6b). Our results suggest that HFD caused a similar pattern of dysbiosis in male and female mice even though female mice did not have obesity, hyperglycemia, glucose intolerance and insulin resistance.

HFD-induced gut microbiota changes correlate with intestinal motility and neuropathy.

To determine the interrelationship between intestinal dysmotility, neuropathy, and gut microbiota changes, we performed correlation and regression analyses. We found that several bacteria, including *Allobaculum*, which were increased by HFD ingestion, were negatively correlated with intestinal motility and nerve cell health (Table 2-1). Conversely, bacteria with lowered relative abundances in HFD mice, such as *Bifidobacterium*, positively correlated with intestinal motility and nerve cell health (Table 2-1). All bacteria (except those with relative abundances lower than 1%) that showed significant correlations with intestinal motility and health may be found in Appendices B-F, Supplementary Tables S2-2,3,4,5. Dysmotility was positively correlated with injury to nNOS neurons both in the duodenum and colon (Appendices B-F, Supplementary Table S2-2,3,4,5,6). Collectively, these results suggest that there are specific interrelationships between intestinal bacteria, motility and myenteric nerve cell health.

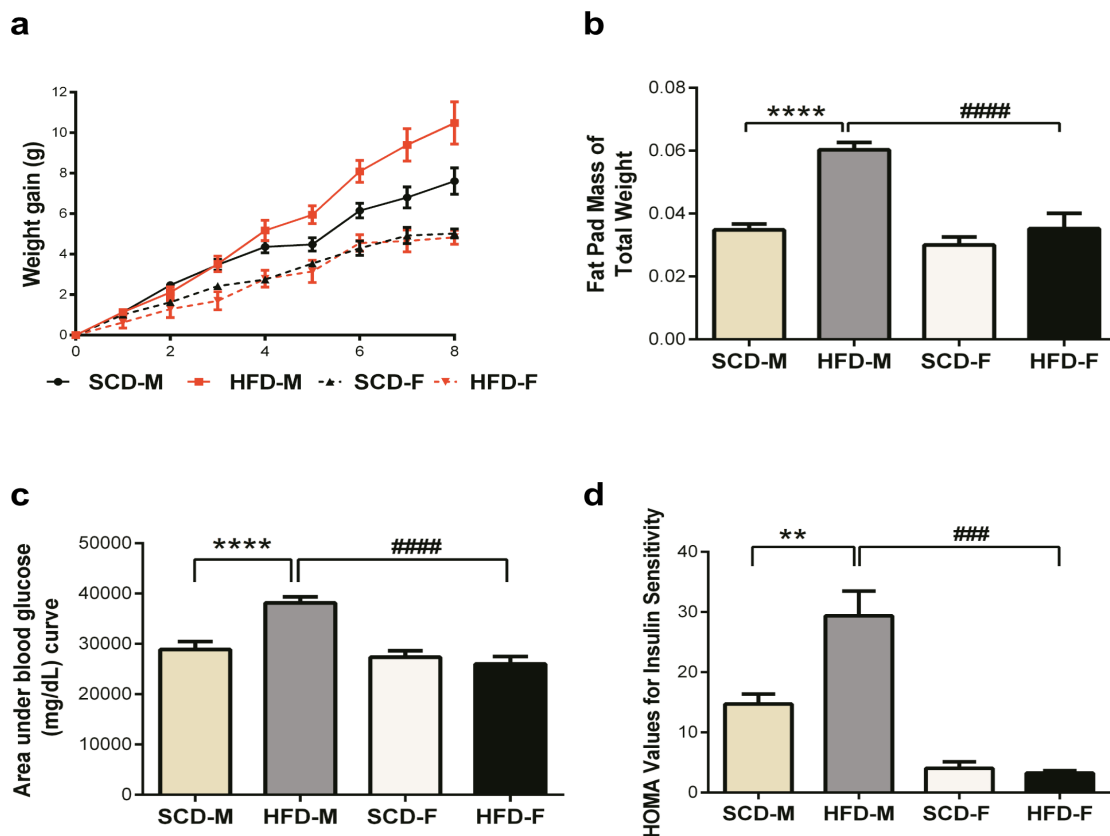


Figure 2-1 HFD has a greater metabolic effect on male mice than on female mice.

Male mice fed HFD (HFD-M) gained statistically higher amounts of weight by week 5 (a) than male SCD mice and this persisted till week 8, while female mice (HFD-F) did not gain weight even after 8 weeks (a). Unlike in female mice, intraperitoneal fat pads made up a significantly higher percentage of the body weights of male mice fed HFD (b). Male HFD mice were glucose intolerant at 8 weeks, evidenced by higher area under blood glucose curve (c), while female HFD mice were not. HFD ingestion resulted in insulin resistance in male mice, but not female mice (d). Data are expressed as mean \pm SEM and were analyzed by one-way analysis of variance followed by Tukey's post-tests. Here and here after, number of animals for experiments were $n=5-10$ per group. Symbols denoting statistical significance are: ns = $P > 0.05$; * P or +P or # P show $P \leq 0.05$; ** P or ++ P, or ## P show $P \leq 0.01$; *** P or +++ P or ### P show $P \leq 0.001$, while **** P, +++++ and ##### P show P value ≤ 0.0001 .

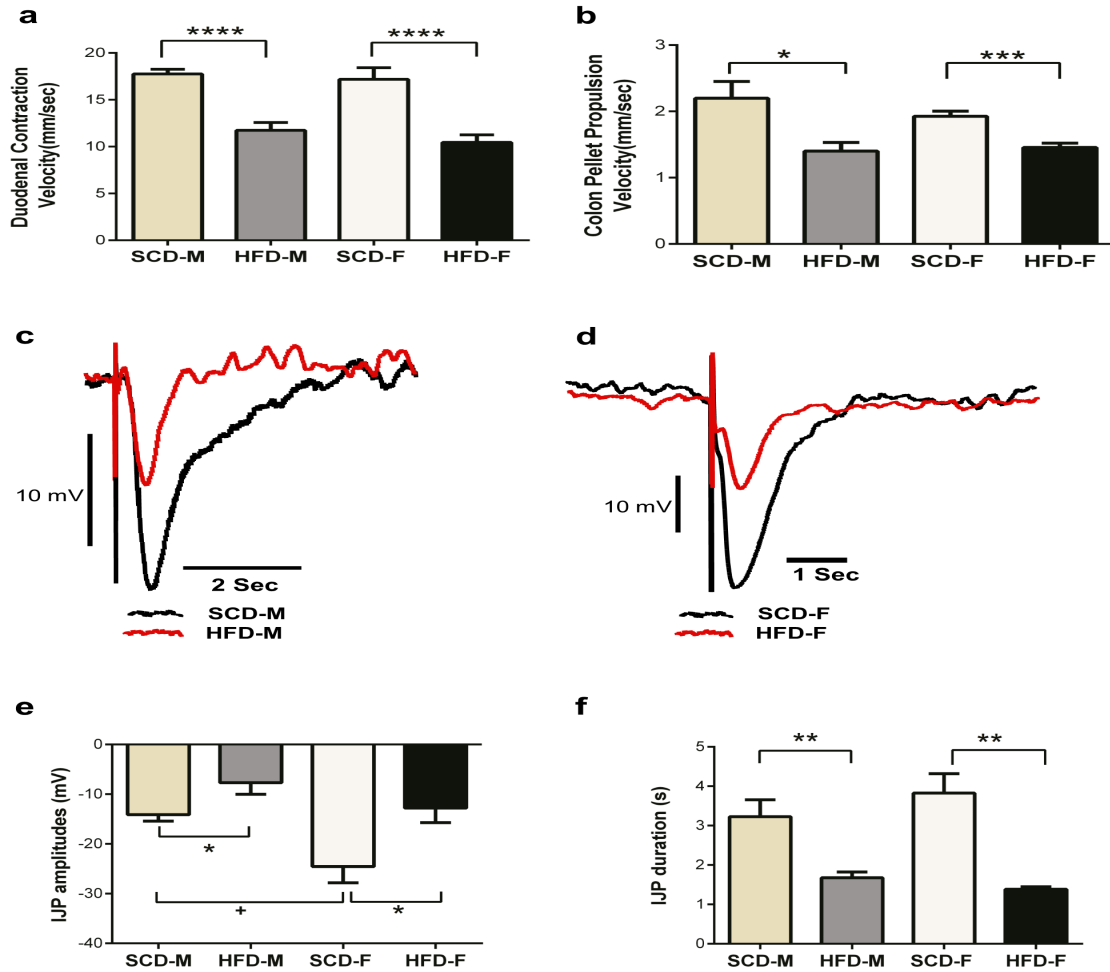


Figure 2-2 HFD results in intestinal dysmotility and disrupts inhibitory intestinal neuromuscular transmission in both male and female mice.

Duodenal contraction velocities (a) and colon pellet propulsion velocities (b) were significantly reduced by HFD ingestion in both male and female mice. HFD ingestion resulted in reduced IJP amplitudes and durations in circular smooth muscle cells in colons of both male and female mice (c-f). SCD female mice had larger IJP amplitudes than SCD male mice (c-e). IJPs were elicited by single stimulus (train duration, 500 ms; frequency, 10 Hz; pulse duration, 0.8 ms; and voltage, 100 V) delivered by two parallel stimulating steel electrodes in the recording chamber. They were measured using glass electrodes penetrating into the circular muscle of muscularis externa from the mucosal surface.

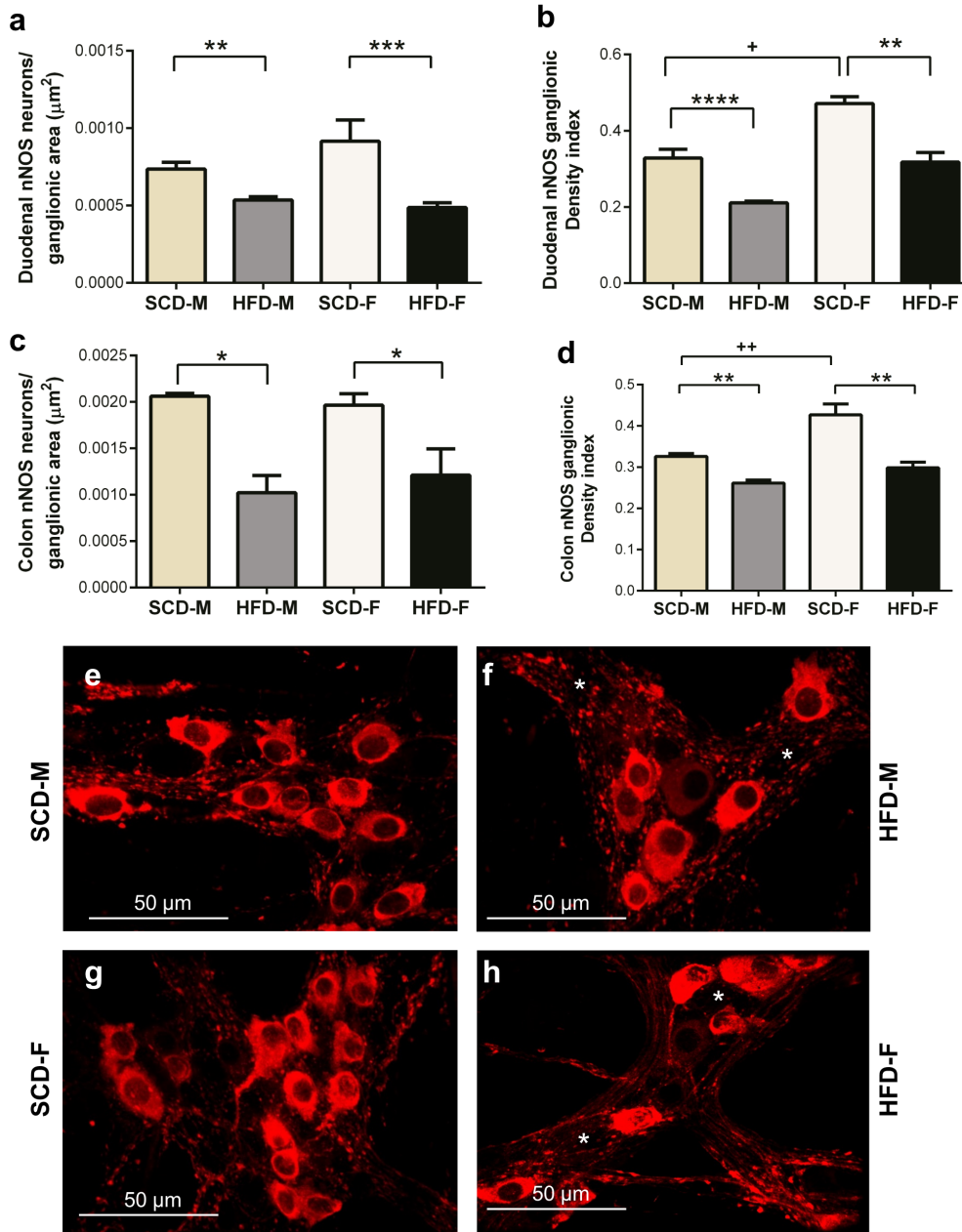


Figure 2-3 HFD reduces intestinal nitrergic myenteric neurons in both male and female mice.

In both duodenum and colon, HFD mice of both sexes had lower numbers of nNOS neurons per ganglionic area than SCD mice (a, c). Likewise, the overall amount of nNOS immunoreactivity (area of stained neurons and varicosities per ganglion area; density index) was reduced in HFD mice of both sexes (b, d). nNOS immunoreactivity was higher in SCD female mice than SCD male mice (b, d). Pictures are sample images showing nNOS staining in colon myenteric ganglia of SCD-M (e), HFD-M (f), SCD-F (g) and HFD-F (h) mice. F and h show fewer nNOS neurons compared to e and g, respectively. White asterisks indicate areas of reduced nNOS immunoreactivity.

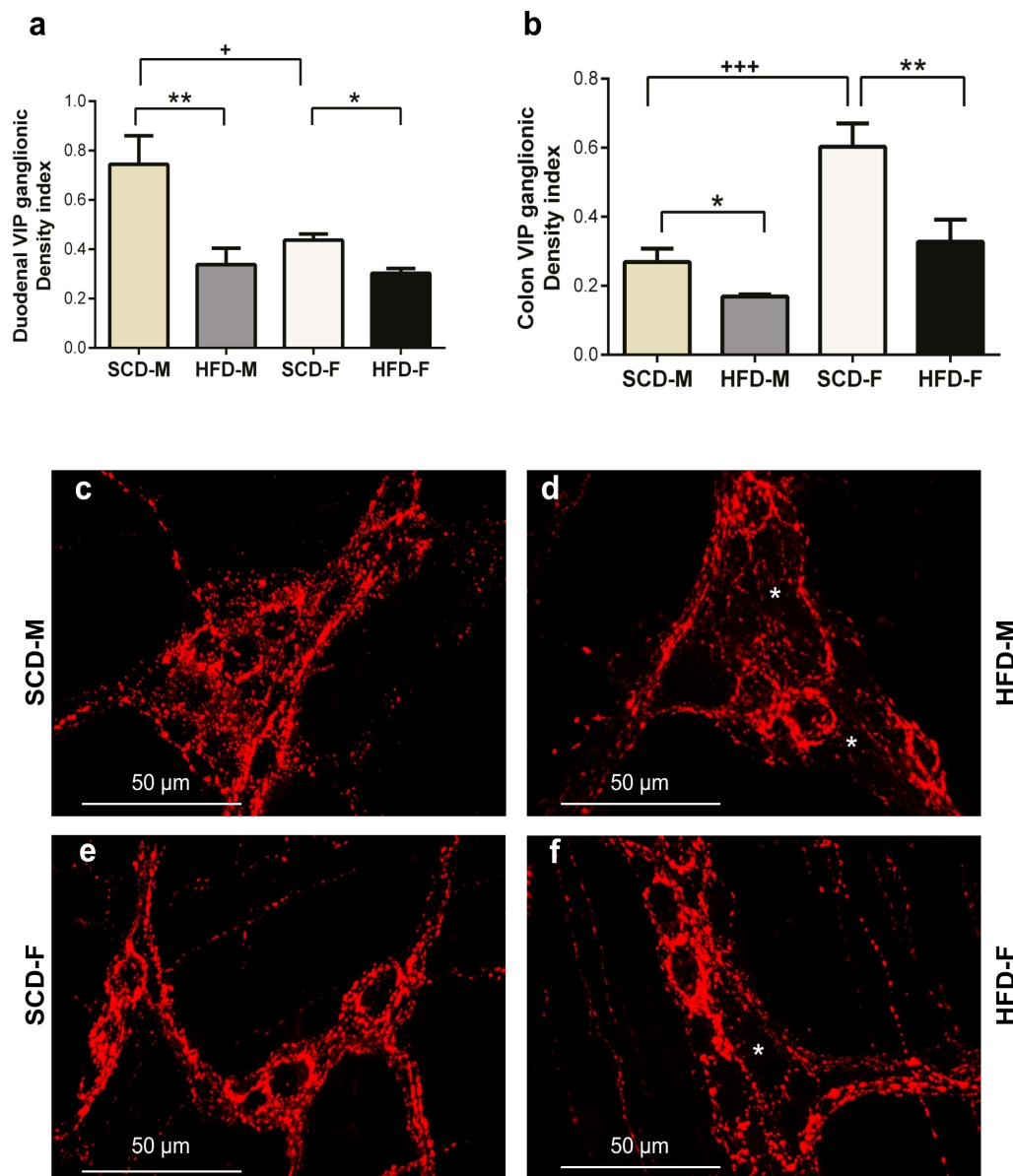


Figure 2-4 HFD reduces myenteric VIP immunoreactive varicosities in the myenteric plexus in both male and female mice intestines.

Similar to nNOS data, SCD male and female mice had higher VIP immunoreactivity in the duodenum and colon than HFD male and female mice (a-b). SCD female mice had higher VIP immunoreactivity in the colon than SCD male mice (b), but male SCD mice had higher VIP immunoreactivity in the duodenum than female SCD mice (a). Pictures are sample images showing VIP staining in SCD-M (c), HFD-M (d), SCD-F (e) and HFD-F (f) mice duodenal myenteric plexus. White asterisks show areas of reduced VIP varicosities (d, f).

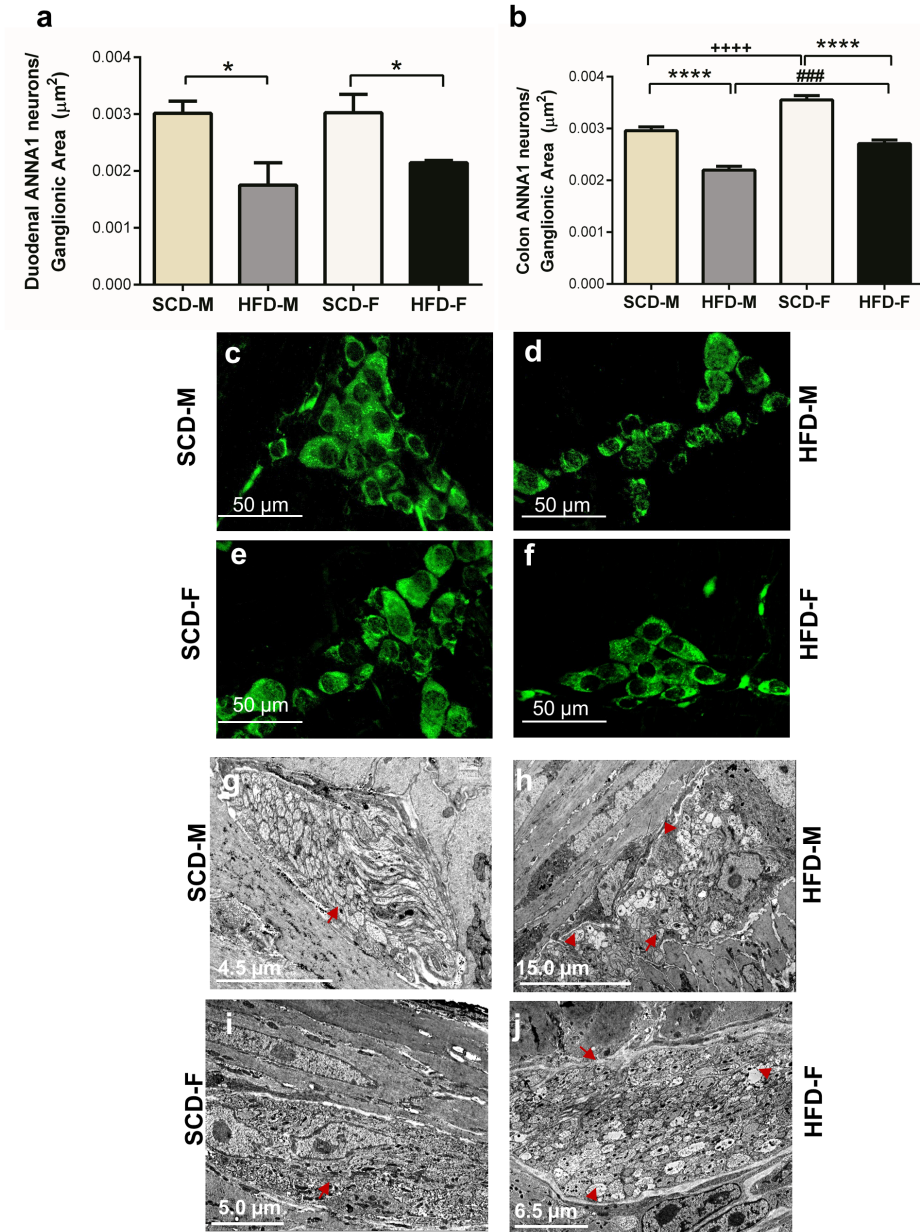


Figure 2-5 HFD reduces the total number of myenteric neurons, and causes axonal swelling and loss of cytoskeletal filaments in the myenteric plexus in both male and female mice.

The total number of neurons labeled with ANNA-1 per ganglionic area was reduced in both male and female mice fed HFD in the duodenum (a) and colon (b). Images of neurons stained by ANNA-1 immunohistochemistry in SCD-M (c), HFD-M (d), SCD-F (e) and HFD-F (f) mice duodenal myenteric plexus. TEM images of SCD (g, i) and HFD (h, j) male and female mice duodenum demonstrate ultrastructural HFD-induced nerve injury. This includes axonal swelling and loss of neurofilaments and microtubules. Red arrows show healthy axons and swollen axons with disrupted neurofilaments and arrowheads indicate microtubules.

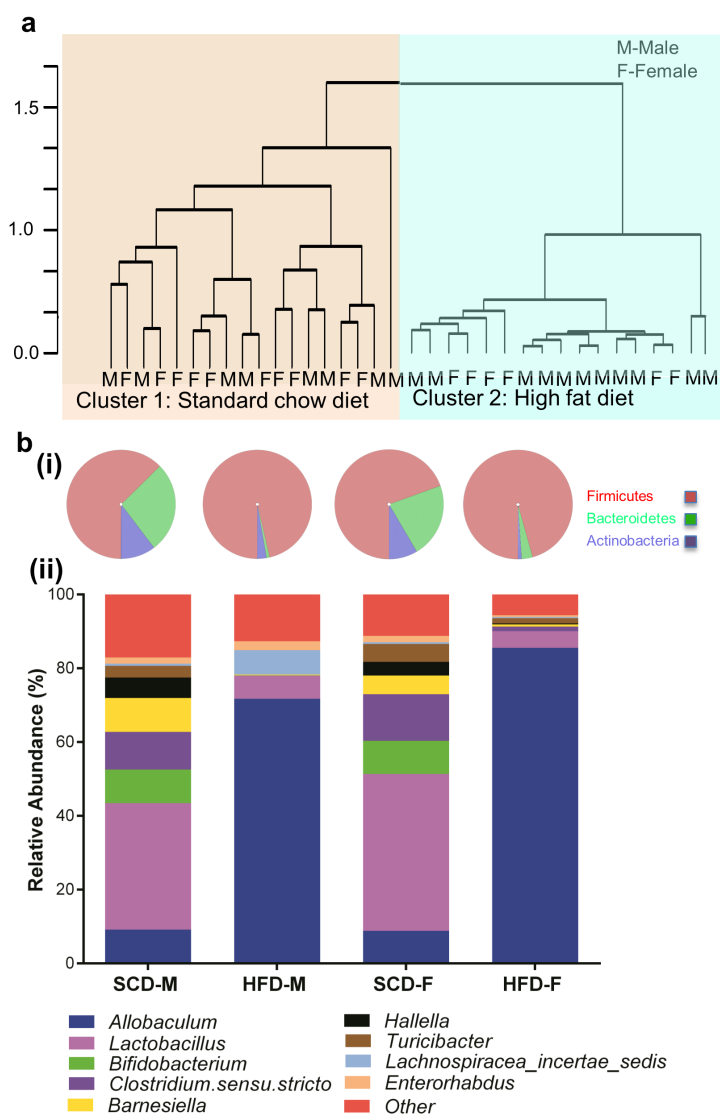


Figure 2-6 HFD is the primary determinant of gut bacterial community composition. Hierarchical clustering revealed samples grouped together by diet and not by sex (a).

The abundance of identified bacteria belonging to the phylum Firmicutes was dramatically increased in HFD mice, while Bacteroidetes and Actinobacteria were reduced by HFD ingestion (b). Stacked bar graphs show specific gut bacteria affected by HFD ingestion regardless of sex (c). Among increased genera, *Allobaculum* was the most prominent, while *Lactobacillus*, *Clostridium sensu stricto*, and *Bifidobacterium* were prominently decreased by HFD ingestion. *For clarity, bacteria with less than 1% relative abundances were grouped and labeled “Other”. Further details on bacteria labeled “Other” may be found on Appendices B-G, Supplementary Table S2-7.

Table 2-1 Bacterial genera that show significant correlations with intestinal motility, neuropathy or both in duodenum and colon.

Only bacterial genera with relative abundances greater than 1% are shown on this table. A detailed list of all organisms with significant correlations to enteric neuropathy and motility may be found in Appendices B-D, supplementary Tables S2-2-4.

#These are bacteria increased by HFD ingestion in both male and female mice.

+These are bacteria decreased by HFD ingestion in both male and female mice.

Organism	Duodenal velocity		Duodenum nNOS		Colon Velocity		Colon nNOS	
	P value	Pearson's r	P value	Pearson's r	P value	Pearson's r	P value	Pearson's r
<i>Allobaculum</i> [#]	0.002	-0.998	0.043	-0.957	0.063	-0.937	0.044	-0.956
<i>Lactococcus</i> [#]					0.078	-0.922	0.020	-0.980
<i>Bifidobacterium</i> ⁺	0.012	0.988	0.047	0.953	0.043	0.957	0.013	0.987
<i>Butyrivibrio</i> ⁺	0.010	0.990	0.051	0.949	0.040	0.960	0.013	0.987
<i>Hallella</i> ⁺	0.038	0.962	0.163	0.837	0.000	1.000	0.026	0.974
<i>Anaerobacter</i> ⁺	0.055	0.945	0.024	0.976				
<i>Clostridium.sen su.stricto</i> ⁺	0.048	0.952	0.022	0.978				
<i>Lactobacillus</i> ⁺	0.033	0.967	0.008	0.992				
<i>TM7_genera_in certae_sedis</i> ⁺	0.050	0.950	0.059	0.941				

Discussion

The purpose of this study was to determine whether slower intestinal propulsive motility, ENS neuropathy, and dysbiosis of the gut microbiota occurred prior to overt diabetes conditions using a HFD mouse model. Consumption of a HFD for 8 weeks caused obesity, hyperglycemia and insulin resistance, and increased leptin, resistin and PAI-1 in male but not female mice. Regardless of these differences in metabolic conditions, both male and female HFD mice exhibited slower intestinal propulsive motility, reduced number of myenteric inhibitory motor neurons in both duodenum and distal colon, and reduced IJPs in colon. HFD ingestion resulted in dysbiosis of the gut microbiota with an overall loss of observed diversity, an increase in the relative abundance of *Firmicutes* and a reduction in *Bacteroidetes* and *Actinobacteria*. HFD also led to a dramatic increase in the abundance of *Allobaculum* accompanied by a striking reduction of *Lactobacillus*, *Bifidobacterium*, and *Clostridium sensu stricto*. Changes in intestinal motility and neuropathy correlated both positively and negatively with shifts in the abundances of specific members of microbiota irrespective of gender. Taken together, our results suggest that slower intestinal propulsive motility, ENS neuropathy, and dysbiosis of the gut microbiota occur prior to glucose intolerance and insulin resistance. Additionally, we found that gender influences the development of HFD-induced metabolic syndrome but not gastrointestinal dysmotility, neuropathy and dysbiosis, which develops prior to overt T2D.

HFD caused obesity, glucose intolerance, and insulin resistance more rapidly in male than female mice. Obesity, glucose intolerance, and insulin resistance, developed in male mice fed a HFD for 8 weeks but not in female mice. Additionally, unlike female mice, male mice had higher circulating concentrations of resistin and PAI-1. These findings are consistent with previous studies showing that 32%-72% Kcal HFD caused increased weight gain and adiposity, as well as hyperglycemia and insulin resistance as early as 4 weeks in male mice^{5,19} while female mice were protected from HFD-induced metabolic syndrome³¹⁻³³. Reasons for these gender differences are not understood, but it is thought that estrogen protects female animals and women against development of the metabolic syndrome and T2D^{31,44}. It is also possible that progesterone protects females against obesity, insulin resistance, and T2D by attenuating HFD-induced low-grade inflammation⁴⁵. Our results are consistent with both of these ideas.

One of our main findings is that despite the lack of obesity and diabetic conditions, HFD females had decreased intestinal motility. The observations in female mice support the view that dysmotility precedes the development of obesity, glucose intolerance and insulin resistance^{19,22}. It is likely that dysmotility occurs in humans of both genders prior to overt obesity and T2D because dysmotility in

this mouse model of T2D closely matches observations in diabetic humans³. Normal rates and patterns of GI motility are crucial for maintaining gut microbiota homeostasis and body metabolism, because a decreased motility correlates with dysbiosis, and increased nutrient absorption, which exacerbates obesity and T2D conditions^{26,46}. Disruptions in the rate and pattern of GI motility could therefore play a vital role in the pathogenesis of obesity and T2D conditions.

In both sexes, HFD-induced slower propulsive motility was associated with neuropathy characterized by loss of nNOS neurons, reduced nNOS and VIP varicosities, reduced total number of neurons, axonal swelling and loss of cytoskeletal filaments in the myenteric plexus. Recorded nerve cell injuries and diminished inhibitory neuromuscular transmission match previous findings in HFD male mice^{5,19,38} and diabetic humans^{3,47}. Moreover, inhibitory neuromuscular transmission (durations and amplitudes of IJPs) was diminished in both sexes fed HFD. In mouse colon, nitric oxide prolongs the waveform of IJPs, while purines determine IJP amplitudes. Our results suggest decreased availability of nitric oxide caused by injury and loss of nNOS neurons³⁸. Additionally, our results suggest the likelihood of decreased availability of purines due to oxidative stress- and inflammation- induced nerve cell damage⁴⁸⁻⁵⁰. Our results match with previous studies suggesting that injury to interstitial cells of Cajal and enteric neuropathy can occur in the absence of hyperglycemia^{19,51,52}. Although inflammation was not evaluated in this study, low serum concentrations of resistin and PAI-1 (thought to mediate inflammation) in female mice support the view that HFD female mice have a delayed development of low-grade systemic inflammation^{32,45}. However, this claim and the role of inflammation in enteric neuropathy in females need to be studied further. The observation of myenteric nerve cell damage in female mice support the view that dyslipidemia due to saturated fatty acids (primarily palmitate) and LPS (endotoxin from Gram-negative bacteria) trigger damage to enteric neurons and dysmotility^{11,19}. Overall, our findings suggest the need for a better understanding of whether neuroinflammation, LPS and saturated fatty acids elicit nerve cell injury and dysmotility in the gut before humans develop obesity and T2D.

Significant gender differences may exist in ENS neurochemical composition and function. The results of this study not only demonstrate the features of T2D enteric neuropathy in female mice, but also show a higher number and immunoreactivity of myenteric inhibitory motor neurons, that match with larger IJP amplitudes in female mice than in male mice. The differences appear to be greater in colon compared to duodenum. These differences support previous findings demonstrating sex differences in motility in humans and in jejunum of mice⁵³⁻⁵⁵. They support the need for a better understanding of gender differences in ENS neurochemical coding and function.

During the past decade, studies have revealed that diabetes is characterized by specific intestinal microbiota^{56,57}. Consistent with findings from previous studies, 16S rRNA sequencing and analysis of the bacterial community in our HFD-mouse model of T2D revealed clustering by diet and not by sex^{56,57}. The relative abundance of *Allobaculum*, a gram positive (in the phylum *Firmicutes*), non-spore forming rod shaped bacterium first isolated from the canine gut⁵⁸, was dramatically increased by HFD ingestion in both male and female mice. *Allobaculum* produces SCFAs including butyrate and lactate⁵⁹, suggesting it has beneficial effects on the host. Additionally, previous studies have linked the increased abundance of this organism to decreased adiposity, weight loss, and an improvement in diabetic symptoms^{17,60}. However, our study found increased *Allobaculum* abundance in HFD mice, and a negative correlation between its abundance and intestinal motility and nerve cell health. This result conflicts with previous studies, but emphasizes the need to study this bacterium more extensively and examine its specific contribution to the pathophysiology of dysmotility and enteric neuropathy in obesity and T2D.

Our study shows significant correlations between gut microbiota dysbiosis, enteric neuropathy and dysmotility. Previous evidence suggests that members of the microbiota modulate GI motility, and enteric neuronal development, function and health^{23,25,26}. However, the link between specific microorganisms, diabetic dysmotility and enteric neuropathy is still in its infancy. Here, we show that several bacteria have positive and negative associations with GI motility and nerve cell health, both across the whole intestine and specific intestinal organs. While this study did not delve into cause and effect relationships, our results pave the way for future studies to address the missing link in the interaction between diet, specific members of the gut microbiota, specific cells in the gut, and associated diabetic GI dysfunctions.

In conclusion, our results reveal that while female mice do not display HFD effects on glucose metabolism and insulin sensitivity after 8 weeks, they still develop slower intestinal motility, neuropathy and dysbiosis of gut microbiota similar to HFD male mice. Further, we show that gut dysbiosis is associated with intestinal dysmotility and neuropathy. These findings suggest that GI dysmotility and neuropathy develop before T2D conditions (mainly hyperglycemia, glucose intolerance and insulin resistance), and therefore play a role in the pathophysiology of T2D. Future investigations should focus on studying the causes of intestinal neuropathy and dysmotility and their cellular mechanisms, and the interactions between specific microbes, intestinal motility and nerve cells. Such studies are critical to improving our understanding of the gut-microbiota-ENS interrelationships in health and disease.

Literature Cited

1. Centers for Disease Control and Prevention. National Diabetes Statistics Report , 2017 Estimates of Diabetes and Its Burden in the Epidemiologic estimation methods. *US Dep. Heal. Hum. Serv.* 2009–2012 (2017). doi:10.1177/1527154408322560
2. Smyth, S. & Heron, A. Diabetes and obesity: the twin epidemics. *Nat. Med.* **12**, 75–80 (2006).
3. Yarandi, S. S. & Srinivasan, S. Diabetic gastrointestinal motility disorders and the role of enteric nervous system: current status and future directions. *Neurogastroenterol. Motil.* **26**, 611–24 (2014).
4. Abrahamsson, H. Gastrointestinal motility disorders in patients with diabetes mellitus. *J. Intern. Med.* **237**, 403–9 (1995).
5. Stenkamp-Strahm, C. M., Kappmeyer, A. J., Schmalz, J. T., Gericke, M. & Balemba, O. High-fat diet ingestion correlates with neuropathy in the duodenum myenteric plexus of obese mice with symptoms of type 2 diabetes. *Cell Tissue Res.* **354**, 381–94 (2013).
6. Anitha, M. *et al.* GDNF rescues hyperglycemia-induced diabetic enteric neuropathy through activation of the PI3K/Akt pathway. *J. Clin. Invest.* **116**, 344–356 (2006).
7. Kunze, W. A. & Furness, J. B. The enteric nervous system and regulation of intestinal motility. *Annu. Rev. Physiol.* **61**, 117–42 (1999).
8. Furness, J. B. The enteric nervous system and neurogastroenterology. *Nat. Rev. Gastroenterol. Hepatol.* **9**, 286–94 (2012).
9. Cefalu, W. T. Animal models of type 2 diabetes: Clinical presentation and pathophysiological relevance to the human condition. *ILAR J.* **47**, 186–198 (2006).
10. Stenkamp-Strahm, C. M. *et al.* Prolonged high fat diet ingestion, obesity, and type 2 diabetes symptoms correlate with phenotypic plasticity in myenteric neurons and nerve damage in the mouse duodenum. *Cell Tissue Res.* **361**, 411–426 (2015).
11. Voss, U., Sand, E., Olde, B. & Ekblad, E. Enteric Neuropathy Can Be Induced by High Fat Diet In Vivo and Palmitic Acid Exposure In Vitro. *PLoS One* **8**, e81413 (2013).
12. Chandrasekharan, B. *et al.* Colonic motor dysfunction in human diabetes is associated with enteric neuronal loss and increased oxidative stress. *Neurogastroenterol. Motil.* **23**, 131-e26 (2011).

13. Farrugia, G. Histologic changes in diabetic gastroparesis. *Gastroenterol. Clin. North Am.* **44**, 31–8 (2015).
14. Grover, M. *et al.* Cellular changes in diabetic and idiopathic gastroparesis. *Gastroenterology* **140**, 1575–85.e8 (2011).
15. Chandrasekharan, B. & Srinivasan, S. Diabetes and the enteric nervous system. *Neurogastroenterol. Motil.* **19**, 951–60 (2007).
16. Vincent, A. M., Russell, J. W., Low, P. & Feldman, E. L. Oxidative stress in the pathogenesis of diabetic neuropathy. *Endocr. Rev.* **25**, 612–28 (2004).
17. Van Hul, M. *et al.* Reduced obesity, diabetes, and steatosis upon cinnamon and grape pomace are associated with changes in gut microbiota and markers of gut barrier. *Am. J. Physiol. Metab.* **314**, E334–E352 (2018).
18. Everard, A. *et al.* Microbiome of prebiotic-treated mice reveals novel targets involved in host response during obesity. *ISME J.* **8**, 2116–2130 (2014).
19. Reichardt, F. *et al.* Western diet induces colonic nitrergic myenteric neuropathy and dysmotility in mice via saturated fatty acid- and lipopolysaccharide-induced TLR4 signalling. *J. Physiol.* **595**, 1831–1846 (2017).
20. Cani, P. D. *et al.* Metabolic endotoxemia initiates obesity and insulin resistance. *Diabetes* **56**, 1761–72 (2007).
21. Aziz, Q., Doré, J., Emmanuel, A., Guarner, F. & Quigley, E. M. M. Gut microbiota and gastrointestinal health: current concepts and future directions. *Neurogastroenterol. Motil.* **25**, 4–15 (2013).
22. Nyavor, Y. E. A. & Balemba, O. B. Diet-induced dysmotility and neuropathy in the gut precedes endotoxaemia and metabolic syndrome: the chicken and the egg revisited. *J. Physiol.* **595**, 1441–1442 (2017).
23. Collins, J., Borojevic, R., Verdu, E. F., Huizinga, J. D. & Ratcliffe, E. M. Intestinal microbiota influence the early postnatal development of the enteric nervous system. *Neurogastroenterol. Motil.* **26**, 98–107 (2014).
24. Grenham, S., Clarke, G., Cryan, J. F. & Dinan, T. G. Brain-gut-microbe communication in health and disease. *Front. Physiol.* **2**, 94 (2011).

25. Quigley, E. M. M. Microflora Modulation of Motility. *J. Neurogastroenterol. Motil.* **17**, 140–147 (2011).
26. Kashyap, P. C. *et al.* Complex interactions among diet, gastrointestinal transit, and gut microbiota in humanized mice. *Gastroenterology* **144**, 967–77 (2013).
27. Haro, C. *et al.* Intestinal Microbiota Is Influenced by Gender and Body Mass Index. *PLoS One* **11**, e0154090 (2016).
28. Sugiyama, M. G. & Agellon, L. B. Sex differences in lipid metabolism and metabolic disease risk. *Biochem. Cell Biol.* **90**, 124–141 (2012).
29. Ford, E. S. Prevalence of the metabolic syndrome defined by the International Diabetes Federation among adults in the U.S. *Diabetes Care* **28**, 2745–9 (2005).
30. Kearney, P. M., Whelton, M., Reynolds, K., Whelton, P. K. & He, J. Worldwide prevalence of hypertension : A systematic review. *J. Hypertens.* **22**, 11–19 (2004).
31. Morselli, E. *et al.* Hypothalamic PGC-1 α Protects Against High-Fat Diet Exposure by Regulating ER α . *Cell Rep.* **9**, 633–645 (2014).
32. Pettersson, U. S., Waldén, T. B., Carlsson, P. O., Jansson, L. & Phillipson, M. Female Mice are Protected against High-Fat Diet Induced Metabolic Syndrome and Increase the Regulatory T Cell Population in Adipose Tissue. *PLoS One* **7**, e46057 (2012).
33. Bridgewater, L. C. *et al.* Gender-based differences in host behavior and gut microbiota composition in response to high fat diet and stress in a mouse model. *Sci. Rep.* **7**, 10776 (2017).
34. Matthews, D. R. *et al.* Homeostasis model assessment: insulin resistance and β -cell function from fasting plasma glucose and insulin concentrations in man. *Diabetologia* **28**, 412–419 (1985).
35. Balemba, O. B., Bhattarai, Y., Stenkamp-Strahm, C., Lesakit, M. S. B. & Mawe, G. M. The traditional antidiarrheal remedy, *Garcinia buchananii* stem bark extract, inhibits propulsive motility and fast synaptic potentials in the guinea pig distal colon. *Neurogastroenterol. Motil.* **22**, 1332–9 (2010).
36. Hoffman, J. M., Brooks, E. M. & Mawe, G. M. Gastrointestinal Motility Monitor (GIMM). *J. Vis. Exp.* (2010). doi:10.3791/2435
37. Wu, R. Y. *et al.* Spatiotemporal maps reveal regional differences in the effects on gut motility for *Lactobacillus reuteri* and *rhamnosus* strains. *Neurogastroenterol. Motil.* **25**, e205–e214 (2013).

38. Bhattarai, Y. *et al.* High-fat diet-induced obesity alters nitric oxide-mediated neuromuscular transmission and smooth muscle excitability in the mouse distal colon. *Am. J. Physiol. Liver Physiol.* **311**, G210–G220 (2016).
39. Spencer, N. J., Hennig, G. W. & Smith, T. K. Spatial and temporal coordination of junction potentials in circular muscle of guinea-pig distal colon. *J. Physiol.* **535**, 565–78 (2001).
40. Yuan, S., Cohen, D. B., Ravel, J., Abdo, Z. & Forney, L. J. Evaluation of methods for the extraction and purification of DNA from the human microbiome. *PLoS One* **7**, e33865 (2012).
41. Payne, A. N. *et al.* The metabolic activity of gut microbiota in obese children is increased compared with normal-weight children and exhibits more exhaustive substrate utilization. *Nutr. Diabetes* **1**, e12 (2011).
42. Ravel, J. *et al.* Vaginal microbiome of reproductive-age women. *Proc. Natl. Acad. Sci. U. S. A.* **108 Suppl**, 4680–7 (2011).
43. Ussar, S. *et al.* Interactions between Gut Microbiota, Host Genetics and Diet Modulate the Predisposition to Obesity and Metabolic Syndrome. *Cell Metab.* **22**, 516–530 (2015).
44. Ozbey, N., Sencer, E., Molvalilar, S. & Orhan, Y. Body fat distribution and cardiovascular disease risk factors in pre- and postmenopausal obese women with similar BMI. *Endocr. J.* **49**, 503–9 (2002).
45. Lei, B. *et al.* Anti-Inflammatory Effects of Progesterone in Lipopolysaccharide-Stimulated BV-2 Microglia. *PLoS One* **9**, e103969 (2014).
46. Fu, X.-Y. *et al.* Effects of gastrointestinal motility on obesity. *Nutr. Metab. (Lond)*. **11**, 3 (2014).
47. Pasricha, P. J. *et al.* Changes in the gastric enteric nervous system and muscle: A case report on two patients with diabetic gastroparesis. *BMC Gastroenterol.* **8**, 21 (2008).
48. Roberts, J. A., Durnin, L., Sharkey, K. A., Mutafova-Yambolieva, V. N. & Mawe, G. M. Oxidative stress disrupts purinergic neuromuscular transmission in the inflamed colon. *J. Physiol.* **591**, 3725–3737 (2013).
49. Bertrand, R. L. *et al.* A Western diet increases serotonin availability in rat small intestine. *Endocrinology* **152**, 36–47 (2011).

50. Sandireddy, R., Yerra, V. G., Areti, A., Komirishetty, P. & Kumar, A. Neuroinflammation and oxidative stress in diabetic neuropathy: futuristic strategies based on these targets. *Int. J. Endocrinol.* **2014**, 674987 (2014).
51. Rivera, L. R. *et al.* Damage to enteric neurons occurs in mice that develop fatty liver disease but not diabetes in response to a high-fat diet. *Neurogastroenterol. Motil.* **26**, 1188–99 (2014).
52. Horváth, V. J., Vittal, H. & Ordög, T. Reduced insulin and IGF-I signaling, not hyperglycemia, underlies the diabetes-associated depletion of interstitial cells of Cajal in the murine stomach. *Diabetes* **54**, 1528–33 (2005).
53. France, M., Skorich, E., Kadrofske, M., Swain, G. M. & Galligan, J. J. Sex-related differences in small intestinal transit and serotonin dynamics in high-fat-diet-induced obesity in mice. *Exp. Physiol.* **101**, 81–99 (2016).
54. Meleine, M. & Matricon, J. Gender-related differences in irritable bowel syndrome: potential mechanisms of sex hormones. *World J. Gastroenterol.* **20**, 6725–43 (2014).
55. Degen, L. P. & Phillips, S. F. Variability of gastrointestinal transit in healthy women and men. *Gut* **39**, 299–305 (1996).
56. Boulangé, C. L., Neves, A. L., Chilloux, J., Nicholson, J. K. & Dumas, M.-E. Impact of the gut microbiota on inflammation, obesity, and metabolic disease. *Genome Med.* **8**, 42 (2016).
57. Turnbaugh, P. J. *et al.* An obesity-associated gut microbiome with increased capacity for energy harvest. *Nature* **444**, 1027–31 (2006).
58. Greetham, H. L. *et al.* *Allobaculum stercoricanis* gen. nov., sp. nov., isolated from canine feces. *Anaerobe* **10**, 301–7 (2004).
59. Tachon, S., Zhou, J., Keenan, M., Martin, R. & Marco, M. L. The intestinal microbiota in aged mice is modulated by dietary resistant starch and correlated with improvements in host responses. *FEMS Microbiol. Ecol.* **83**, 299–309 (2013).
60. Li, H. *et al.* Relationship between gut microbiota and type 2 diabetic erectile dysfunction in Sprague-Dawley rats. *J. Huazhong Univ. Sci. Technol. - Med. Sci.* **37**, 523–530 (2017).

Chapter 3: Intestinal luminal contents from mice fed high fat diet impair intestinal motility by injuring enteric neurons and smooth muscle cells

Abstract

Damage to enteric neurons and impaired gastrointestinal muscle contractions cause motility disorders in 70% of diabetic patients. Nerve damage and altered gastrointestinal movements occur before overt diabetes, but triggers of these changes are not fully known. We tested the hypothesis that bowel contents of mice with and without high fat diet- (HFD-) induced diabetic conditions contain molecules that can impair gastrointestinal movements by damaging neurons and disrupting muscle contractions. Small and large intestinal segments were collected from healthy mice (fed standard chow diet; SCD) and filtrates of bowel contents from HFD or SCD mice were perfused through them. Bowel filtrates from HFD mice reduced intestinal movements, but those from SCD mice had no effect. Cultured intestinal muscle preparations were used to determine whether these HFD filtrates and their solid phase extraction (SPE) fractions disrupt muscle contractions by injuring nerve and smooth muscle cells. Bowel filtrates and aqueous SPE fractions from HFD mice blocked muscle contractions, caused a loss of myenteric neurons through inflammation, and reduced smooth muscle excitability. Lipopolysaccharide and palmitate caused a loss of neurons but did not affect muscle contractions. This study provides new data suggesting that unknown molecules from the bowel trigger enteric neuropathy and dysmotility before diabetes occurs.

Introduction

It is estimated that 50% of the 385 million adults globally living with obesity and type 2 diabetes (T2D)¹ suffer from debilitating complications as a result of nerve cell damage (neuropathy)². Such complications include gastrointestinal (GI) motility disorders³ which are dysphagia, gastroesophageal reflux disease, gastroparesis, enteropathy (constipation and diarrhea, incontinence) and pain. These disorders affect up to 70% of T2D patients and pose a significant socioeconomic burden^{4,5}. Diabetic GI motility-related disorders are caused by neuropathy in the enteric nervous system (ENS) and smooth muscle dysfunction^{6,7}.

The ENS consists of networks of two ganglionated plexuses—the submucosal plexus and myenteric plexus, and associated extrinsic parasympathetic, sympathetic and sensory nerve fibers supplying the gut. The submucosal plexus neurons mainly regulate GI absorption and secretion, while the myenteric

plexus neurons regulate the contraction and relaxation of muscle^{8,9}. Diabetic dysmotility is associated with damage to the myenteric plexus including loss of nitrergic myenteric neurons, which co-express neuronal nitric oxide synthase (nNOS) plus vasoactive intestinal peptide (VIP), axonal swelling and loss of cytoskeletal filaments^{4,10,11}. These diabetic ENS injuries are commonly thought to be caused by oxidative stress, advanced glycation end products and sorbitol accumulation in neurons^{4,12}.

Diabetic gastrointestinal motility disorders and ENS neuropathy are considered to be complications of diabetes, elicited by hyperglycemia, hyperlipidemia and vascular damage, and inflammation^{4,13}. However, recent studies suggest that GI dysmotility and associated ENS neuropathy develop before hyperglycemia and insulin resistance^{14,15}. Saturated fatty acids (palmitate in particular), microbial metabolites, and bacterially derived lipopolysaccharide (LPS) are thought to be responsible for triggering GI dysmotility and ENS neuropathy in obese and diabetic patients^{14,16-18}. Further, LPS from gut microbiota and dietary palmitate are thought to act synergistically to trigger damage in ENS nerve cells. This suggests that diet-bacteria-host interactions have a crucial role in the pathophysiology of GI diabetic neuropathy and dysmotility^{14,19}.

The GI lumen houses a vast number of microbes, and contains numerous bioactive molecules derived from diet, the host cells or gut microbiota^{20,21}. The gut microbiota composition in obese and diabetic patients is different from that of lean, healthy individuals^{22,23}. These differences are largely caused by diet²⁴⁻²⁶ and other factors including GI motility. The gut microbiota are important modulators of ENS function and GI motility^{18,27,28} and alterations of the gut microbial communities alters ENS functions and GI motility^{26,28,29} through the production of short chain fatty acids and other metabolites^{30,31} and cell wall constituents³². Some of these molecules can damage enteric neurons, smooth muscle and other cells that regulate motility and thus disrupt GI motility^{4,14}. However, knowledge of potentially toxic molecules from GI lumen contents and the cellular mechanisms responsible for triggering ENS neuropathy and GI dysmotility in obesity, T2D and other motility-related disorders is extremely limited. We hypothesize that toxic molecules other than LPS and palmitate from the GI luminal contents trigger diabetic GI dysmotility and ENS neuropathy by damaging smooth muscle and enteric neurons. We tested this hypothesis using a HFD mouse model.

HFD animal models are used to study T2D and diabetic neuropathy because T2D is commonly associated with consuming a high fat western diet³³. HFD ingestion and T2D are also associated with alterations of the gut microbiota³⁴ and dysmotility. In addition, HFD-induced diabetic ENS injuries in laboratory mice and rats correspond with ENS injuries in T2D humans^{10,33}. We have previously shown that GI dysmotility and a loss of myenteric inhibitory motor neurons occur in male and female C57BL6 mice fed a high fat diet (HFD) for 8 weeks^{10,15}. The aim of this study was to test our

hypothesis by determining whether ileocecal luminal contents from mice fed HFD trigger dysmotility by damaging nitrergic myenteric neurons and disrupting smooth muscle function.

Methods and Materials

Mice

The University of Idaho Animal Care and Use Committee approved study procedures. We purchased six to seven weeks old male and female C57Bl/6J mice from Jackson Laboratories (Bar Harbor, ME), and housed them on a 12-hour light cycle in the Laboratory Research Animal Facility at the University of Idaho with *ad libitum* access to food and water. After acclimation for 1-2 weeks, mice (8-weeks old) were split into two groups and fed either a standard chow diet (SCD) composed of 6.2% fat (Teklad Global 2018, Teklad Diets, Madison WI) or a HFD containing 72% fat (70% kcal fat diet with 2% additional corn oil, TestDiet, Richmond, IN) for 8 weeks¹⁵. For experiments with DHE, we used the first filial generation of GCaMP6 mice obtained by crossing female B6J.Cg-Gt (ROSA) 26Sortm95.1(CAG-GCaMP6f) Hze/MwarJ (Stock# 028865) mice with male B6.129-Nos1^{<tm1(cre)Mgmj>/J} (Stock# 017526). These mice were fed SCD only. Mice were euthanized by exsanguination under deep isoflurane anesthesia. We collected ileocecal supernatants from both HFD and SCD mice by cutting open the cecum and distal ileum samples along the mesentery and using sterile forceps to push out contents into ice-chilled sterile 2ml tubes. Samples were stored at -80 °C.

Gastrointestinal motility assays to determine how ileocecal supernatants affect intestinal propulsion

We conducted all motility assays using the Gastrointestinal Motility Monitoring system (GIMM, Med-Associates Inc., Saint Albans, VT) for filming duodenal contractions and pellet propulsion as previously described¹⁵. Ileocecal contents from mice were weighed and subsequently suspended in the appropriate volume of ice-chilled Krebs solution. Ileocecal contents were mixed with Krebs solution in a ratio of 1:100 weight/volume. This ratio was maintained for all subsequent experiments. Solid materials were filtered out with a Whatman grade 1 filter paper (ThermoFisher Scientific, Waltham, MA) to obtain ileocecal supernatants (ICS), which were superfused at a flow rate of 0.5ml/min through intestinal segments after recording four baseline videos. Baseline videos were obtained by intraluminal superfusion with Krebs at a similar flow rate. In another approach, supernatants were sterile filtered with a 0.22µm filter (Sigma, St. Louis, MO, USA) to collect sterile ICS and tested in a similar manner. The effect of HFD itself was tested by preparing a suspension in Krebs (matching ratio) and superfusing it into isolated intestinal segments. We calculated duodenal contraction velocities after converting videos into spatiotemporal maps as previously described¹⁵.

Pellet propulsion velocities were calculated in GIMM by measuring the distance traveled over the time taken by the pellet to reach the aboral end of the colon¹⁵.

Solid-phase extraction (SPE) fractionation of ileocecal supernatants (ICS)

Ileocecal contents from HFD and SCD mice were suspended in deionized water and filtered with 0.22 µm filters to collect ICS samples, which were freeze-dried and stored at -80 °C before being separated using solid-phase extraction⁶¹ (SPE). SPE was conducted using established already published procedures⁶¹. Freeze-dried ICS samples were solubilized in sterile distilled water or methanol and separated by SPE into water (hereafter, SPE1), and 20% (SPE2), 50% (SPE3), and 100% (SPE4) methanolic fractions and stored at -20°C. Samples were reconstituted in culture medium at 1:100 dilution and filter sterilized before use.

Identifying whether ileocecal supernatants and their fractions inhibit muscle contractions by using cultured muscularis preparations

The duodenojejunal and distal colon segments were removed from mice euthanized by exsanguination under deep isoflurane anesthesia and placed immediately in ice-cold Hepes buffer (20 mM HEPES (pH 7.4), 115 mM NaCl, 5.4 mM KCl, 2.2 mM CaCl and 0.8 mM MgCl₂, 13.8 mM glucose; all reagents from Sigma, St. Louis, MO, USA) containing 2% penicillin-streptomycin (Sigma, St. Louis, MO, USA). The samples were then pin-stretched in Sylgard lined petri dishes and opened along the mesenteric border. After multiple washes in Hepes buffer with 2% penicillin-streptomycin, samples were pin stretched mucosa up and dissected to obtain muscularis (muscularis externa) with fine forceps. Approximately 1cm long pieces of muscularis were then cultured in Neurobasal A medium (Thermofisher Scientific, Waltham, MA) supplemented with B27 according to manufacturer's instructions (Thermofisher Scientific, Waltham, MA). Samples were cultured in the presence of ileocecal supernatants from HFD or SCD mice (HFD-ICS or SCD-ICS), their fractions (HFD-SPE1 or SCD- SPE1), control molecules, or left untreated. Control molecules were used at the following concentrations: 0.5ng/ml LPS (L4391), 30µM sodium palmitate (P9767), and 20mM glucose (all from Sigma, St. Louis, MO, USA). All test substances were solubilized in culture media and filter sterilized with 0.22 µm filters before use. Tissues were cultured in 24 well plates for 24 hours in a tissue culture incubator at a temperature of 37°C, relative humidity of 95% and CO₂ concentration of 5%. 30-second long videos were recorded with a camera-equipped Nikon light microscope (Nikon, Melville, NY) using the 5x objective lens to determine the effect of supernatants on muscle contractions. Duodenojejunal samples were videotaped after 1 hour of equilibration and before test molecules were added (Time 0), 6 hours and 24 hours later. Videos were analyzed in a blinded fashion by counting the number of contractions in the time period of the video. Samples were

immediately fixed and stained to analyze neuronal damage as described below. To measure contractions in distal colon muscularis, samples were loosely pinned and stretched in a tissue bath then cultured. The tissues were then transferred onto the stage of an inverted Nikon Ti-S microscope and visualized using 10x objectives. They were washed for 10 minutes and then equilibrated in Krebs for additional 30 minutes at 36.5°C. Phasic contractions were recorded on videos and analyzed in a blinded fashion by counting the number of contractions for one minute.

Immunohistochemistry analysis of nerve cell damage

Tissues were fixed overnight in 4% paraformaldehyde with 0.2% picric acid and washed twice in phosphate buffered saline before proceeding with staining. Immunohistochemistry staining for neuronal nitric oxide synthase (nNOS, 1:300, Abcam, Cambridge, MA) to localize nitrergic myenteric neurons was performed as previously described¹⁰. Total neuron population analysis was completed using an antibody for anti-neuronal nuclear antibody 1 (ANNA1 positive human serum, 1:20,000, kind gift from Dr. Vanda A. Lennon, Mayo Clinic). Tissue inflammation was evaluated by staining with an antibody to TNF α , which was pre-conjugated to a far-red fluorescent dye (TNF α , 1:500, Abcam, Cambridge, MA). Oxidative stress was evaluated with anti-glutathione synthase antibody (GS, 1:200, Abcam, Cambridge, MA). Nitrosative stress was measured by staining with an antibody to inducible nitric oxide synthase (iNOS, 1:500, Abcam, Cambridge, MA). We used Donkey anti-rabbit 594 or 488 and donkey anti-human 488 secondary antibodies (Jackson ImmunoResearch, West Grove, PA), both at 1:300, to label nNOS, iNOS, GS and ANNA1, respectively. Tissues were mounted on objective slides using VectaShield mounting medium (Vector Labs, Burlingame, CA).

Quantification of the number of neurons and density indices

Tissues were photographed using a wide field camera on a Nikon/Andor Spinning disk microscope with a 40x objective lens (Nikon, Melville, NY) and analyzed with Nikon NIS Elements software using previously described procedures¹⁰.

Determining whether ileocecal supernatants and their fractions reduce inhibitory neuromuscular transmission

Approximately one and a half cm long segment of the proximal distal colon was immediately pinned in a Sylgard-lined chamber in ice-chilled HEPES solution and opened along the mesenteric border. Samples were pinned-stretched mucosal surface up in recording chambers and mucosal and submucosal layers were teased off with sharp forceps. Samples were treated with HFD-ICS, SCD-ICS, HFD-SPE1 and SCD-SPE1 via HEPES, or left untreated for 6 hours at room temperature. Solutions were changed after 3 hours. Stainless steel stimulating electrodes were placed in the recording chamber (one electrode at the oral and another at the aboral end of the sample). Tissues

were transferred onto the stage of an inverted Nikon Ti-S microscope, washed with Krebs solution (mmol L⁻¹: NaCl, 121; KCl, 5.9; CaCl², 2.5; MgCl², 1.2; NaHCO³, 25; NaH²PO⁴, 1.2; and glucose, 8; all from Sigma, St. Louis, MO, USA; aerated with 95% O₂/5% CO₂) for 10 minutes and visualized using 10x or 20x objectives. Tissues were then equilibrated at ~36.5°C by continuous superfusion (~10 ml/min) with constantly aerated (95% O₂-5% CO₂), re-circulating Krebs solution for 1 hour. After equilibration, we measured inhibitory junction potentials (IJPs) in the circular smooth muscle cells by using sharp glass electrodes with tip resistance of 90-180 mega Ohms. IJPs were evoked by electrical field stimulation (single pulses, 0.8 ms duration, 10 Hz frequency, 100 Volts) using established procedures⁷. These experiments were performed in solutions containing nisoldipine and atropine (Sigma, St. Louis, MO, USA) at 1.5 μM concentration to block muscle contractions.

Identifying whether ileocecal supernatants and their fractions inhibit the excitability of smooth muscle cells

Proximal distal colon samples were prepared and cultured in the presence of HFD-ICS or SCD-ICS or HFD-SPE1 or SCD- SPE1 or left untreated for 6 hours as described above. Microelectrode recording was used to measure spontaneous slow wave and action potential activities in circular smooth muscle cells by using sharp glass electrodes with tip resistance of 90-180 mega Ohms. Smooth muscle cell swelling and the overall tissue health were analyzed during IJP and slow wave recording. Muscle pictures were taken with 20x objective lens and a Q-Imaging Micropublisher camera.

Oxidative stress analysis by dihydroethidium staining

Superoxide levels were measured by quantifying fluorescence of the superoxide marker dihydroethidium (DHE, Life Technologies, Carlsbad, CA)⁶² as previously described³⁷. Briefly, muscularis preparations obtained from nNOS-GCaMP6 mice were cultured for 12 hours in test solutions and then incubated with 2 μM DHE dissolved in DMEM at 37°C for 1 hour. Using nNOS-GCaMP6 mice samples enabled us to visualize nNOS neurons (green fluorescence) in myenteric ganglia. DHE red fluorescence levels were quantified in live ganglia after mounting samples and capturing 15-20 random fields of view with a 40x objective lens and a wide field camera on a Nikon/Andor Spinning disk microscope (Nikon, Melville, NY). We analyzed resulting images with Nikon NIS Elements software using previously described methods¹⁰.

Quantification of inflammatory cytokines in culture medium

After 24 hours of culture, muscularis samples were removed and the culture supernatant frozen at -80 °C until further analysis. Concentrations of inflammatory cytokines were measured using the

multiplex magnetic bead-based immunoassay Luminex system and Milliplex mouse kits (Millipore, Billerica, MA, USA), according to the manufacturer's protocol. Data were analyzed using xPonent 3.1 software (Austin, TX, USA).

Statistical analysis

Data are expressed as mean \pm standard error mean of duplicate experiments. ICS induced response on motility and muscle contractions were assessed by calculating the percentage of response compared to basal velocities and number of contractions recorded in the same samples. Statistical analyses were performed using GraphPad Prism 5 software (GraphPad Software Inc, La Jolla, CA). A two-tailed unpaired Student's t-test was used to compare means of SCD-ICS and HFD-ICS with means of untreated control samples. A parametric ANOVA with Tukey's post- hoc test was used to correct for multiple comparisons when analyzing data from more than two groups. Statistical significance between groups was determined at $P < 0.05$.

Results

Ileocecal supernatants from mice fed HFD (HFD-ICS) cause dysmotility in duodenum and colon ex vivo

Ileocecal contents from HFD obese male mice with diabetic conditions, HFD female mice without obesity or diabetic conditions and SCD male and female mice were suspended in Krebs solution. Upon intraluminal perfusion, HFD-ICS rapidly slowed down duodenal contractions and colonic pellet propulsion velocities (Figs. 3-1**a-b**). Ileocecal supernatants from mice fed SCD (SCD-ICS) did not affect propulsive motility in the duodenum or colon. Similar results were obtained upon using sterile ileocecal supernatants (collected by 0.22 μm filters), suggesting microbial cells were not directly responsible for these effects. A suspension of HFD in Krebs did not affect motility suggesting HFD ingredients were not directly involved in triggering dysmotility. Altogether, these results suggest that luminal contents of mice fed HFD contain water-soluble antimotility molecules.

HFD-ICS inhibits contractions of duodenal and colon muscularis externa and damages smooth muscle cells

We next determined the effects of HFD-ICS on smooth muscle contractions using cultured muscularis preparations from mouse duodenum and colon. Compared with baseline contractions (1 hour after culture), untreated muscularis preparations were contracting at a similar rate and had healthy looking smooth muscle cells after 24 hours in culture. HFD-ICS completely blocked muscle contractions of

both duodenal and colon muscularis externa after 24 hours of culture (Figs. 3-2**a-b**). In contrast, SCD-ICS, lipopolysaccharide (LPS), palmitate, LPS + palmitate combined (LPS/Palm.), glucose, and a suspension of HFD in culture medium (not shown) did not affect muscularis contractions after 24 hours. Additionally, after 6-12 hours, smooth muscle cells from samples cultured with HFD supernatants were swollen and some of the damaged cells fell off from muscularis preparations. SCD-ICS did not cause smooth muscle cell swelling after 12 hours (Fig. 3-2**c**). Also, we observed that compared with untreated controls and SCD-ICS after 6 hours, some of the myenteric neurons in muscularis preparations cultured in HFD-ICS were readily visible by Hoffman's modulation contrast and appeared to be larger than neurons in untreated or treated with SCD-ICS. Taken together, these results suggest the presence of toxic molecules in the HFD-ICS that disrupt intestinal muscle contractions by damaging smooth muscle and other cells in the muscularis layer.

HFD-ICS induce damage to duodenal and colon nitrergic myenteric neurons

Following the observations suggesting that HFD-ICS have molecules that inhibit intestinal propulsive movements by blocking muscle contractions, we determined whether HFD-ICS impaired motility by damaging nitrergic myenteric neurons, which are mainly inhibitory motor neurons. This is because in the ENS, nitrergic myenteric neurons are readily susceptible to injuries elicited by HFD and diabetes in animal models and diabetic humans^{4,10}. In addition, there is a correlation between ENS neuropathy and dysmotility¹⁵. After 24 hours of culture, both duodenal and colon muscularis preparations were fixed and stained by immunohistochemistry with anti-neuronal nuclear antibody 1 (ANNA1) to label all myenteric neurons and neuronal nitric oxide synthase (nNOS) antibody to localize nitrergic myenteric neurons³⁵. HFD-ICS reduced the percentage of nNOS neurons in myenteric ganglia similar to LPS, palmitate and LPS/Palm (Figs. 3-3**a-b**). The percentage of myenteric nNOS neurons was not affected by SCD-ICS. These results suggest that there are neurotoxic molecules in the ileocecal contents of mice ingesting HFD, which cause dysmotility by damaging myenteric inhibitory motor neurons.

HFD-ICS reduces inhibitory neuromuscular transmission

Diabetic- and HFD-induced damage to nitrergic myenteric neurons diminish inhibitory neuromuscular transmission by decreasing the amplitude and duration of inhibitory junction potentials (IJPs), the electrical signals mainly triggered by nitric oxide and purines to elicit relaxation of smooth muscle cells^{7,15}. To link HFD-ICS-induced dysmotility to disrupted nitrergic myenteric neuronal function, we studied the effects HFD-ICS have on IJPs in circular smooth muscle cells of cultured distal colon muscularis using published procedures^{7,15}. Compared with untreated controls and SCD-ICS, HFD-ICS reduced the amplitudes but did not affect the duration of IJPs (Figs. 3-4**a-c**).

Interestingly, SCD-ICS increased the durations of IJPs (Fig. 3-4b). These observations suggest that HFD-ICS can impair inhibitory neuromuscular transmission to smooth muscle.

HFD-ICS inhibits the excitability of smooth muscle cells (SMCs) in the distal colon

The altered excitability of SMCs contributes to both HFD-induced dysmotility in animal models and diabetic GI dysmotility in humans⁷. However, whether intestinal contents of diabetic patients or animal subjects ingesting a HFD have molecules that inhibit the excitability of smooth muscle has never been studied. We used standard intracellular microelectrode recording³⁶ to determine whether HFD-ICS block smooth muscle contractions by inhibiting the excitability of SMCs by measuring slow wave and action potentials in circular SMCs in the distal colon. We observed that HFD-ICS depolarized SMCs after 4-12 hours of culture and inhibited the discharge of slow waves and action potentials (Figs. 3-5a-f). HFD-ICS disrupted the rhythmic firing of slow waves and action potentials in SMCs, causing prolonged quiescent periods. HFD-ICS also caused irregular bursting of action potentials on prolonged slow wave plateaus, leading to what resembled migrating motor complexes. Interestingly, the effects of HFD-ICS on the excitability of colonic SMCs matched the effects of HFD ingestion (Figs. 3-5e-f). SCD ingestion and SCD-ICS did not affect the discharge of slow wave action potentials (Figs. 3-5c-d). These findings suggest that HFD-ICS contain toxic molecules that inhibit the excitability of SMCs and alter the rhythmic pattern of slow waves and associate action potentials. Taken together, our results thus far suggest that HFD-ICS have neurotoxic antimotility molecules that block intestinal contractions by injuring both enteric neurons and smooth muscle cells.

The neurotoxic and antimotility molecules are mainly present in the aqueous solid phase extraction (SPE) fractions of HFD-ICS

In initial efforts to isolate and identify the neurotoxic antimotility molecules in HFD-ICS that inhibit muscle contractions and damage nitrergic myenteric neurons, sterile HFD-ICS and SCD-ICS samples were freeze-dried and stored at -80 °C. We then reconstituted these samples in either double distilled water or methanol and used solid phase extraction (SPE) to collect (aqueous, SPE1) or 20% (SPE2), 50% (SPE3), and 100% (SPE4) methanolic fractions. An initial bioactivity screening of these fractions using isolated duodenal contraction assays showed that SPE1 and SPE4 from HFD-ICS mimicked the effects of HFD ingestion and HFD-ICS by reducing the propulsive velocity of duodenal contractions. However, SPE1 from HFD-ICS showed a stronger effect than SPE4. Therefore, we used cultured duodenojejunal muscularis preparations to determine whether SPE1 and SPE4 from HFD-ICS and SCD-ICS inhibit muscle contractions and damage nitrergic myenteric neurons. Intracellular microelectrode recording³⁶ was used determine whether SPE1 block smooth muscle contractions by inhibiting the excitability of SMCs by measuring slow wave and action potentials in circular SMCs in

the distal colon. Like the HFD-ICS, its SPE1 fraction (HFD-SPE1) entirely blocked muscularis contractions (Fig. 3-6a), caused swelling of SMCs (Fig. 3-6b), and reduced the percentage of nNOS neurons (Figs. 3-6c, d). Both HFD-SPE4 and SCD-SPE4 did not affect muscularis contractions or the percentage of nNOS neurons (Figs 6a, c). Unlike HFD-SPE1, the aqueous fraction of SCD-ICS (SCD-SPE1) did not affect muscle contractions, damage SMCs or reduce the percentage of nNOS neurons (Figs. 3-6a-d). Importantly, like HFD-ICS, HFD-SPE1 depolarized and inhibited the excitability of circular SMCs in muscularis preparations from distal colon after 6 hours (Fig. 3-6 e-f). These results support the view that neurotoxic antimotility molecules in HFD-ICS are primarily water soluble, stable at low temperatures and can be isolated by using SPE.

Oxidative stress is likely not required for enteric neurons and smooth muscle damage caused by ileocecal supernatants from HFD mice (HFD-ICS)

Previous studies have demonstrated that oxidative stress is the main factor that causes diabetic enteric neuropathy⁴. We, therefore, hypothesized that neurotoxic molecules in HFD-ICS and its SPE1 damaged enteric neurons through oxidative stress. To test this idea, duodenojejunal muscularis samples were cultured in HFD-ICS, HFD-SPE1, SCD-ICS, SCD-SPE1, LPS control or untreated control. Then, samples were stained with the superoxide-specific fluorescent indicator dihydroethidium (DHE)³⁷. We also fixed and then stained treated muscularis samples with an anti-glutathione synthase antibody to measure the expression of glutathione, an essential antioxidant produced by both neurons and glia in response to oxidative stress^{38,39}. We observed that the DHE stained area per ganglionic area was unchanged by the treatments above except LPS, which increased the DHE stained area after 12 hours (Figs. 3-7a-b). Additionally, we found the anti-glutathione synthase stained ganglionic area was not changed by either HFD-ICS or SCD-ICS but was increased by LPS (Figs. 3-7c-d). These results suggest that oxidative stress is likely not activated or required for damage caused by toxic molecules in HFD-ICS. Noteworthy, most nNOS neurons did not appear to be immunoreactive for anti-glutathione synthase (Fig. 3-7d).

HFD-ICS induces inflammation but likely does not increase nitrosative stress

Inflammation is one of the major pathways through which diabetic enteric neuropathy occurs and usually leads to oxidative and/or nitrosative stress⁴⁰. We determined whether HFD-ICS induced inflammation and nitrosative stress in cultured duodenojejunal muscularis externa by measuring inflammatory cytokines and markers (TNF α , IL-6, MCP1 and PAI-1) in culture supernatant, and immunohistochemical staining for TNF α and iNOS after 24 hours of culture. Compared to the untreated control samples and SCD-ICS, HFD-ICS increased TNF α concentration in culture medium (Fig. 3-8a). LPS treatment caused a dramatic increase of the concentrations of TNF α (Fig. 3-8a).

However, HFD-ICS did not affect IL-6 levels compared with untreated control and SCD-ICS (Fig. 3-8b). LPS caused a dramatic increase in IL-6 concentration (Fig. 3-8b). A qualitative examination of neuroinflammation and nitrosative stress by TNF α and inducible nitric oxide synthase (iNOS) immunohistochemistry, respectively revealed that TNF α immunoreactivity was increased in myenteric ganglia after treatment with both SCD-ICS and HFD-ICS (Fig. 3-8c) compared with untreated control. However, like LPS, HFD-ICS treated samples had more neurons expressing TNF α compared to SCD-ICS treated samples. In contrast to LPS, HFD-ICS and SCD-ICS did not appear to increase the number nNOS and non-nNOS neurons expressing iNOS (Fig. 3-8c, arrows). This data suggests that HFD-ICS damages enteric neurons by inducing TNF α mediated neuroinflammation.

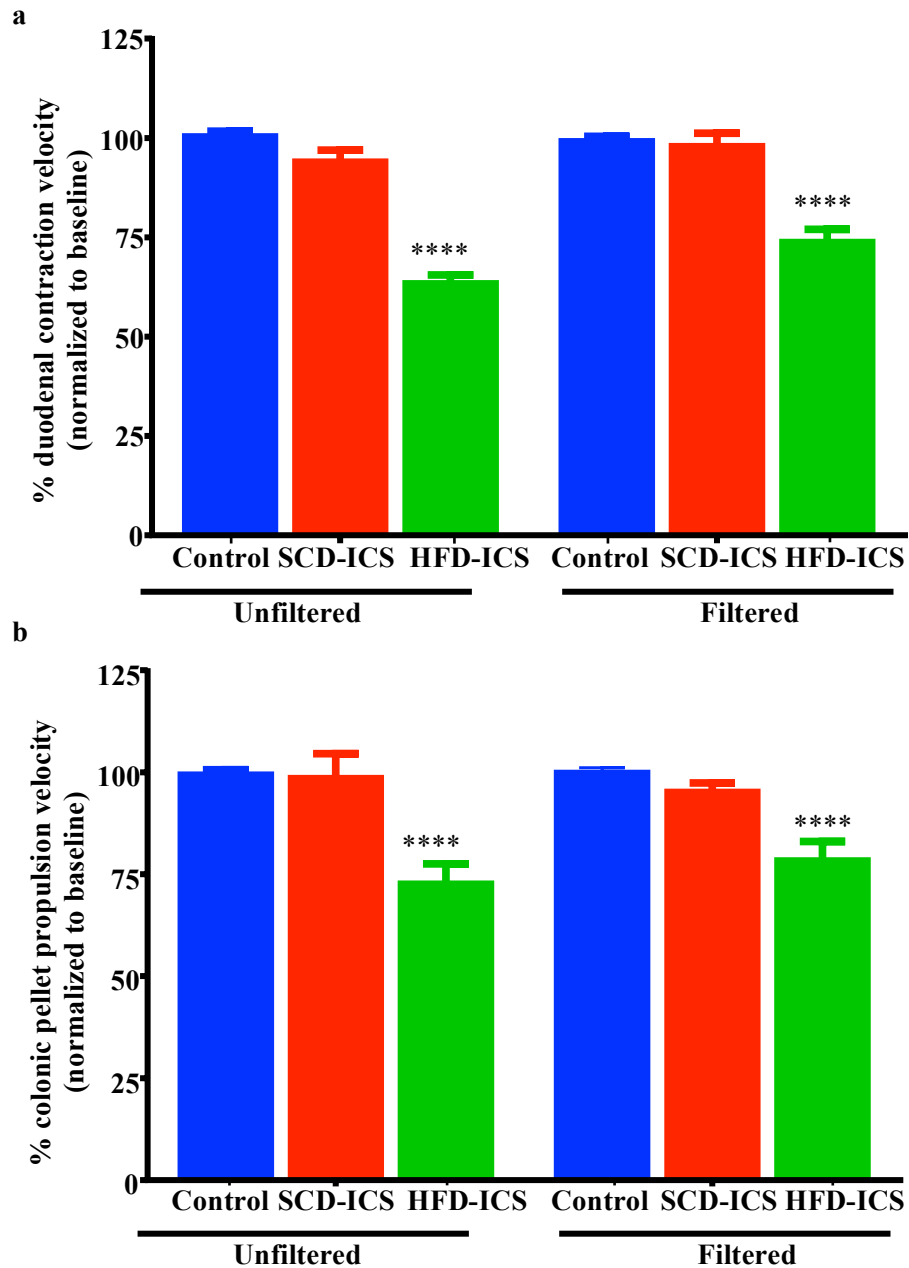


Figure 3-1 HFD-ICS induces dysmotility in both duodenum and colon *ex vivo*.

Duodenal contraction velocities (a) and colon pellet propulsion velocities (b) were significantly reduced by HFD-ICS after 5 minutes of perfusion compared with control and SCD-ICS. Filtering ICS with a 0.22 μm filter, which removed microbial cells and other cells, did not change its effects on motility. Data are expressed as mean \pm SEM and were analyzed by one-way analysis of variance followed by Tukey's post-tests in all figures. Here and here after, number of animals for experiments were n=5-10 per group. Symbols denoting statistical significance are: ns = $P > 0.05$; * P shows $P \leq 0.05$; ** P shows $P \leq 0.01$; *** P shows $P \leq 0.001$, while **** P , shows P value ≤ 0.0001 .

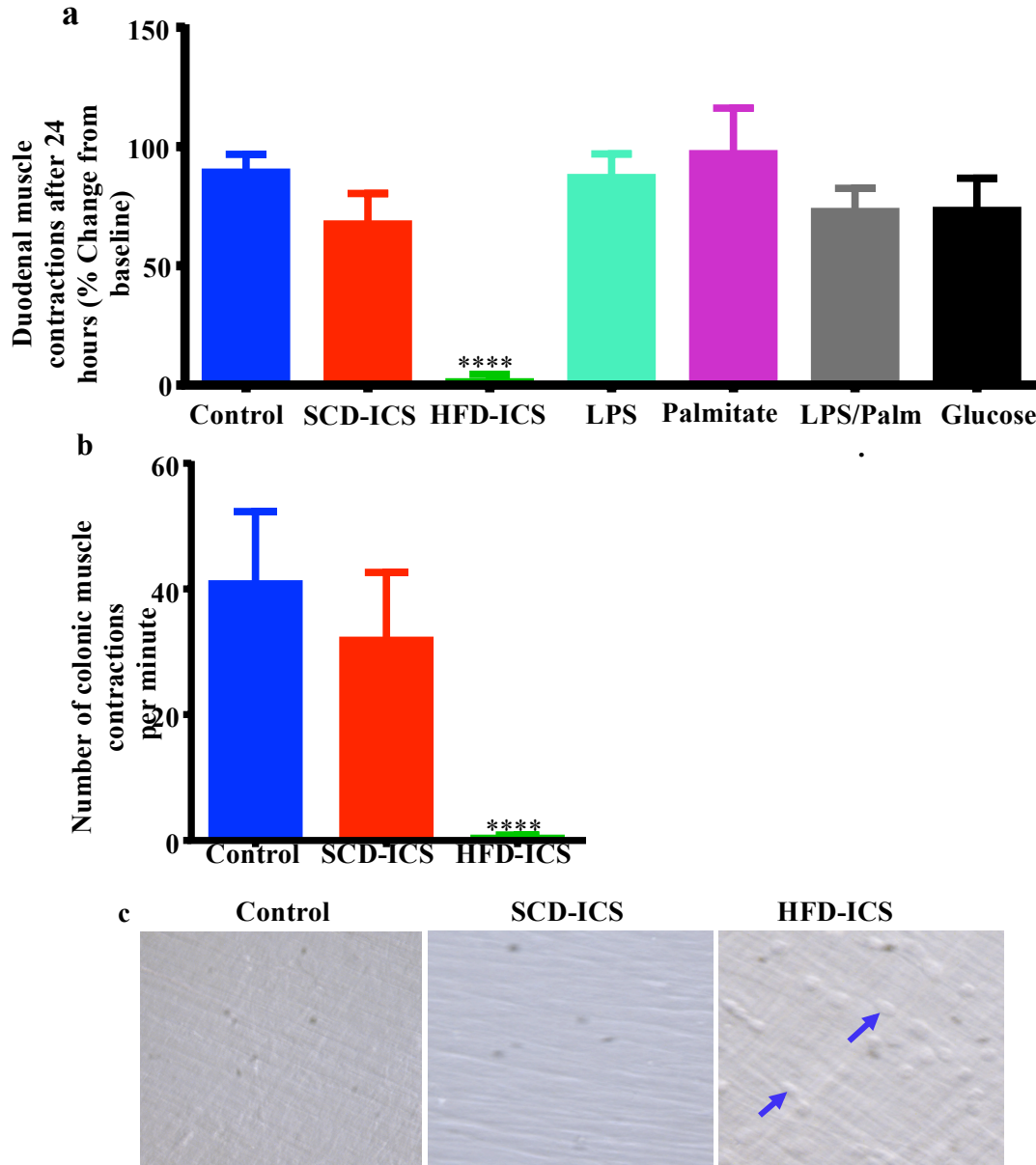


Figure 3-2 HFD-ICS reduces contractions of small and large intestine muscularis preparations and damages smooth muscle cells (SMCs).

After 24 hours of culture, HFD-ICS reduced the number of contractions of muscularis preparations from duodenum (a) and distal colon (b) when compared to untreated control. SCD-ICS, LPS, palmitate, LPS/palmitate combination and glucose did not affect muscularis contractions. Compared with untreated control (control) and SCD-ICS, HFD-ICS caused swelling of SMCs suggesting it damaged these and other cells in muscularis preparation (c, arrows; 6 hours).

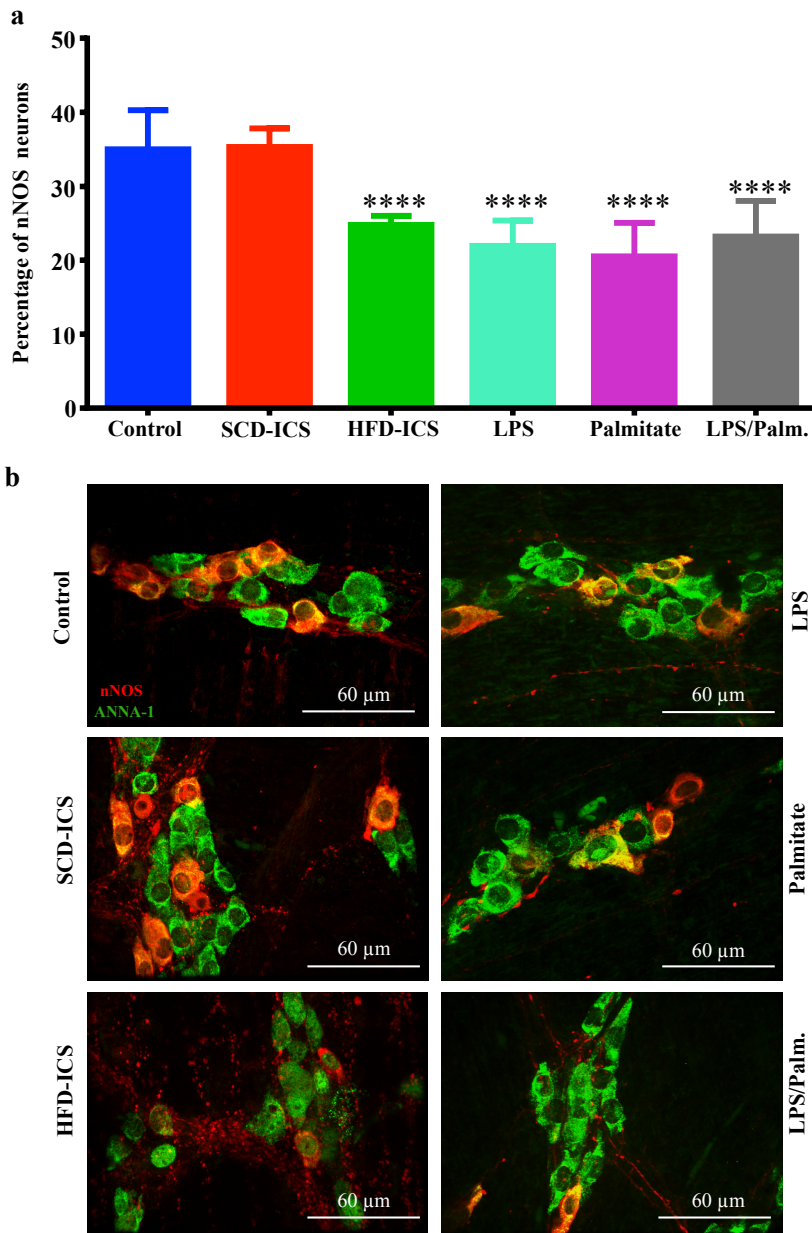


Figure 3-3 HFD-ICS reduces the percentage of nNOS neurons in the myenteric plexus in duodenum.

The percentage of nNOS neurons out of the total number of myenteric neurons (labeled with ANNA1) per ganglionic area was lower in samples treated with HFD-ICS for 24 hours (a), which was similar to samples treated with LPS, palmitate, and LPS/palmitate when compared to untreated control and SCD-ICS. (b) Sample images showing overlays of nNOS (red) and ANNA1 (green) staining in duodenal myenteric ganglia of untreated control, SCD-ICS, HFD-ICS, LPS, palmitate, and LPS/palmitate treated samples.

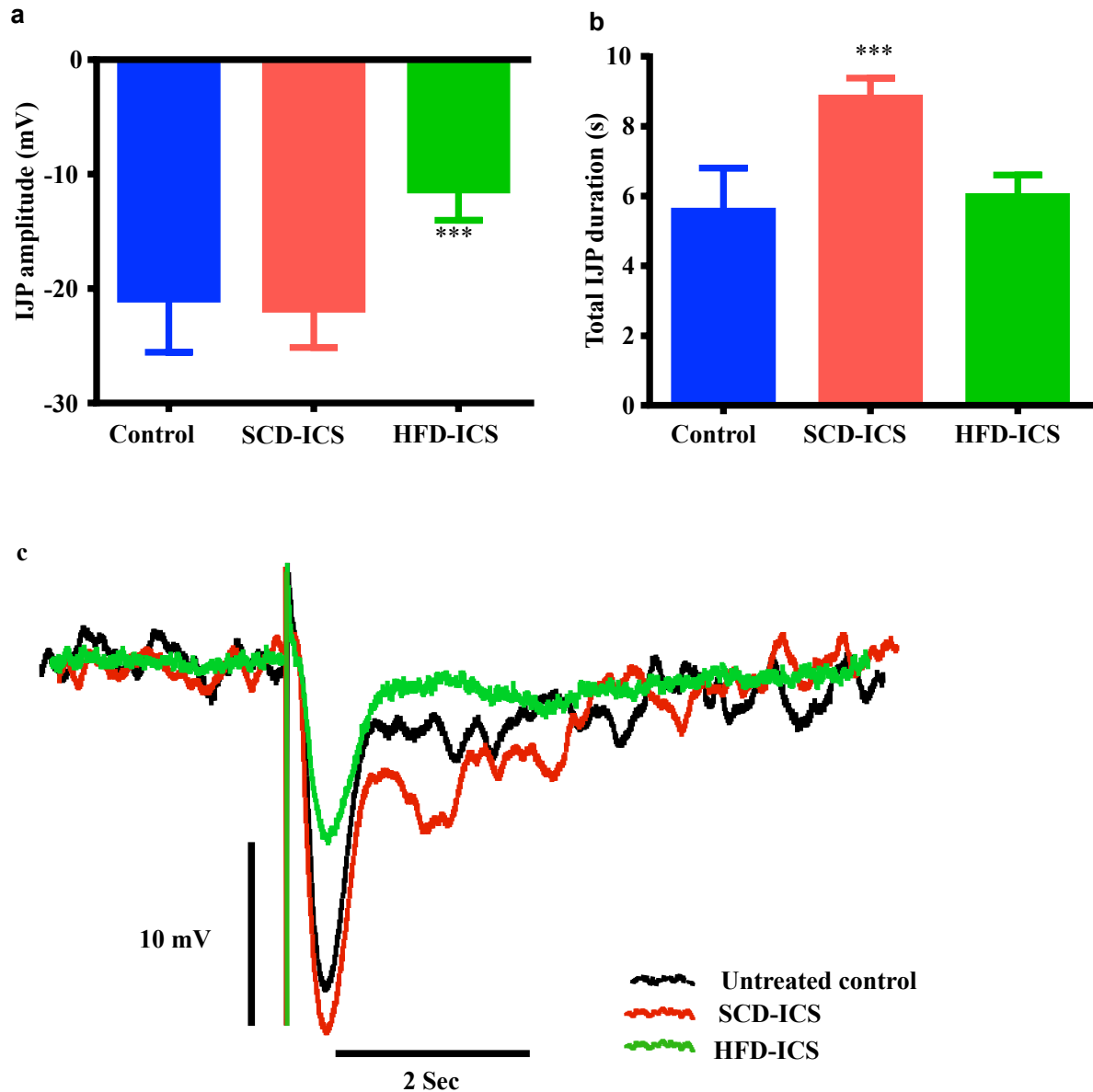


Figure 3-4 HFD-ICS impairs intestinal inhibitory neuromuscular transmission to circular smooth muscle in distal colon.

Treatment with HFD-ICS reduced IJP amplitudes (a) but did not change IJP durations (b) in circular smooth muscle cells in distal colon muscularis. SCD-ICS did not change IJP amplitudes but increased durations. (c) Traces of representative IJPs from untreated control, SCD-ICS and HFD-ICS treated muscularis.

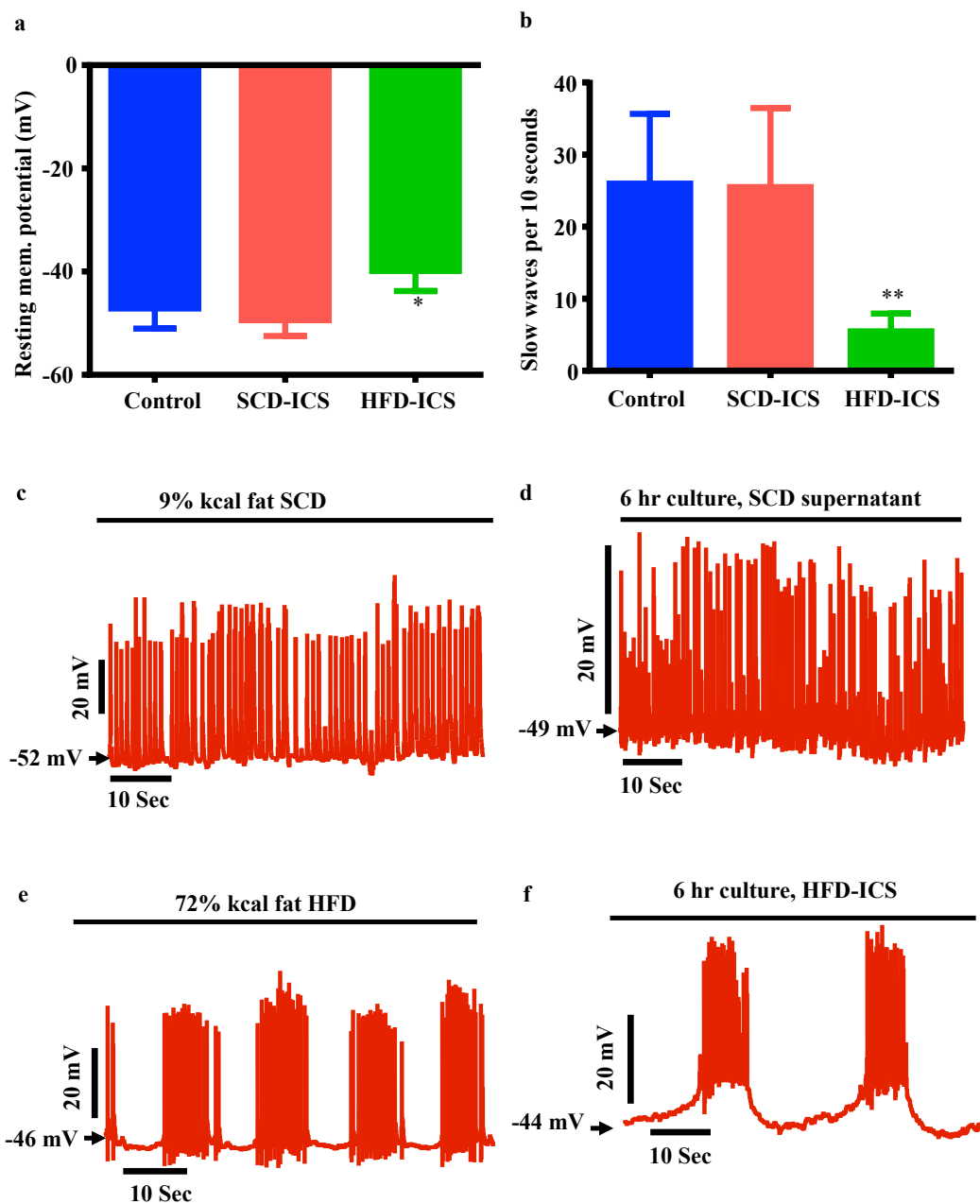
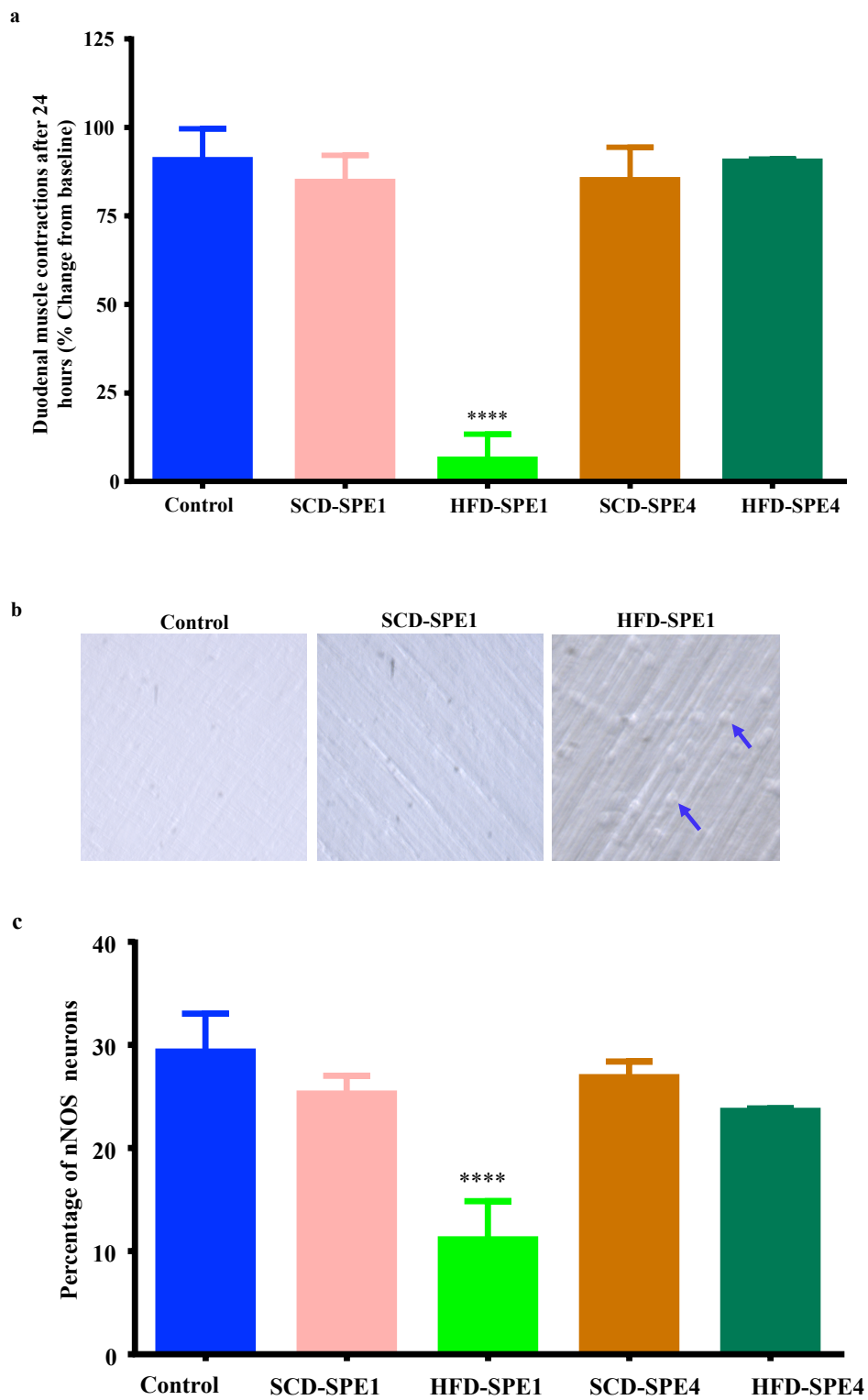
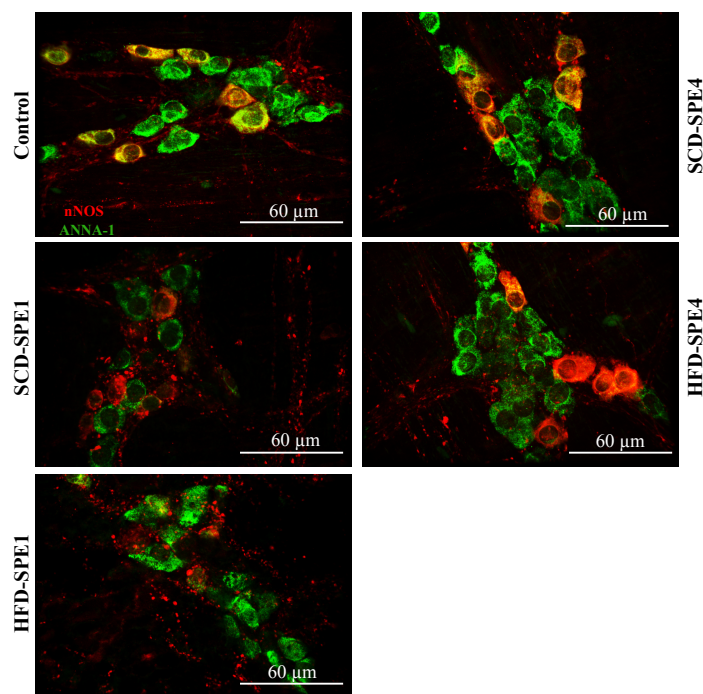


Figure 3-5 HFD ICS inhibits the excitability of smooth muscle cells.

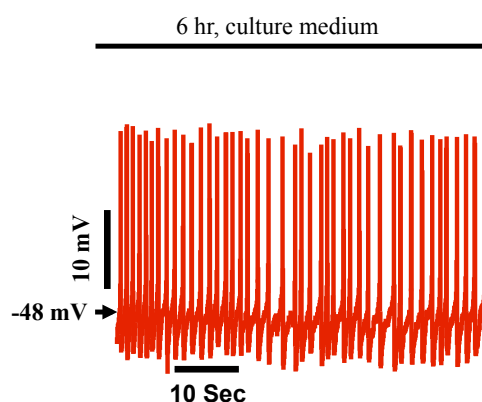
Compared to SCD-ICS, HFD-ICS depolarized resting membrane potentials in circular smooth muscle cells in distal colon muscularis (**a**) and reduced the frequency of slow waves (**b**) after 6 hours of treatment. Compared to the rhythmic discharge of slow waves-action potentials from mice fed SCD (**c**) and colon muscularis treated with SCD-ICS (**d**) both HFD ingestion (**e**) and HFD-ICS treatment (**f**) induced irregular discharge of slow waves-action potentials. They caused a bursting pattern of slow waves-action potentials and prolonged quiescent intervals.



d



e



f

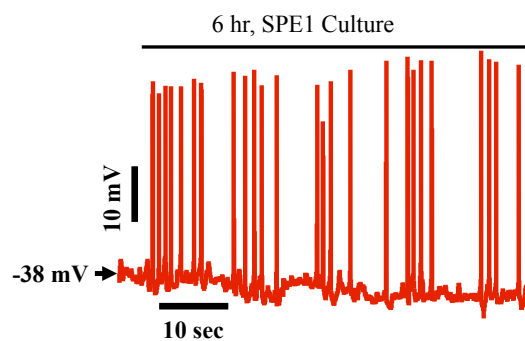
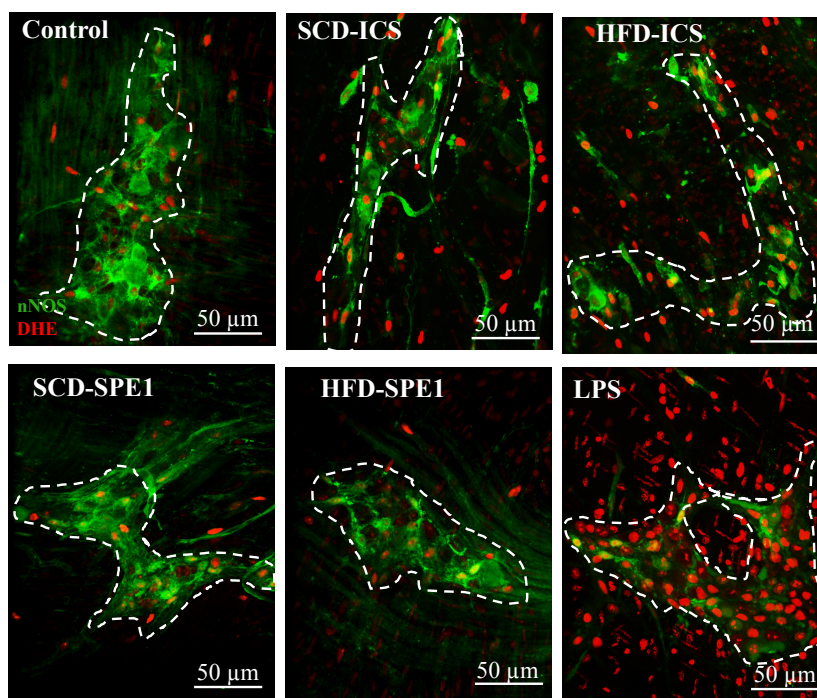
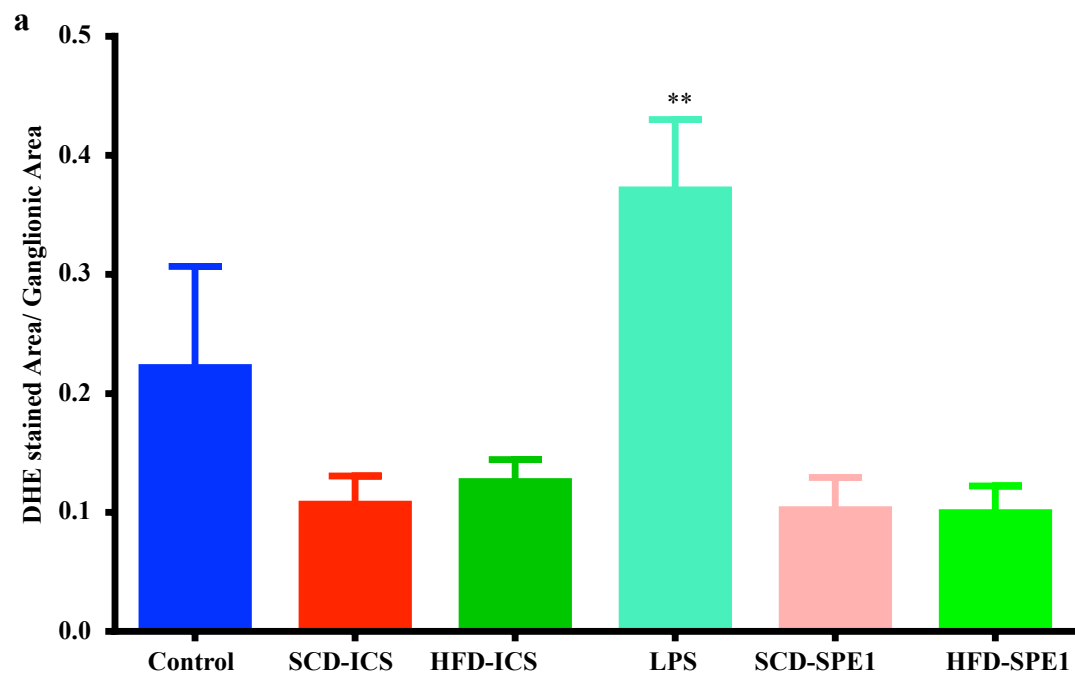


Figure 3-6 Aqueous SPE fractions of HFD-ICS (HFD-SPE1) block muscularis contractions by damaging smooth muscle cells and nNOS neurons, and inhibiting the excitability of SMCs.

Like HFD-ICS, HFD-SPE1 treatment blocked muscularis contractions after 24 hours (a). Also, similar to HFD-ICS, HFD-SPE1 damaged smooth muscle cells, evidenced by SMCs swelling after 6 hours (b, arrows), and reduced the percentage of nNOS neurons out of the total number of myenteric neurons labeled with ANNA1 per ganglionic area after 24 hours (c). Sample images (d) showing overlays of nNOS (red) and ANNA1 (green) staining in duodenum myenteric ganglia of control, SCD-SPE1, HFD-SPE1, SCD-SPE4, and HFD-SPE4 treated samples. Similar to HFD-ICS, HFD-SPE1 depolarized resting membrane potentials in circular CSMs in distal colon muscularis preparations and inhibited the discharge of slow waves and action potentials (e-f, compare with Figs 5c-f).



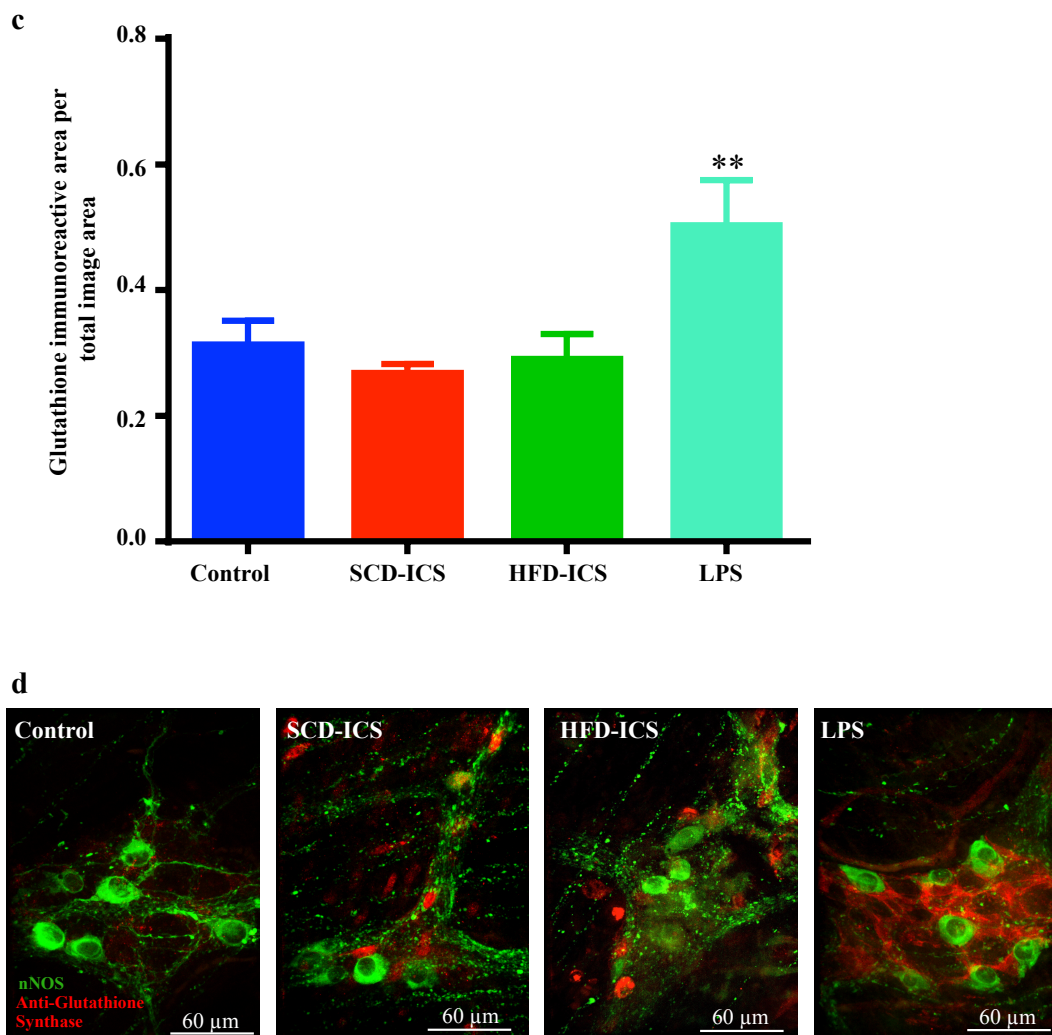
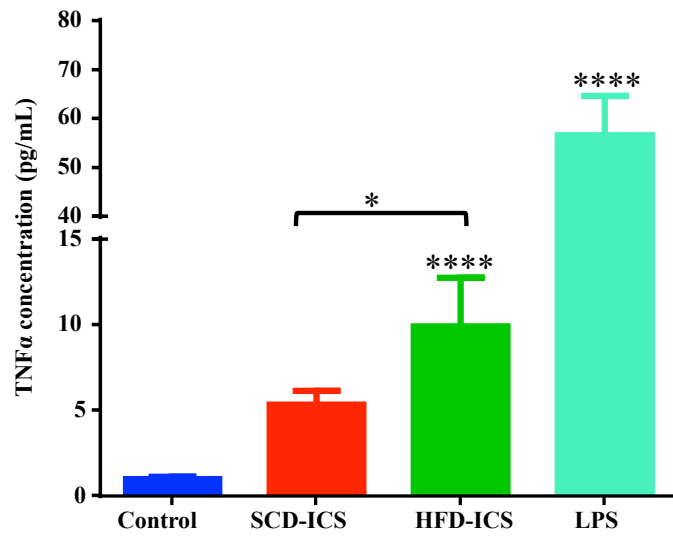
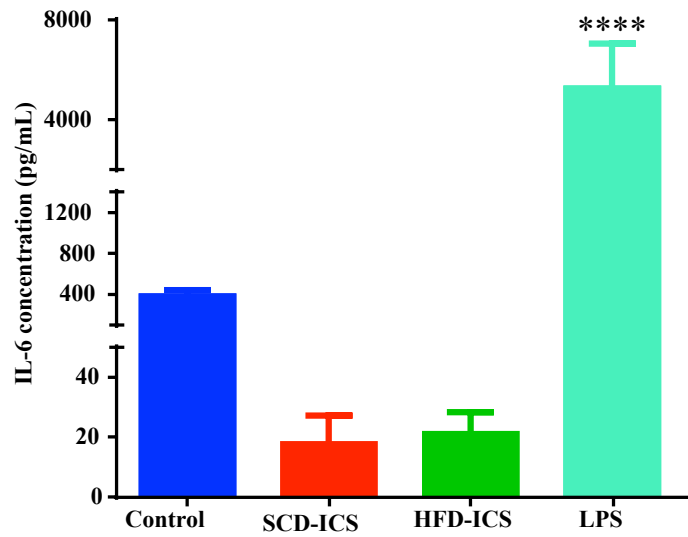


Figure 3-7 HFD-ICS does not induce oxidative stress in myenteric neurons.

HFD-ICS and its aqueous SPE1 fraction did not increase the amount of DHE staining per ganglionic area (a). Sample images (b) showing nNOS (green) and DHE (red fluorescent) staining in duodenal myenteric ganglia of control, SCD-ICS, HFD-ICS, LPS, SCD-SPE1 and HFD-SPE1 treated samples. HFD-ICS did not affect anti-glutathione synthase immunoreactivity per ganglionic area (c). Sample images (d) showing that nNOS neurons (green immunoreactivity) rarely expressed anti-glutathione synthase (red) in duodenal myenteric ganglia of control, SCD-ICS, HFD-ICS, and LPS treated samples. LPS increased DHE and anti-glutathione synthase staining suggesting it caused oxidative stress in myenteric ganglia.

a**b**

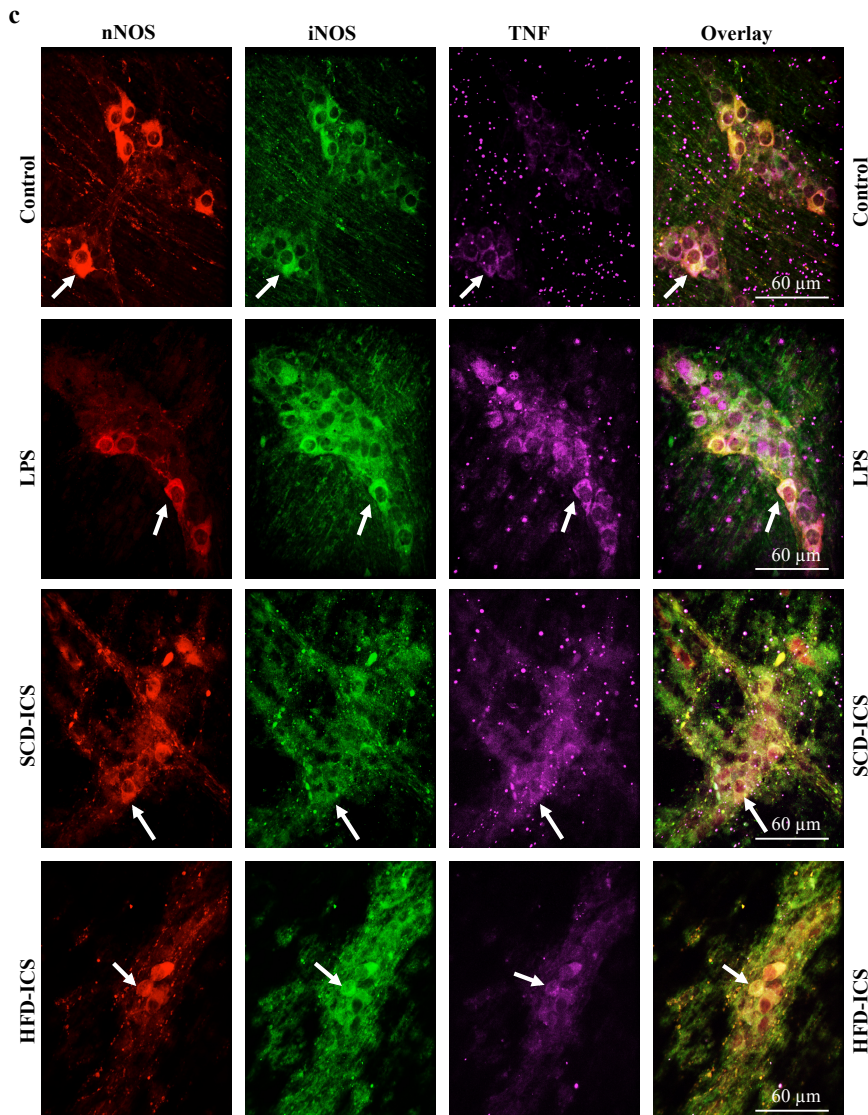


Figure 3-8 HFD-ICS treatment induces the production of TNF α but does not cause nitrosative stress.

After 24 hours of treatment, like LPS, HFD-ICS resulted in higher concentrations of TNF α (a) in culture media but did not affect the concentrations of IL-6 (b). We did not have sufficient amounts of HFD-SPE1 to perform these experiments. Images (c) to demonstrate qualitative analysis of inducible nitric oxide synthase (iNOS, green) and TNF α immunoreactivity (purple) in nNOS neurons (red) in control, SCD-ICS, HFD-ICS and LPS treated samples. Overlays show neurons expressing all markers (white arrows). Similar to LPS treatment, HFD-ICS treatment increased the number of neurons expressing TNF α , but did not appear to increase the number of neurons expressing iNOS. LPS increased both iNOS and TNF α compared to HFD-ICS, SCD-ICS and control samples.

Discussion

The objective of this study was to determine whether ileocecal luminal contents from male and female mice fed a HFD (HFD-ICS) contain molecules that impair intestinal motility by damaging and disrupting ENS neurons and smooth muscle functions. We observed that HFD-ICS contains yet to be identified neurotoxic and antimotility molecules that impair intestinal motility by damaging nitrergic myenteric neurons, disrupting inhibitory neuromuscular transmission, and by damaging smooth muscle cells and inhibiting their excitability. LPS, high glucose levels, and palmitate did not replicate these effects of HFD-ICS. Furthermore, we found that HFD-ICS induced inflammation, which is known to play a role in the cellular mechanisms by which damage to ENS neurons and smooth muscle occurs. Our initial efforts to identify antimotility and neurotoxic molecules from HFD-ICS led us to discover that the aqueous SPE1 fraction of HFD-ICS mimicked the effects of HFD-ICS in blocking muscle contractions. HFD-SPE1 also damaged nitrergic myenteric neurons, and inhibited the excitability of smooth muscle cells, indicating that the neurotoxic and antimotility molecules in HFD-ICS can be isolated, which is the focus of our future studies. Collectively, these results support our hypothesis that unknown antimotility and neurotoxic molecules in intestinal contents are involved in causing HFD-induced and diabetic GI neuropathy and dysmotility, and the view that diabetic ENS neuropathy and dysmotility occur before overt T2D^{14, 15}.

The known causes of ENS neuropathy and dysmotility in type two diabetes (T2D) include hyperglycemia, dyslipidemia, oxidative/nitrosative stress, inflammation, advanced glycation end products, deficiency of neurotrophic factors, and alterations of the gut microbiota^{11,41-43}. However, mounting evidence from recent studies suggests a shift in the theory about the pathophysiology of ENS neuropathy and dysmotility by proposing that dietary saturated fatty acids and endotoxin from gut microbiota trigger ENS neuropathy and dysmotility before hyperglycemia, insulin resistance and overt T2D^{14,15,19,41}. These studies indicate that LPS, palmitate and other saturated fatty acids are the molecules that link diet-gut microbiota-host interactions to obesity, insulin resistance, T2D, and damage to ENS neurons and dysmotility^{14,41}. However, the literature is still not very conclusive about what actually triggers ENS neuropathy and dysmotility in T2D. The results of this study support the view that the triggers of ENS neuropathy and dysmotility arise from gut contents and provide evidence of the existence of unknown soluble neurotoxic and antimotility molecules in ileocecal contents of HFD mice other than LPS, palmitate and glucose^{11,14}. These results arguably suggest that we have not identified all potential neurotoxic and antimotility molecules from intestinal luminal contents for the following reasons: First, even though saturated fatty acids are thought to trigger dysmotility before endotoxemia, hyperglycemia and insulin resistance, their effects appear to be region specific¹⁴ and palmitate did not block muscle contractions in this study. Second, since the

neurotoxic and antimotility molecules in HFD-SPE1 are likely soluble in water, this excludes palmitate and other long-chain saturated fatty acids, leaving LPS and glucose as the likely already known antimotility molecules present in HFD-ICS and HFD-SPE1. However, neither LPS nor glucose blocked muscle contractions in this study despite inducing neuropathy. This highlights a critical gap of knowledge because besides causing motility disorders, ENS neuropathy and smooth muscle dysfunction contribute to the pathogenesis of obesity and T2D by causing alterations of gut microbiota, and disrupting mucosal barrier function, ENS-brain signaling and glucose metabolism^{16,44}. Additionally, although the unknown neurotoxic and antimotility molecules are in ileocecal contents, they affected duodenal and colon myenteric neurons and SMCs in a similar manner, suggesting they can damage neurons and SMCs in any region of the gut and likely other body organs. Since ENS neuropathy and dysmotility are among the earliest GI pathologies, identifying such molecules and their molecular mechanisms of action could reveal new biomarkers and therapeutic targets for GI motility disorders in T2D.

GI motility disorders in obesity and T2D are caused by ENS dysfunction and subsequent aberrant signaling⁴⁵. Furthermore, dysmotility is also associated with thickening and dysfunction of GI smooth muscle in both humans and animal models^{4,7,46}. These pathologies cause decreased contractile force and peristaltic dyscoordination which lead to altered GI transit time^{4,42,45,47}. Our results suggest that antimotility and neurotoxic molecules in HFD-ICS and its HFD-SPE1 are responsible for triggering damage to nitrergic myenteric neurons and SMCs in HFD mice⁷ causing decreased neuromuscular transmission (IJP) and the discharge of slow waves and action potentials. To our knowledge, this is the first study to suggest the presence of antimotility molecules in the intestinal content of HFD mice that disrupt the excitability of SMCs by depolarizing and inhibiting the discharge of slow waves and action potentials. Noteworthy, the inhibition of smooth muscle excitability caused bursting of the action potentials on prolonged slow waves that correspond with migrating motor complexes (MMCs), suggesting that toxic antimotility molecules in HFD-ICS and HFD-SPE1 increased MMCs. This could explain the increased hypercontractility observed in the duodenum of HFD mice^{44,48,49}. Although the cellular mechanisms underlying diabetic GI muscle dysfunction are largely not known, they are thought to include altered smooth muscle excitability, IP₃-mediated Ca²⁺ mobilization, mitochondrial and potassium (K⁺) channel functions, and caveola disarray as a sequel to oxidative stress and inflammation triggered by hyperglycemia and hyperlipidemia^{36,48,50,51}. Future studies will investigate whether HFD-ICS, its HFD-SPE1 and isolated molecules damage and disrupt the excitability of SMCs via these or other mechanisms.

The findings reported here match previous observations in diabetic humans and animal models, indicating that the unknown antimotility and neurotoxic molecules play a crucial role in triggering HFD-induced and diabetic enteric neuropathy and GI dysmotility. These data show that the unknown antimotility and neurotoxic molecules in HFD-ICS, and its HFD-SPE1, damage the ENS and SMCs in the same manner as HFD ingestion in a mouse model of T2D. Furthermore, HFD-ICS and HFD-SPE1 fraction significantly reduced the number of myenteric nNOS neurons and diminished inhibitory neuromuscular transmission similarly to results observed in previous studies in diabetic humans and animal models including HFD mice^{7,13,54}. SMCs damage and disruption of smooth muscle excitability elicited by HFD-ICS and HFD-SPE1 matches observation in HFD mice and reported observations in diabetic humans and animal models^{36,48,50,51}. Therefore, our results strongly suggest that toxic molecules from intestinal contents have a crucial role in the pathophysiology of HFD-induced and diabetic ENS neuropathy and dysmotility. However, more studies are needed to correlate HFD-ICS and its HFD-SPE1-induced ENS injuries with T2D enteric neuropathy and SMCs injuries and to identify neurotoxic and antimotility molecules in HFD-ICS and HFD-SPE1.

In diabetic ENS neuropathy, necrosis and loss of ENS neurons is thought to be caused by oxidative/nitrosative stress and neuroinflammation^{4,51}. Similarly, LPS and hyperglycemia both cause apoptosis of ENS neurons by activating these pathways^{14,38}. The present study showed that culturing muscularis samples in HFD-ICS for 24 hours elicited inflammation without causing oxidative stress (assessed by measuring DHE and anti-GS staining in muscularis preparations). These observations give support to the idea that unknown molecules in HFD-ICS and SPE1 damage myenteric neurons through activation of neuroinflammation. Unlike HFD-ICS, LPS caused both inflammation (elevated TNF α and IL-6 in culture medium) and strong oxidative stress. The fact that HFD-ICS did not affect DHE and GS was unexpected, especially because of the significant loss of nitrergic myenteric neurons and because oxidative stress usually occurs in conjunction with inflammation⁴⁰. These preliminary results must be interpreted cautiously because we cannot confidently rule out the involvement of oxidative/nitrosative stress in the nerve damage induced by toxic molecules in HFD-ICS without analyzing time-dependent effects and high purity isolated molecules. Further studies are therefore necessary to determine the specific mechanisms utilized by HFD-ICS, HFD-SPE1 and the isolated antimotility and neurotoxic molecules to damage ENS neurons. For instance, investigating the role of NF- κ B and Nrf2 pathways, two important pathways that control oxidative stress and inflammation and mediate cellular homeostasis⁴⁰ is necessary.

Previous studies have shown that colonizing the rectum of healthy germ free mice with fecal slurries from conventional mice fed HFD activate inflammation after two weeks even though these germ free mice ingested regular chow diet⁵². In addition, these studies showed that the onset of intestinal inflammation (induction of TNF α) preceded and correlated with the development of insulin resistance and obesity. To some extent, these findings support our assumptions that the production of the antimotility/neurotoxic molecules occur before insulin resistance and suggests that the gut microbiota have a key role in producing these antimotility/neurotoxic molecules. We previously showed that intestinal nerve cell injury and dysmotility occur in female mice fed HFD prior to hyperglycemia, glucose intolerance and insulin resistance¹⁵. In the present study, HFD-ICS from obese male mice presenting with hyperglycemia, glucose intolerance and insulin resistance and HFD-ICS from lean HFD female mice without hyperglycemia, glucose intolerance and insulin resistance blocked muscle contractions by damaging and disrupting ENS and smooth muscle function. The aqueous SPE1 fractions from these supernatants caused a similar pathology. Altogether, these results suggest that likely antimotility and neurotoxic molecules in HFD-ICS and its HFD-SPE1 fraction have key roles in inducing neuropathy and dysmotility before glucose intolerance, insulin resistance and obesity.

Could our findings be implicated in the pathophysiology of other intestinal neurodegenerative and smooth muscle illnesses linked to alterations of gut microbiota, mucosal barrier dysfunction, and GI inflammation? HFD ingestion causes alterations of the gut microbiota, intestinal inflammation, disrupted mucosal barrier function and LPS endotoxemia¹⁶. It also results in increased GI transit, and damage to enteric neurons^{10,14,15}. Intestinal permeability is increased in obese and diabetic patients and promotes an abnormal passage of luminal substances into the intestinal wall^{53,54}. Alterations of the gut microbiota is also linked to the production of toxic molecules causing decreased colonic muscle contractility in irritable bowel disease⁵⁵ and visceral hypersensitivity in colicky infants⁵⁶. Furthermore, there is an increasing number of studies providing evidence to link CNS neurologic diseases, notably autism spectrum disorder, Parkinson's disease, and Alzheimer's disease to alterations of the gut microbiota and GI dysfunctions^{57,58}. Patients with autism spectrum disorder, Parkinson's disease and Alzheimer's disease also display intestinal dysmotility and enteric neuropathy, dysbiosis, intestinal inflammation, disrupted mucosal barrier function and neuroinflammation^{57,59,60}. However, toxic molecules from the GI lumen are largely unknown. It is likely that neurotoxic and antimotility molecules in HFD-ICS and HFD-SPE1 can cross the disrupted mucosal barrier and injure cells in the GI wall and other body organs. However, whether this the case in other GI disorders or CNS neurologic diseases remain to be determined. Therefore, future studies to identify toxic molecules from HFD-ICS and HFD-SPE1 are crucial.

The data from this study strongly suggests that HFD ingestion results in the production of unknown antimotility and neurotoxic molecules in the gut. These molecules, likely produced before hyperglycemia and insulin resistance, trigger dysmotility, enteric neuropathy, SMCs injury and inflammation before the onset of diabetic symptoms. Additional studies to identify the specific molecule(s) by the combination of metabolomics and bioactivity assays are therefore needed. These studies also warrant *in vivo* studies in healthy mice and a parallel translational analysis in obese and diabetic humans. Altogether, these findings highlight the significance of identifying specific neurotoxic and antimotility molecules in ileocecal contents of HFD mice due to their potential essential role in GI motility disorders, diabetes and other diseases associated with injury to neurons or smooth muscle.

Literature Cited

1. Guariguata, L. *et al.* Global estimates of diabetes prevalence for 2013 and projections for 2035. *Diabetes Res. Clin. Pract.* **103**, 137–149 (2014).
2. Singh, R., Kishore, L. & Kaur, N. Diabetic peripheral neuropathy: Current perspective and future directions. *Pharmacological Research* **80**, 21–35 (2014).
3. Smyth, S. & Heron, A. Diabetes and obesity: the twin epidemics. *Nat. Med.* **12**, 75–80 (2006).
4. Yarandi, S. S. & Srinivasan, S. Diabetic gastrointestinal motility disorders and the role of enteric nervous system: current status and future directions. *Neurogastroenterol. Motil.* **26**, 611–24 (2014).
5. Feldman, M. & Schiller, L. R. Disorders of gastrointestinal motility associated with diabetes mellitus. *Ann. Intern. Med.* **98**, 378–84 (1983).
6. Krishnan, B., Babu, S., Walker, J., Walker, A. B. & Pappachan, J. M. Gastrointestinal complications of diabetes mellitus. *World J. Diabetes* **4**, 51 (2013).
7. Bhattarai, Y. *et al.* High-fat diet-induced obesity alters nitric oxide-mediated neuromuscular transmission and smooth muscle excitability in the mouse distal colon. *Am. J. Physiol. Liver Physiol.* **311**, G210–G220 (2016).
8. Furness, J. B. The enteric nervous system and neurogastroenterology. *Nat. Rev. Gastroenterol. Hepatol.* **9**, 286–94 (2012).
9. Hansen, M. B. The Enteric Nervous System I: Organisation and Classification. *Pharmacol. Toxicol.* **92**, 105–113 (2003).
10. Stenkamp-Strahm, C. M., Kappmeyer, A. J., Schmalz, J. T., Gericke, M. & Balemba, O. High-fat diet ingestion correlates with neuropathy in the duodenum myenteric plexus of obese mice with symptoms of type 2 diabetes. *Cell Tissue Res.* **354**, 381–94 (2013).
11. Anitha, M. *et al.* GDNF rescues hyperglycemia-induced diabetic enteric neuropathy through activation of the PI3K/Akt pathway. *J. Clin. Invest.* **116**, 344–356 (2006).
12. Vincent, A. M., Russell, J. W., Low, P. & Feldman, E. L. Oxidative stress in the pathogenesis of diabetic neuropathy. *Endocr. Rev.* **25**, 612–28 (2004).

13. Bagyánszki, M. & Bódi, N. Diabetes-related alterations in the enteric nervous system and its microenvironment. *World J. Diabetes* **3**, 80–93 (2012).
14. Reichardt, F. *et al.* Western diet induces colonic nitrenergic myenteric neuropathy and dysmotility in mice via saturated fatty acid- and lipopolysaccharide-induced TLR4 signalling. *J. Physiol.* **595**, 1831–1846 (2017).
15. Nyavor, Y. *et al.* Intestinal nerve cell injury occurs prior to insulin resistance in female mice ingesting a high-fat diet. *Cell Tissue Res.* **376**, 325–340 (2019).
16. Cani, P. D. *et al.* Metabolic endotoxemia initiates obesity and insulin resistance. *Diabetes* **56**, 1761–72 (2007).
17. Voss, U., Sand, E., Olde, B. & Ekblad, E. Enteric Neuropathy Can Be Induced by High Fat Diet In Vivo and Palmitic Acid Exposure In Vitro. *PLoS One* **8**, e81413 (2013).
18. Aziz, Q., Doré, J., Emmanuel, A., Guarner, F. & Quigley, E. M. M. Gut microbiota and gastrointestinal health: current concepts and future directions. *Neurogastroenterol. Motil.* **25**, 4–15 (2013).
19. Nyavor, Y. E. A. & Balemba, O. B. Diet-induced dysmotility and neuropathy in the gut precedes endotoxaemia and metabolic syndrome: the chicken and the egg revisited. *J. Physiol.* **595**, 1441–1442 (2017).
20. Sender, R., Fuchs, S. & Milo, R. Revised Estimates for the Number of Human and Bacteria Cells in the Body. *PLOS Biol.* **14**, e1002533 (2016).
21. Skelly, A. N., Sato, Y., Kearney, S. & Honda, K. Mining the microbiota for microbial and metabolite-based immunotherapies. *Nat. Rev. Immunol.* **19**, 305–323 (2019).
22. Turnbaugh, P. J. *et al.* An obesity-associated gut microbiome with increased capacity for energy harvest. *Nature* **444**, 1027–31 (2006).
23. Qin, J. *et al.* A metagenome-wide association study of gut microbiota in type 2 diabetes. *Nature* **490**, 55–60 (2012).
24. Nicholson, J. K. *et al.* Host-gut microbiota metabolic interactions. *Science* **336**, 1262–7 (2012).
25. Flint, H. J., Scott, K. P., Louis, P. & Duncan, S. H. The role of the gut microbiota in nutrition and health. *Nat. Rev. Gastroenterol. Hepatol.* **9**, 577–589 (2012).

26. Kashyap, P. C. *et al.* Complex interactions among diet, gastrointestinal transit, and gut microbiota in humanized mice. *Gastroenterology* **144**, 967–77 (2013).
27. Collins, J., Borojevic, R., Verdu, E. F., Huizinga, J. D. & Ratcliffe, E. M. Intestinal microbiota influence the early postnatal development of the enteric nervous system. *Neurogastroenterol. Motil.* **26**, 98–107 (2014).
28. Quigley, E. M. M. Microflora Modulation of Motility. *J. Neurogastroenterol. Motil.* **17**, 140–147 (2011).
29. Manichanh, C., Borruel, N., Casellas, F. & Guarner, F. The gut microbiota in IBD. *Nat. Rev. Gastroenterol. Hepatol.* **9**, 599–608 (2012).
30. Jahng, J., Jung, I. S., Choi, E. J., Conklin, J. L. & Park, H. The effects of methane and hydrogen gases produced by enteric bacteria on ileal motility and colonic transit time. *Neurogastroenterol. Motil.* **24**, 185–90, e92 (2012).
31. Hurst, N. R., Kendig, D. M., Murthy, K. S. & Grider, J. R. The short chain fatty acids, butyrate and propionate, have differential effects on the motility of the guinea pig colon. *Neurogastroenterol. Motil.* **26**, 1586–96 (2014).
32. Mao, Y.-K. *et al.* Bacteroides fragilis polysaccharide A is necessary and sufficient for acute activation of intestinal sensory neurons. *Nat. Commun.* **4**, 1465 (2013).
33. Islam, M. S. Animal models of diabetic neuropathy: progress since 1960s. *J. Diabetes Res.* **2013**, 149452 (2013).
34. Everard, A. *et al.* Microbiome of prebiotic-treated mice reveals novel targets involved in host response during obesity. *ISME J.* **8**, 2116–2130 (2014).
35. Qu, Z.-D. *et al.* Immunohistochemical analysis of neuron types in the mouse small intestine. *Cell Tissue Res.* **334**, 147–61 (2008).
36. France, M., Bhattarai, Y., Galligan, J. J. & Xu, H. Impaired propulsive motility in the distal but not proximal colon of BK channel β 1-subunit knockout mice. *Neurogastroenterol. Motil.* **24**, e450-9 (2012).
37. Brown, I. A. M., McClain, J. L., Watson, R. E., Patel, B. A. & Gulbransen, B. D. Enteric Glia Mediate Neuron Death in Colitis Through Purinergic Pathways That Require Connexin-43 and Nitric Oxide. *Cell. Mol. Gastroenterol. Hepatol.* **2**, 77–91 (2016).

38. Chandrasekharan, B. *et al.* Colonic motor dysfunction in human diabetes is associated with enteric neuronal loss and increased oxidative stress. *Neurogastroenterol. Motil.* **23**, 131-e26 (2011).
39. Brown, I. A. M. & Gulbransen, B. D. The antioxidant glutathione protects against enteric neuron death in situ, but its depletion is protective during colitis. *Am. J. Physiol. Liver Physiol.* **314**, G39–G52 (2018).
40. Sandireddy, R., Yerra, V. G., Areti, A., Komirishetty, P. & Kumar, A. Neuroinflammation and oxidative stress in diabetic neuropathy: futuristic strategies based on these targets. *Int. J. Endocrinol.* **2014**, 674987 (2014).
41. Anitha, M. *et al.* Intestinal Dysbiosis Contributes to the Delayed Gastrointestinal Transit in High-Fat Diet Fed Mice. *Cell. Mol. Gastroenterol. Hepatol.* **2**, 328–339 (2016).
42. Gotfried, J., Priest, S. & Schey, R. Diabetes and the Small Intestine. *Curr. Treat. Options Gastroenterol.* **15**, 490–507 (2017).
43. Abrahamsson, H. Gastrointestinal motility disorders in patients with diabetes mellitus. *J. Intern. Med.* **237**, 403–9 (1995).
44. Fournel, A. *et al.* Apelin targets gut contraction to control glucose metabolism via the brain. *Gut* **66**, 258–269 (2017).
45. Ohlsson, B. *et al.* Oesophageal dysmotility, delayed gastric emptying and autonomic neuropathy correlate to disturbed glucose homeostasis. *Diabetologia* **49**, 2010–2014 (2006).
46. Farrugia, G. Histologic changes in diabetic gastroparesis. *Gastroenterol. Clin. North Am.* **44**, 31–8 (2015).
47. Horváth, V. J. *et al.* Diabetes-Related Dysfunction of the Small Intestine and the Colon: Focus on Motility. *Curr. Diab. Rep.* **15**, 94 (2015).
48. Chandrasekharan, B. & Srinivasan, S. Diabetes and the enteric nervous system. *Neurogastroenterol. Motil.* **19**, 951–60 (2007).
49. Abot, A. *et al.* Galanin enhances systemic glucose metabolism through enteric Nitric Oxide Synthase-expressed neurons. *Mol. Metab.* **10**, 100–108 (2018).
50. Galligan, J. J. Mechanisms of excitatory synaptic transmission in the enteric nervous system. *Tokai J. Exp. Clin. Med.* **23**, 129–36 (1998).

51. Giacco, F. & Brownlee, M. Oxidative Stress and Diabetic Complications. *Circ. Res.* **107**, 1058–1070 (2010).
52. Ding, S. *et al.* High-Fat Diet: Bacteria Interactions Promote Intestinal Inflammation Which Precedes and Correlates with Obesity and Insulin Resistance in Mouse. *PLoS One* **5**, e12191 (2010).
53. Jayashree, B. *et al.* Increased circulatory levels of lipopolysaccharide (LPS) and zonulin signify novel biomarkers of proinflammation in patients with type 2 diabetes. *Mol. Cell. Biochem.* **388**, 203–210 (2014).
54. Cani, P. D. *et al.* Changes in gut microbiota control metabolic endotoxemia-induced inflammation in high-fat diet-induced obesity and diabetes in mice. *Diabetes* **57**, 1470–81 (2008).
55. Guarino, M. P. *et al.* Supernatants of irritable bowel syndrome mucosal biopsies impair human colonic smooth muscle contractility. *Neurogastroenterol. Motil.* **29**, 1–9 (2017).
56. Eutamène, H. *et al.* Luminal contents from the gut of colicky infants induce visceral hypersensitivity in mice. *Neurogastroenterol. Motil.* **29**, e12994 (2017).
57. Roy Sarkar, S. & Banerjee, S. Gut microbiota in neurodegenerative disorders. *Journal of Neuroimmunology* **328**, 98–104 (2019).
58. Jolanta Wasilewska, J. & Klukowski, M. Gastrointestinal symptoms and autism spectrum disorder: links and risks – a possible new overlap syndrome. *Pediatr. Heal. Med. Ther.* **153** (2015).
59. Cersosimo, M. G. & Benarroch, E. E. Pathological correlates of gastrointestinal dysfunction in Parkinson's disease. *Neurobiol. Dis.* **46**, 559–564 (2012).
60. Chalazonitis, A. & Rao, M. Enteric nervous system manifestations of neurodegenerative disease. *Brain Research* **1693**, 207–213 (2018).
61. Stark, T. & Hofmann, T. Isolation, Structure Determination, Synthesis, and Sensory Activity of N -Phenylpropenoyl- l -amino Acids from Cocoa (*Theobroma cacao*). *J. Agric. Food Chem.* **53**, 5419–5428 (2005).
62. Benov, L., Szejnberg, L. & Fridovich, I. Critical evaluation of the use of hydroethidine as a measure of superoxide anion radical. *Free Radic. Biol. Med.* **25**, 826–831 (1998).

Chapter 4: High fat diet-induced alterations to gut microbiota and gut-derived lipoteichoic acid contributes to the development of enteric neuropathy

Abstract

High-fat diet, microbiota alterations and lipopolysaccharide (LPS) are thought to cause enteric diabetic neuropathy and intestinal dysmotility. However, the role of the gut microbiota, lipoteichoic acid (LTA) from Gram-positive bacteria and short chain fatty acids (SCFAs) in the development of diabetic enteric neuropathy and intestinal dysmotility is not well understood. The aim of this study was to examine the role of the gut microbiota, LTA and SCFAs in the development of diabetic enteric neuropathy and intestinal dysmotility. We fed germ free (GF) and conventionally raised (CR) mice either a high-fat diet (HFD) or standard chow diet (SCD) for 8 weeks. We then analyzed the microbial community composition in cecum of CR mice using 16S rRNA sequencing and damage to myenteric neurons using immunohistochemistry. We also studied the effects of LPS, LTA, and SCFAs on duodenal muscularis contractions and myenteric neurons using cultured preparations. HFD ingestion reduced the total number and the number of nitrergic myenteric neurons per ganglion in the duodenum of CR but not in GF-HFD mice. GF mice had fewer neurons per myenteric ganglion compared to CR mice. CR mice fed a HFD had increased abundance of Gram-positive bacteria. LTA and LPS did not affect the frequency of duodenal muscularis contractions after 24 hours of culture but reduced the density of nitrergic myenteric neurons, and increased oxidative stress and TNF α production in myenteric ganglia. SCFAs did not affect muscularis contractions or injure myenteric neurons. Gut microbial alterations leading to increased Gram-positive bacterial LTA levels may cause enteric neuropathy.

Introduction

Over 70% of diabetic patients suffer from gastrointestinal (GI) motility disorders including dysphagia, gastroparesis, constipation, diarrhea, incontinence and pain^{1,2}. Enteric nervous system (ENS) neuropathy, characterized by loss of nitrergic neurons expressing neuronal nitric oxide synthase (nNOS) and vasoactive intestinal peptide neurons (VIP) in the myenteric plexus¹ is a major contributing factor to these diabetic GI motility-related disorders.

Enteric neuropathy in diabetes is has been linked to alteration of the gut microbiota^{3,4}.

Lipopolysaccharide (LPS), the cell wall component of Gram-negative bacteria is thought to be the microbial mediator that causes ENS neuropathy⁴. Additionally, it was recently shown that LPS and

dietary palmitate act synergistically to cause myenteric neuron loss³. These observations suggest that interaction between diet, gut microbes and the host have a crucial role in the pathophysiology of GI diabetic neuropathy and motility disorders^{3,5}.

Diet has a significant impact on the gut microbiota composition and function⁶. High fat diet (HFD) consumption is associated with potentially deleterious alterations in gut microbiota⁷⁻⁹, decreased fecal concentrations of SCFAs^{10,11}, type two diabetes (T2D) symptoms of hyperglycemia and insulin resistance^{9,12}, enteric neuropathy¹², and intestinal dysmotility in human and animal models of T2D³⁻⁵. All these conditions are commonly observed in T2D patients¹³. Gut microbiota alterations in T2D humans and mice is often characterized by a significant increase in the abundance of Firmicutes, a phylum comprised mostly of Gram-positive bacteria, and a decrease in Bacteroidetes, comprised of Gram-negative bacteria^{9,14}. This observation correlates with the increased presence of Gram-positive gut bacteria in the blood of T2D patients¹⁵, and likely increases the intestinal and circulating levels of Gram-positive bacterial cell wall component, lipoteichoic acid (LTA). It has been shown that LTA binds to TLR-2 receptors¹⁶ and induces neuronal damage in cultured rat cerebellum cells through oxidative- stress dependent mechanisms^{17,18}. LTA also enhances IL-6 expression in various cells¹⁹, and could have a role in increasing IL-6 levels observed in mice fed HFD⁹ and T2D patients²⁰. Apart from LPS and LTA, gut microbes also influence host health by producing short chain fatty acids (SCFAs) derived from fermenting indigestible carbohydrates and proteins²¹. Although increased concentrations of SCFAs may be involved in reducing obesity and inflammation, and increasing insulin sensitivity^{22,23}, there is evidence suggesting that butyrate damages nitrergic myenteric neurons, *ex vivo*²⁴. Despite all of the observations above, most studies of enteric neuropathy and dysmotility have focused primarily on LPS^{3,4}, leaving a knowledge gap regarding the role of LTA and SCFAs in the development of GI dysmotility and enteric neuropathy.

We have previously shown that gut microbiota alterations and the development of enteric neuropathy and GI dysmotility occur before the onset of diabetic conditions in female C57BL6 mice fed HFD for 8 weeks⁹. We have also showed that ileocecal contents from HFD fed mice damage nitrergic myenteric neurons and inhibit intestinal motility by blocking muscularis contractions²⁵. The aim of this study was to determine how HFD induced gut microbiota alterations impacts the development of enteric neuropathy. We also sought to determine whether LTA from Gram-positive bacteria and SCFAs contribute to GI dysmotility by damaging enteric neurons and disrupting muscle contractions.

Methods and Materials

Mice

The institutional Animal Care and Use Committee approved all animal studies. All gnotobiotic mouse experiments were done in the Mayo Clinic germ free mouse facility. Seven weeks old male Swiss Webster germ free (GF) mice were fed either a HFD^{26,27} (n=5, containing 60% kcal fat diet; Research Diets, D10011202), or standard chow diet (SCD, n=5, containing 6% kcal fat diet) for 8 weeks in GF isolators. Duodenal tissues were collected post euthanasia at the end of the experiment. The University of Idaho Animal Care and Use Committee approved the study protocols for conventionally raised (CR) mice. Six to seven weeks old C57Bl/6J male mice were purchased from Jackson Laboratories (Bar Harbor, ME) and housed in the Laboratory Animal Research Facility. At 8 weeks, mice were separated into two groups and fed either a SCD composed of 6.2% fat (n=8, 6% kcal fat diet; Teklad Global 2018, Teklad Diets, Madison WI) or a HFD containing 72% fat (n=8, 70% kcal fat diet with 2% additional corn oil; TestDiet, Richmond, IN) *ad libitum* for 8 weeks. Mice were euthanized by exsanguination under deep isoflurane anesthesia. The cecal contents were collected and immediately frozen at -80°C for microbial community profiling. For experiments with dihydroethidium (DHE), we used samples from eight to ten weeks old first generation (F1, n=8) GCaMP6f mice obtained by crossing female B6J.Cg-Gt (ROSA) 26Sortm95.1(CAG-GCaMP6f) Hze/MwarJ (Stock# 028865) mice with male B6.129-Nos1^{tm1}(cre)Mgmj>/J (Stock# 017526). These mice were fed SCD only.

16S rRNA analysis of the gut microbiota and taxonomic assignment of reads

Genomic DNA was extracted from cecal contents using enzymatic and mechanical lysis as previously described²⁷. The variable V1-V3 regions of bacterial 16S rRNA genes were amplified and sequenced as previously described⁹. Hierarchical clustering and principal components analysis (PCoA)²⁸ were used to assess similarities and differences in bacterial community composition across conventional SCD and HFD mice with MicrobiomeAnalyst (<https://www.microbiomeanalyst.ca/>) and custom R code.

Identifying the effects of LTA and SCFAs on muscle contractions using cultured muscularis

Twelve week-old C57Bl/6J mice were purchased from Jackson Laboratories (Bar Harbor, ME), and housed in the Laboratory Research Animal Facility for a week. Mice were euthanized and the duodenum and upper jejunum was removed and placed immediately in ice cold Hepes buffer supplemented with 2% Penicillin-Streptomycin (Sigma, St. Louis, MO, USA). The samples were then pin-stretched in Sylgard lined petri dishes and opened along the mesenteric border. After multiple washes in Hepes Buffer with 2% Penicillin-Streptomycin, samples were pin stretched mucosa up and

dissected with fine forceps to obtain the muscularis externa (muscularis). Approximately 1cm long pieces of muscularis were then cultured in Neurobasal A medium (Thermofisher, Waltham, MA, USA) supplemented with the serum substitute B27 according to manufacturer's instructions (Thermofisher, Waltham, MA, USA). Tissues were cultured in 24 well plates for 24 hours in a tissue culture incubator at a temperature of 37°C, relative humidity of 95% and CO₂ concentration of 5%. 30-second long videos were recorded with a camera equipped Nikon light microscope using the 5x objective lens to determine the effect of test molecules on muscle contractions. All test molecules were solubilized in culture media and filter sterilized before use at the following concentrations: 0.5ng/ml LPS (L4391), 0.5ng/ml LTA (L4391), 30mM sodium acetate (P9767), 30mM sodium propionate (P9767), and 30mM sodium butyrate (P9767) (all from Sigma, St. Louis, MO, USA). Samples were videotaped after 1 hour of equilibration and before test molecules were added (Time 0) and 24 hours later. Videos were analyzed in a blinded fashion by counting the number of contractions that occurred during 30 seconds. The samples were then fixed and stained to assess neuronal health as described below.

Immunohistochemistry analysis of nerve cell damage

After filming tissues for measuring the rates of contractions, tissues were fixed overnight in 4% paraformaldehyde with 0.2% picric acid and dissected as previously described²⁹. Immunohistochemistry staining for neuronal nitric oxide synthase (nNOS, 1:300, Abcam, Cambridge, MA) and vasoactive intestinal peptide (VIP, 1:1000, Abcam, Cambridge, MA) to localize myenteric inhibitory motor neurons was performed as previously described¹¹. Total neuron population analysis was completed using an antibody for anti-neuronal nuclear antibody 1 (ANNA1 positive human serum, 1:20,000, kind gift from Dr. Vanda A. Lennon, Mayo Clinic). Tissue inflammation was evaluated by staining with an antibody to TNF α (TNF α , 1:500, Abcam, Cambridge, MA). Increased antioxidant production in tissue was evaluated with an antibody to anti-glutathione synthase (GS, 1:200, Abcam, Cambridge, MA). Nitrosative stress was measured by staining with an antibody to inducible nitric oxide synthase (iNOS, 1:500, Abcam, Cambridge, MA). We used Donkey anti-rabbit 594 or 488 and donkey anti-human 488 secondary antibodies (Jackson ImmunoResearch, West Grove, PA), both at 1:300, to label nNOS, iNOS, GS and ANNA1, respectively. Tissues were mounted on objective slides using VectaShield Mounting Medium (Vector Labs, Burlingame, CA).

Dihydroethidium Staining

Superoxide levels were measured by quantifying fluorescence of the superoxide marker dihydroethidium (DHE)³⁰ as previously described³¹. Briefly, LMMP whole mount preparations were incubated with 2 μ M DHE (Life Technologies, Carlsbad, CA) dissolved in DMEM at 37°C for 1

hour. Fluorescence levels were quantified in live ganglia after mounting samples and capturing 15 to 20 random fields of view with a 40x objective lens and a wide field camera on a Nikon/Andor Spinning disk microscope (Nikon, Melville, NY) and analyzed with Nikon NIS Elements software using similar methods as previously described¹¹.

Quantification of number of neurons and density indices

Tissues were photographed using a wide field camera on a Nikon/Andor Spinning disk microscope with a 40x objective lens (Nikon, Melville, NY) and analyzed with Nikon NIS Elements software using similar methods as previously described²⁸.

Statistical analysis

Statistical analyses were conducted using GraphPad Prism 5 software (GraphPad Software Inc, La Jolla, CA) unless otherwise indicated. A repeated measure ANOVA with Bonferroni post- hoc test was used to correct for multiple comparisons. Statistical significance was determined at $P < 0.05$. The effects of the test molecules on muscle contractions were assessed by calculating the percentage of response compared to basal contractions recorded at time point 0 in the same samples. Data in bar graphs are expressed as mean \pm SEM and analyzed by one-way ANOVA followed by Tukey's post-tests.

Results

The gut microbiota is important in the development of enteric neuropathy

Gut microbiota alterations have been associated with enteric neuropathy, but it is unclear if this is a cause or effect of the neuropathy. In order to test the relevance of gut microbiota in development of diet-related enteric neuropathy⁹, we examined the duodenal myenteric plexus of GF and CR mice fed HFD or SCD for 8 weeks for loss of inhibitory motor neurons in the myenteric ganglia. HFD ingestion decreased the total number of neurons per ganglionic area in CR mice but not GF mice (Fig. 4-1a). In addition, HFD decreased the number of nNOS neurons (Fig. 4-1b), the density of nNOS immunoreactivity (Fig. 4-1c) and percentage of nNOS neurons per total number of neurons (Fig. 4-1d) per ganglionic area in CR mice. In contrast, GF mice fed HFD did not display a decrease in either the number (Fig. 4-1b) or percentage (Fig. 4-1d) of nNOS neurons per ganglionic area. Of note, GF mice fed both SCD and HFD had fewer total numbers of neurons and nitrergic myenteric neurons per ganglion area compared with CR mice (Fig. 4-1a-c). However, GF HFD mice had higher amounts of nNOS immunoreactive varicosities per ganglionic area (Fig. 4-1d). HFD ingestion reduced the VIP

immunoreactivity in CR mice, but not in GF mice (Fig. 4-2a-b). These results suggest that the gut microbiota is important in the high fat diet associated loss of inhibitory neurons.

HFD ingestion increases the population of cecal gram-positive bacteria

We have previously shown that neuropathy in CR mice is associated with shifts in the fecal microbiota that included increased Firmicutes and decreased Bacteroidetes⁹. We sought to determine if HFD fed CR mice exhibit similar changes (Fig. 4-3a). HFD ingestion increased the abundance of Gram-positive Firmicutes in CR mice while decreased Gram-negative Bacteroidetes abundance (Fig. 4-3b). In addition to the phylum level changes we also observed significant changes in specific genera; *Allobaculum* was increased following HFD ingestion while *Lactobacillus* and *Akkermansia* were decreased (Fig. 4-3c). These results match our previous observations using fecal samples where we have shown increased Firmicutes and decreased Bacteroidetes and observed that *Allobaculum* was increased following HFD ingestion while *Lactobacillus* and *Akkermansia* were decreased⁹.

Microbiota derived LPS, LTA and SCFAs do not affect contractions of cultured duodenojejunal muscularis externa

We have previously shown that ileocecal supernatants from CR mice fed a HFD inhibit contractions in duodenum and in cultured duodenal muscularis externa²⁵. Hence we next determined whether LTA, LPS and SCFAs inhibit intestinal smooth muscle contractions using cultured muscularis externa preparations from CR mice fed SCD. After 24 hours of culture, the frequency of contractions of untreated muscularis preparations was unchanged compared to baseline contractions recorded after 1-hour equilibration (0 hour time point; Fig. 4-4a). Treatment with LPS and LTA (Fig. 4-4a) did not affect the frequency of muscle contractions after 24 hours. Similarly, 30 mM concentrations of acetate, propionate and butyrate had no effect on contractions (Fig. 4-5a). These results suggest that these bacterially derived molecules do not affect muscle contractions.

LTA induces enteric neuropathy similar to that elicited by LPS

LPS is known to cause ENS neuron loss and reduce the number of nitrergic myenteric neurons in cultured preparations, which is similar to the neuropathy elicited by HFD and diabetes in animal models and diabetic humans⁴. We next determined whether LTA could also contribute to reduction in the number of myenteric nitrergic neurons in cultured duodenal muscularis preparations. We observed that in muscularis cultured for 24 hours, LPS and LTA decreased the number of nNOS neurons per ganglionic area (Fig. 4-4b) and the percentage of nNOS neurons per total number of neurons per

ganglionic area (Figs. 4-4c-d). These results suggest that similar to HFD ingestion, LPS, and LTA can result in reduction of the number of myenteric nitrergic neurons.

SCFAs do not affect myenteric neurons

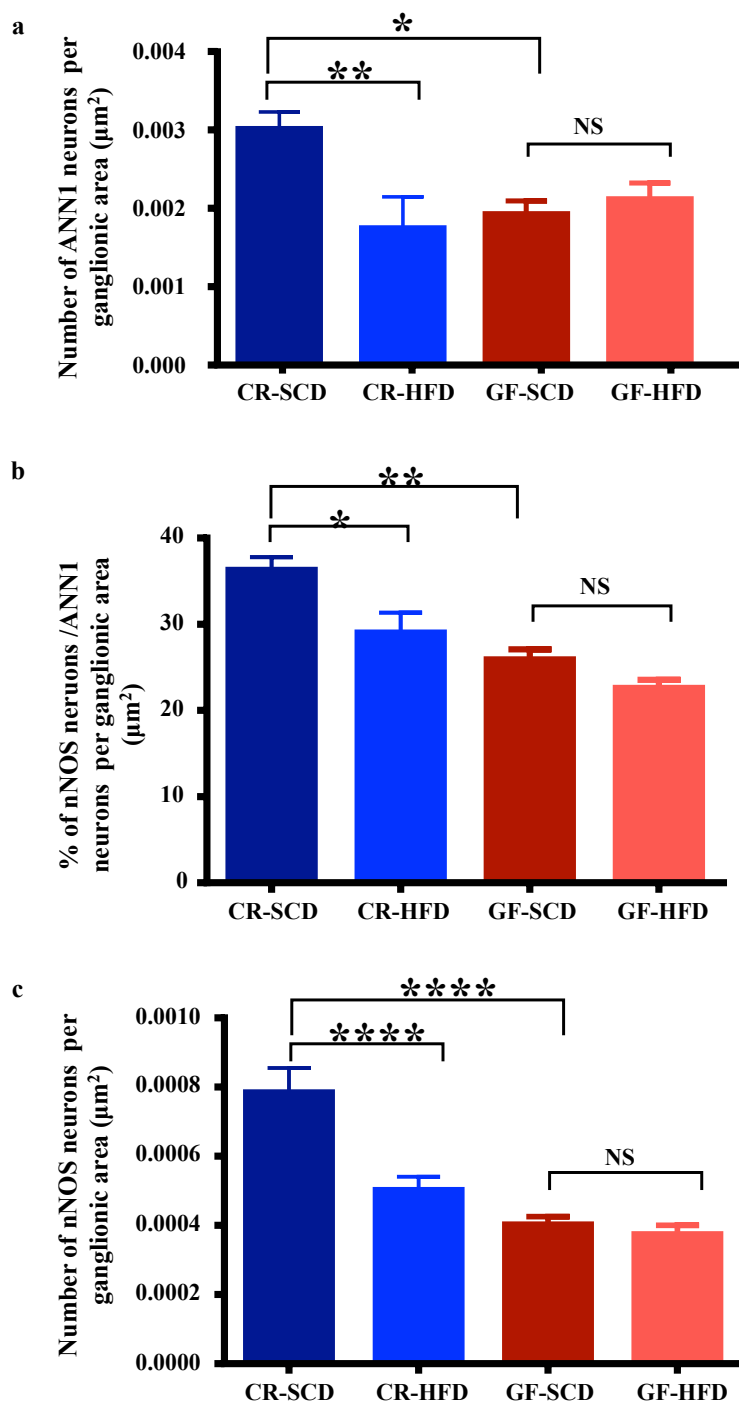
It was previously shown that butyrate decreased the proportion of nNOS neurons in cultured primary rat myenteric neurons from colon²³. We studied whether 30mM acetate, propionate and butyrate affects the number of myenteric nitrergic neurons in cultured duodenojejunal muscularis. We found that compared to untreated controls, 30mM acetate, propionate and butyrate did not affect (Fig. 4-5b-d) myenteric nNOS neuronal population in cultured muscularis preparations.

LTA induces oxidative stress

Previous studies have demonstrated that LPS-induced enteric nerve cell injury results from increased oxidative stress^{4,34}. We therefore hypothesized that; similar to LPS, LTA induced damage to myenteric nitrergic neurons was associated with oxidative stress. To test this idea, duodenojejunal muscularis samples were cultured in LTA or LPS and stained with the superoxide-specific fluorescent indicator dihydroethidium (DHE)^{31,35}. We also stained fixed treated muscularis samples with an anti-glutathione antibody to measure the expression of glutathione, an essential antioxidant produced in response to oxidative stress³⁵. Compared to untreated control samples, the total DHE staining per ganglionic area (Fig. 4-6a) and in the entire field of view (Fig. 4-6b) was increased by LTA and LPS treatment after 12 hours (Figs. 4-6a-c). Additionally, the anti-glutathione staining per ganglionic area (Fig. 4-6d) and the number of anti-glutathione positive cells (Figs. 4-6e-f) were dramatically increased in LTA and LPS treated samples. This suggests that like LPS, LTA causes increased oxidative stress in myenteric ganglia.

LTA triggers nitrosative stress and inflammation

TNF α mediated inflammation leading to oxidative-nitrosative stress is the major pathway through which LPS induced enteric neuropathy occurs³⁴. We therefore determined whether LTA has a similar effect. We examined LTA-induced TNF α -mediated inflammation and nitrosative stress by staining muscularis preparations with antibodies to TNF α and iNOS. Samples treated with LPS and LTA demonstrated more TNF α and iNOS staining (Fig. 4-7) when compared to untreated controls. TNF α and iNOS labeling was observed in nNOS and other types of myenteric neurons in ganglia from samples treated with LPS and LTA. This suggests that similar to LPS, LTA induces damage to enteric neurons through inflammation and nitrosative stress.



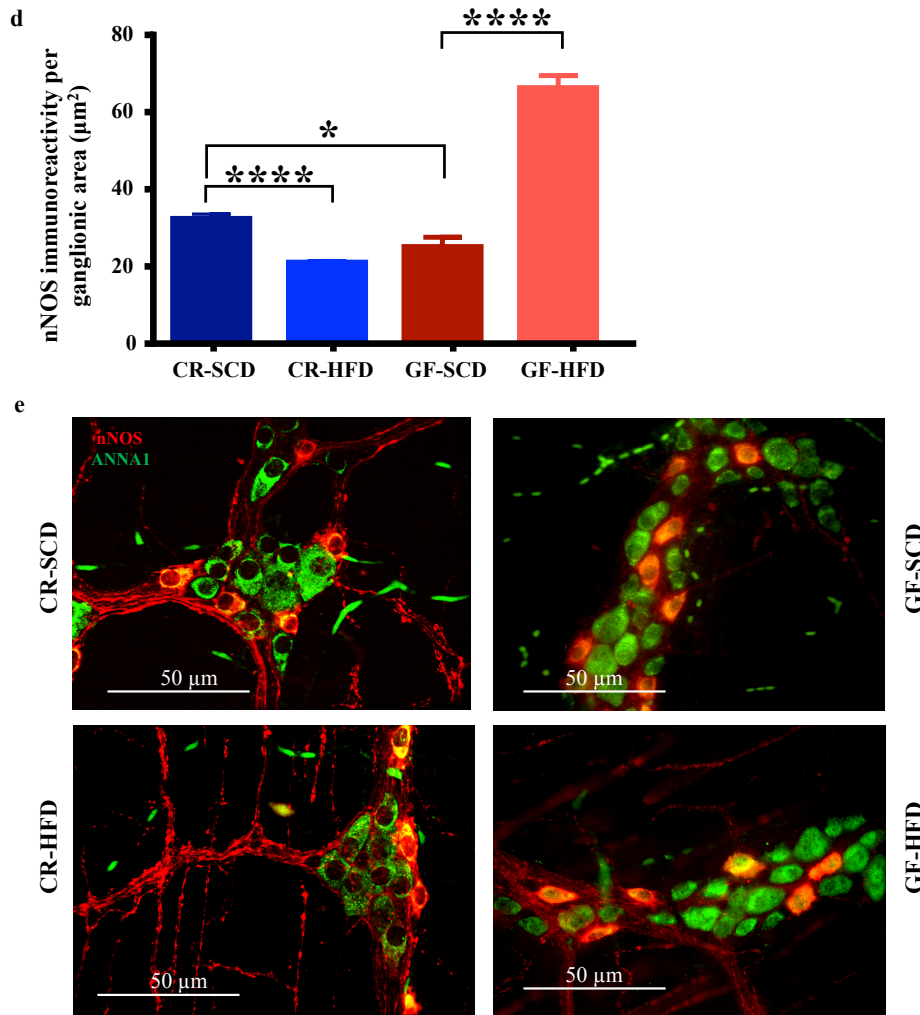


Figure 4-1. The gut microbiota is required for HFD-induced injury to nitrenergic myenteric neurons.

a, HFD reduced the total number of duodenal myenteric neurons in conventionally raised mice (CR) but had no effect myenteric neurons in GF mice after 8 weeks. b, HFD reduced the percentage of nNOS neurons out of the total number of myenteric neurons (labeled with ANNA1) per ganglionic area in CR-HFD mice but it did not affect the percentage of nNOS neurons in GF mice. c-d, HFD reduced the number of nNOS neurons per ganglionic area (c), and the density of nNOS immunoreactive neurons and varicosities per ganglionic area (d) in CR mice. In contrast, HFD did not affect the number of duodenal myenteric nNOS in HFD-GF mice (c), but HFD GF mice had a higher density of nNOS immunoreactivity per ganglion. Noteworthy, GF mice had few total number of neurons and nNOS neurons per ganglion compared to CR mice (a-b). e. Sample images showing overlays of nNOS (red) and ANNA1 (green) staining in duodenal myenteric ganglia of CR-SCD, CR-HFD, GF-SCD and GF-HFD mice. Data are expressed as mean \pm SEM and were analyzed by one-way analysis of variance followed by Tukey's post-tests in all figures. Here and here after, number of animals for experiments were $n=5-10$ per group. Symbols denoting statistical significance are: ns = $P > 0.05$; * P shows $P \leq 0.05$; ** P shows $P \leq 0.01$; *** P shows $P \leq 0.001$, while **** P , shows P value ≤ 0.0001 .

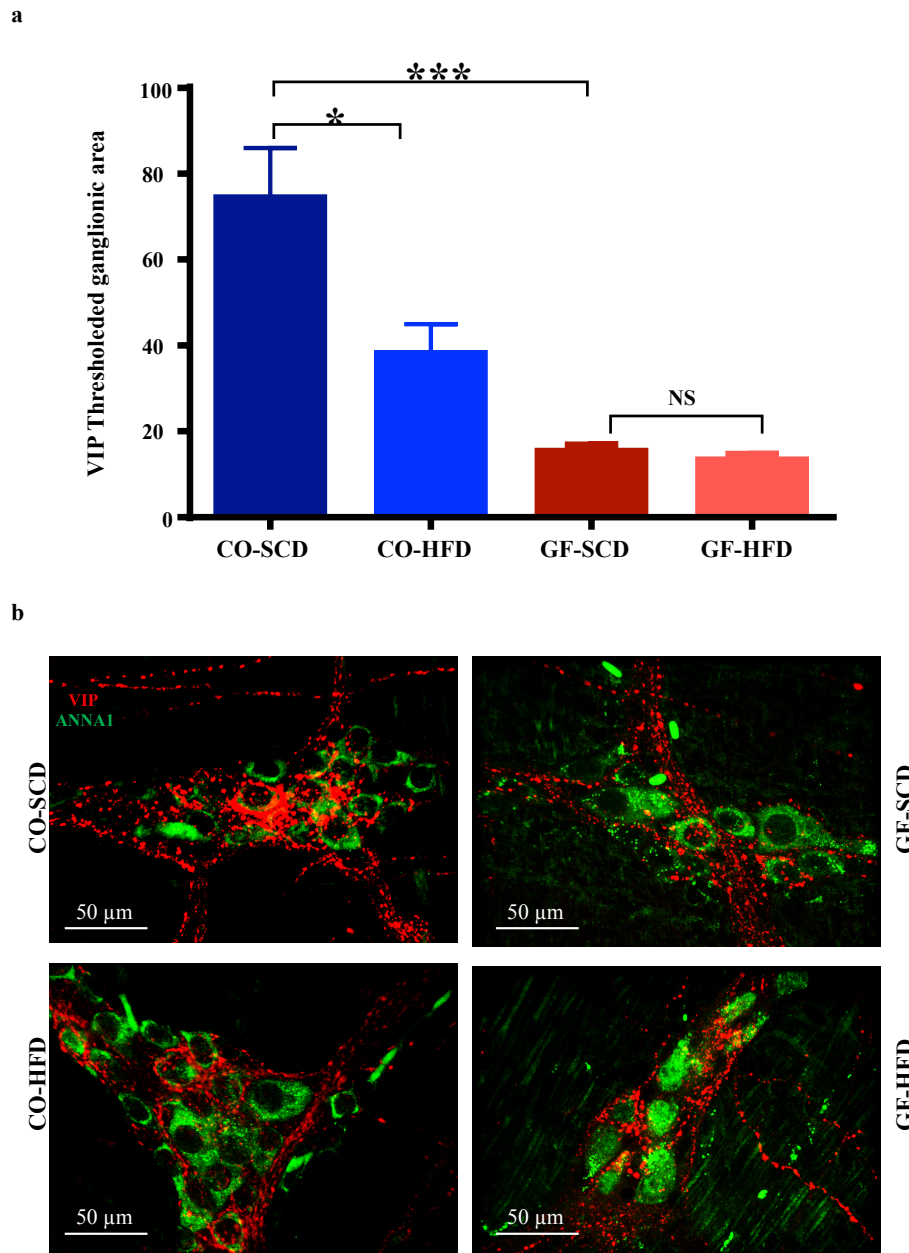
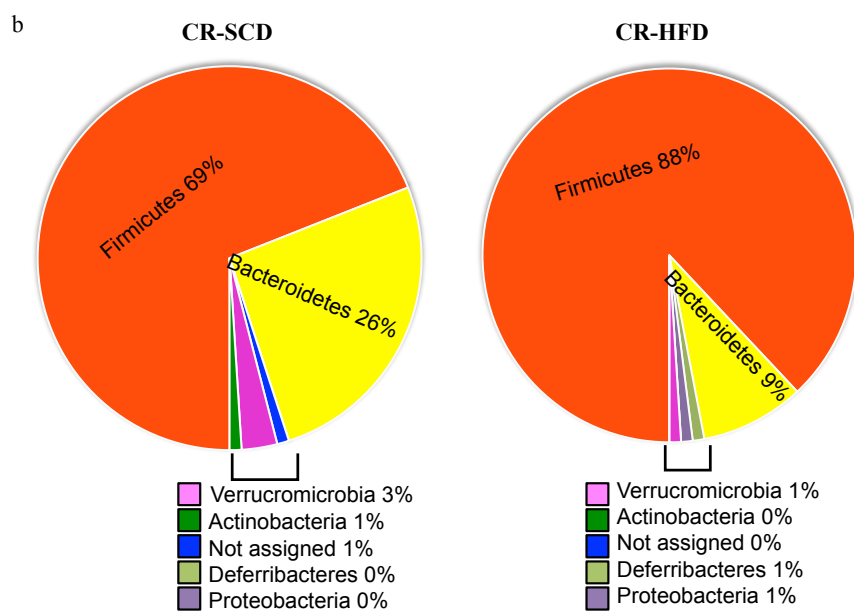
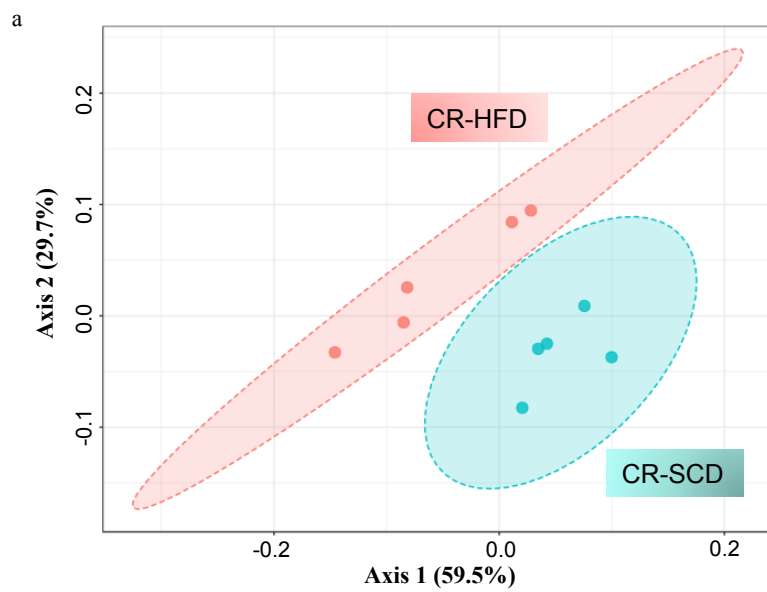


Figure 4-2 The microbiota is necessary for HFD-induced injury to myenteric VIP neurons in mouse duodenum.

a, In the duodenum of GF mice, HFD did not affect myenteric VIP immunoreactivity, but the VIP immunoreactivity was reduced in CR-HFD mice. GF-SCD mice had lower VIP immunoreactivity in duodenum myenteric plexus when compared to CR-SCD mice. b, Sample images showing overlays of VIP (red) and ANNA1 (green) staining in duodenal myenteric ganglia of CR-SCD, CR-HFD, GF-SCD and GF-HFD mice.



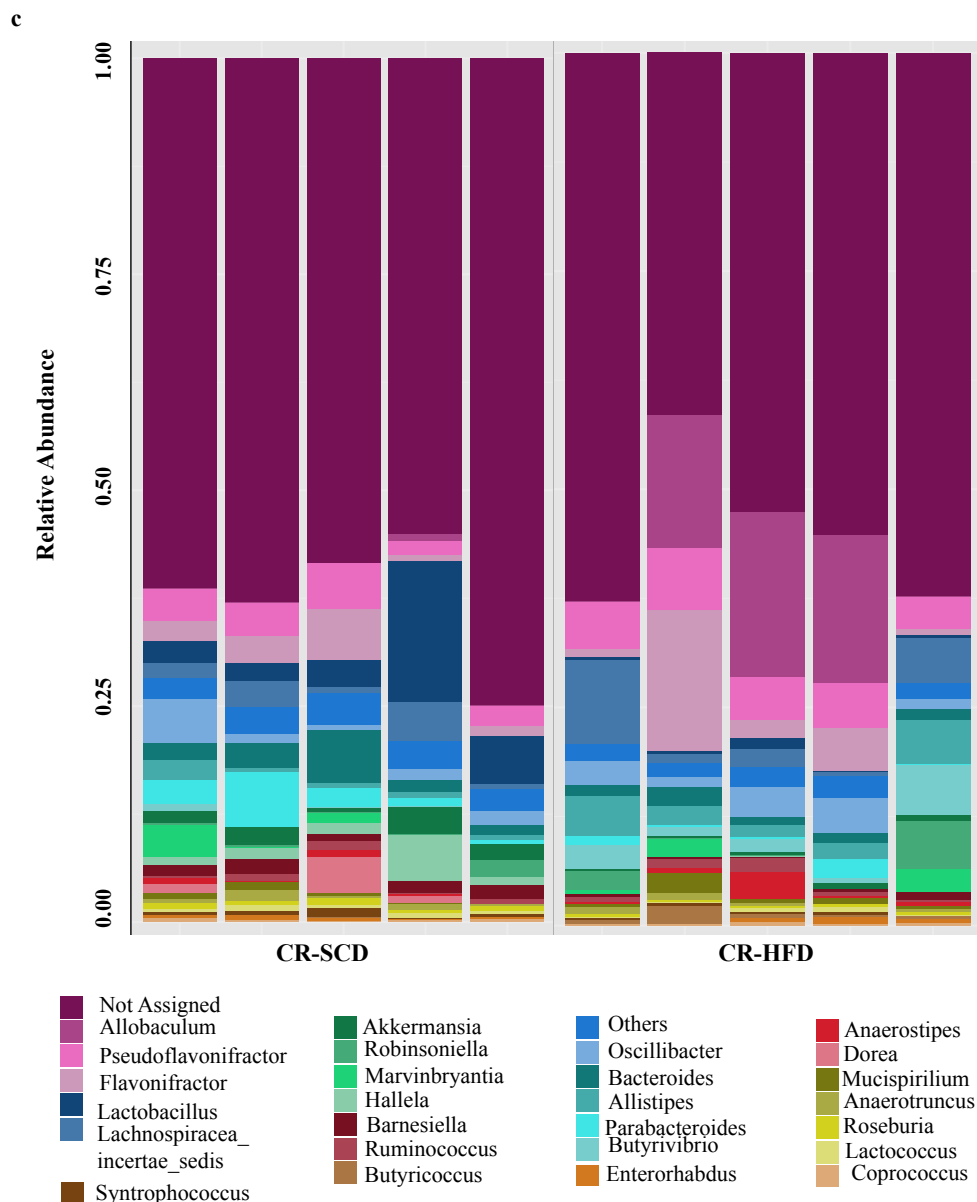


Figure 4-3 HFD ingestion caused microbial alterations in the cecum, which was marked by increased gram-positive bacteria.

a, Principal component analysis revealed that cecal microbial communities from CR mice clustered together by diet, indicating diet shifted the community composition. b, Cecal microbiota of CR-HFD mice had higher Firmicutes and lower Bacteroidetes compared to CR-SCD mice, indicating an increase in gram-positive bacteria in the cecum of CR-HFD mice. c, HFD induced shifts in specific genera in the cecum of CR mice.

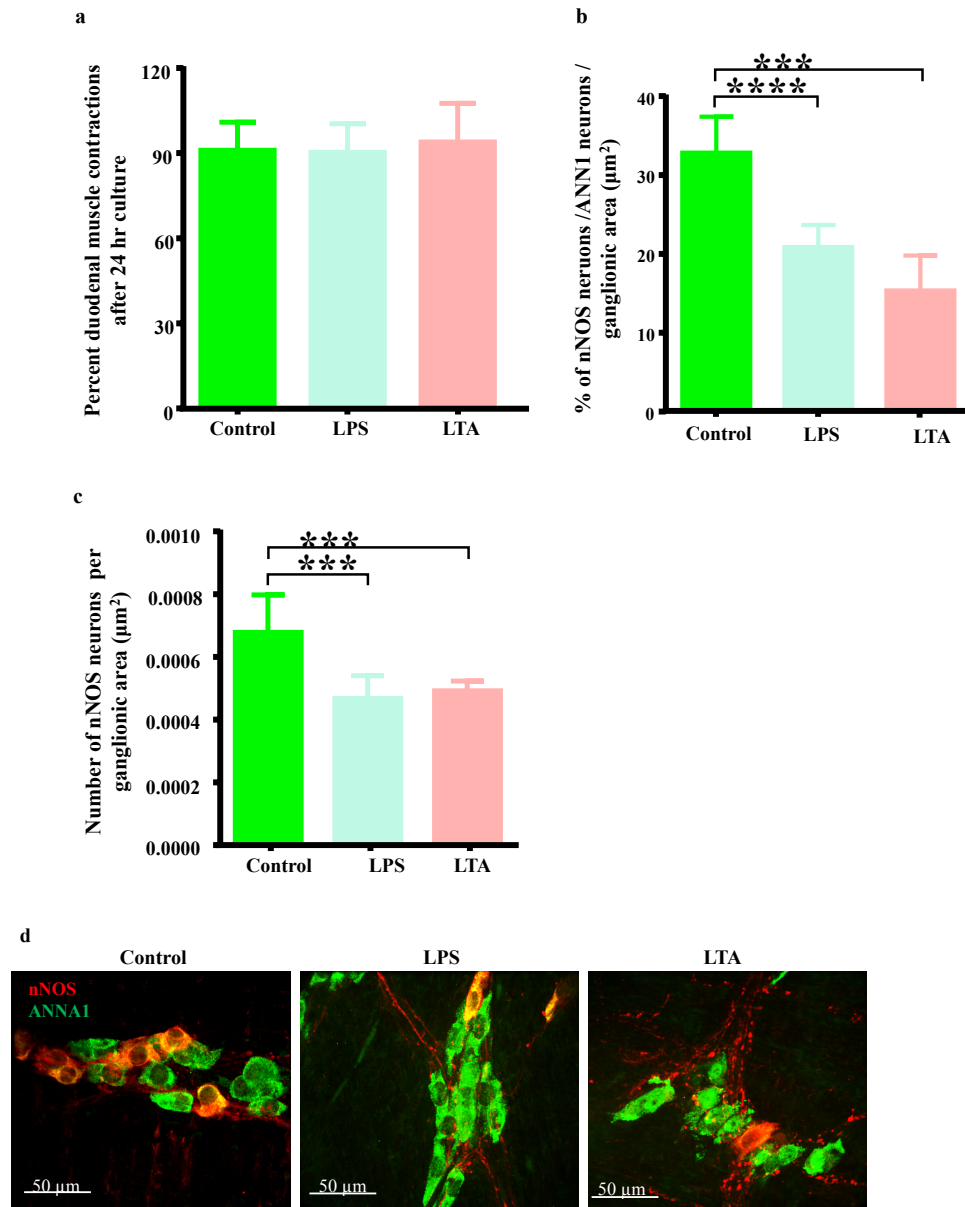


Figure 4-4 Bacterially derived cellular components, LTA and LPS damage nitrenergic myenteric neurons without affecting intestinal muscle contractions in culture.

a, The number of muscle contractions per second was not affected by 24 hours of treatment with LPS and LTA when compared with untreated control samples. b-c, Similar to LPS treatment, LTA induced damage to nitrenergic myenteric neurons in cultured duodenal muscularis samples. Both LTA and LPS reduced the percentage of nNOS neurons per total number of neurons in myenteric ganglia and the number of myenteric of nNOS neurons per ganglionic area after 24 hours. d, Sample images showing overlays of nNOS (red) and ANNA1 (green) staining in duodenal myenteric ganglia of untreated control, LPS and LTA treated duodenal muscularis.

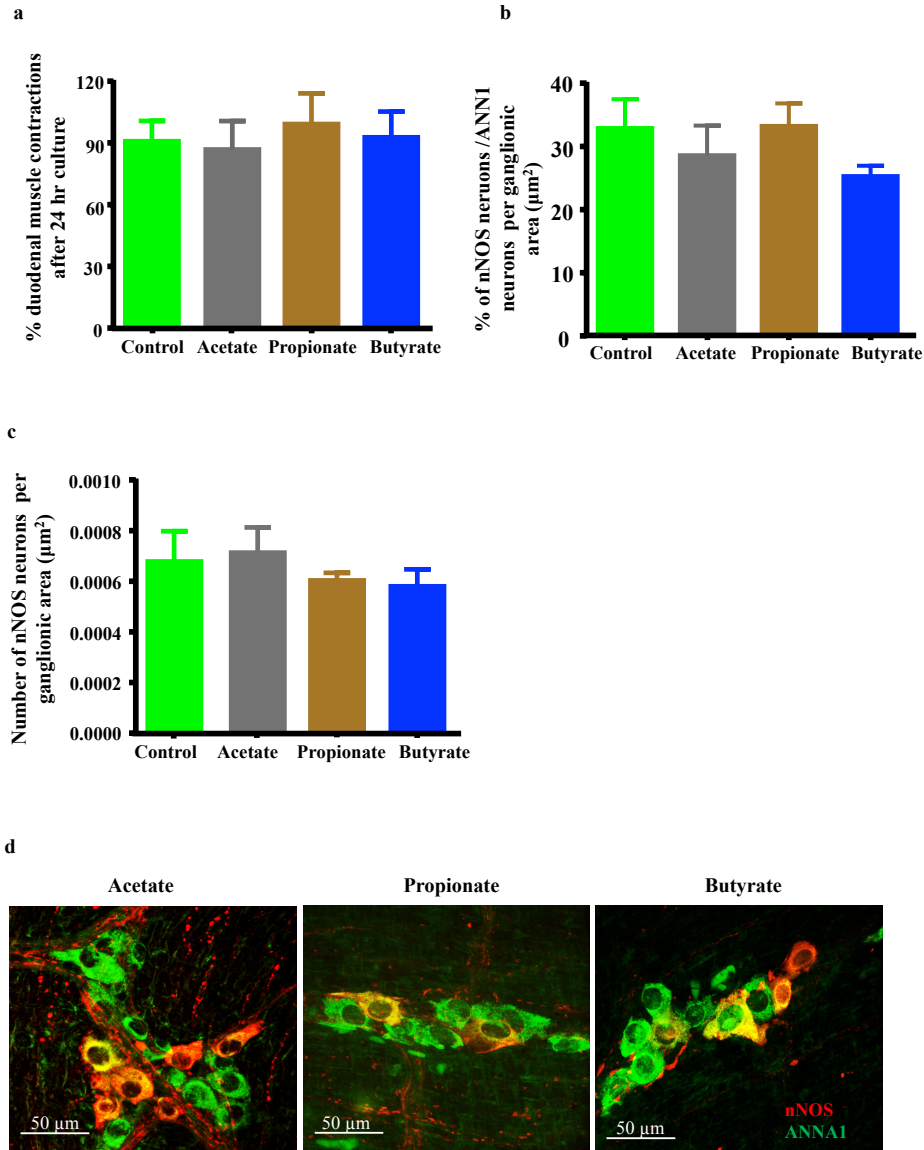
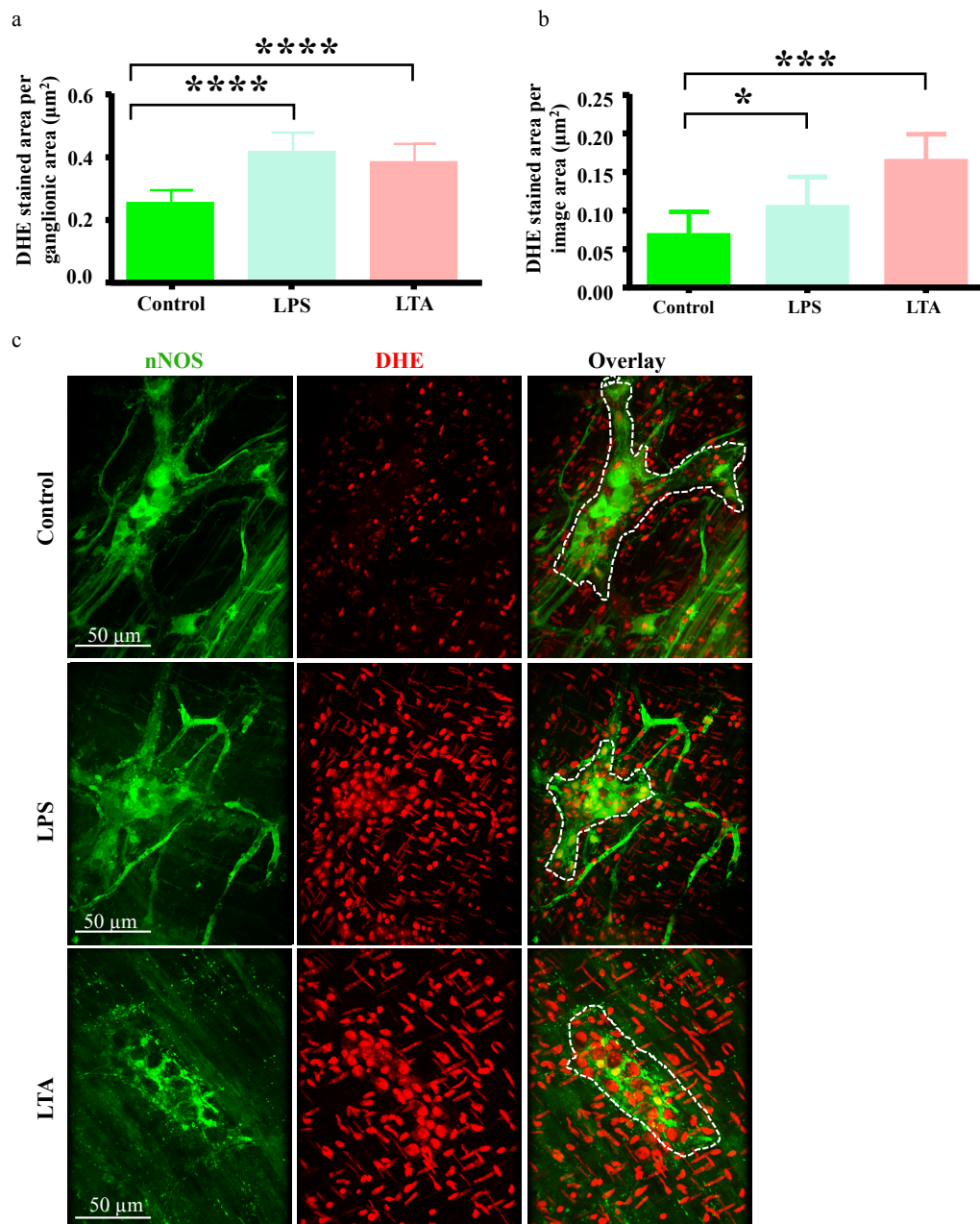


Figure 4-5 Bacterially derived SCFAs do not affect contractions or injure nNOS neurons in cultured duodenojejunal muscularis.

a, The number of muscle contractions per second was not affected by 24 hours of treatment with 30mM concentrations of SCFAs when compared with untreated control samples. b-c, SCFAs did not affect the percentage of nNOS neurons per total number of neurons in myenteric ganglia and the number of myenteric of nNOS neurons per ganglionic area after 24 hours. d, Sample images showing overlays of nNOS (red) and ANNA1 (green) staining in duodenal myenteric ganglia of untreated control, acetate, propionate and butyrate treated duodenal muscularis.



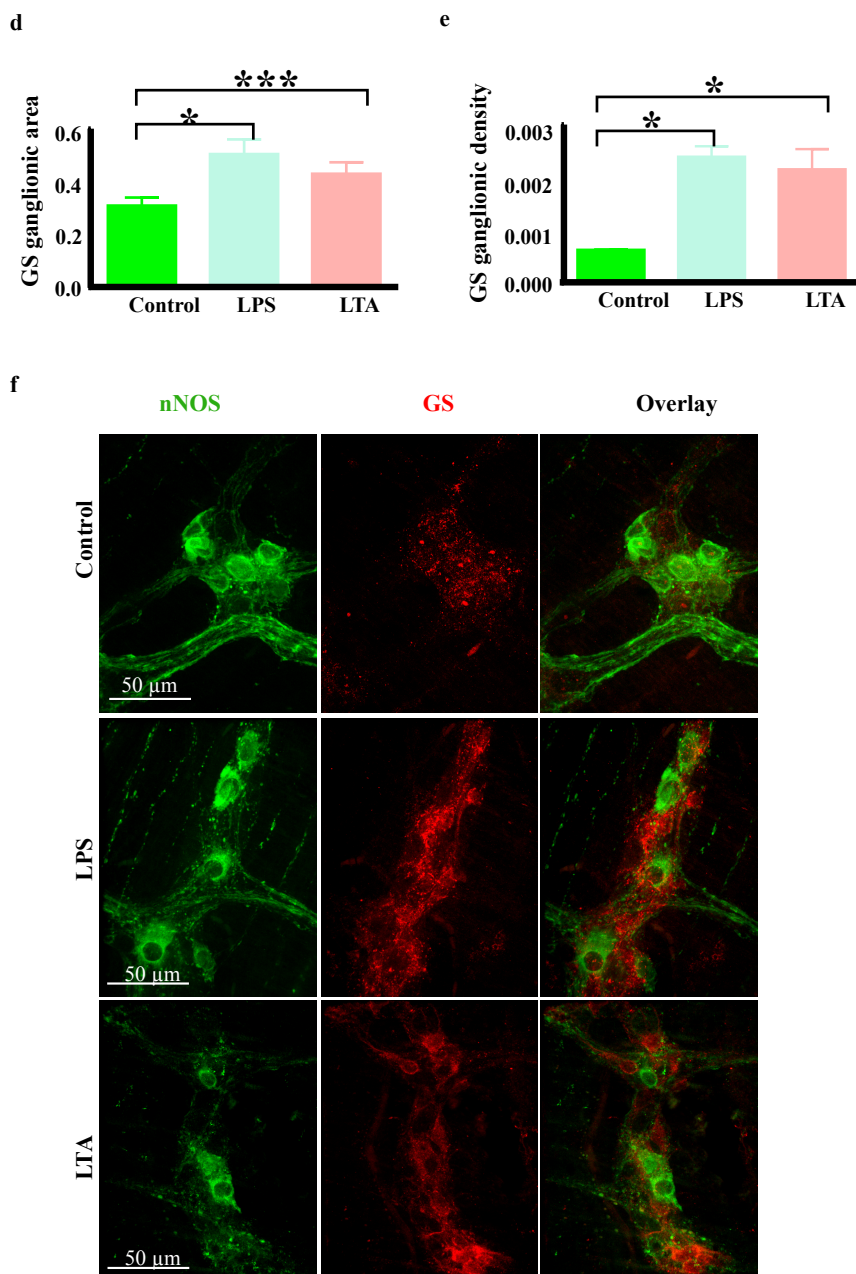


Figure 4-6 LTA induces oxidative stress in myenteric neurons.

a-b, Like LPS, LTA increased the amount of DHE staining per ganglionic area (a) and in the entire field of view (b) after 12 hours. c, Sample images showing nNOS (green) and DHE (red) staining in duodenal myenteric ganglia of control, LPS and LTA treated samples. d-e, Like LPS, LTA increased the anti-glutathione synthase immunoreactivity (d) and increased the GS positive neurons per ganglionic area (e). f, Sample images showing nNOS neurons (green) and anti-glutathione synthase (red) immunoreactivities in duodenal myenteric ganglia of control, LPS and LTA treated (12hr) muscularis.

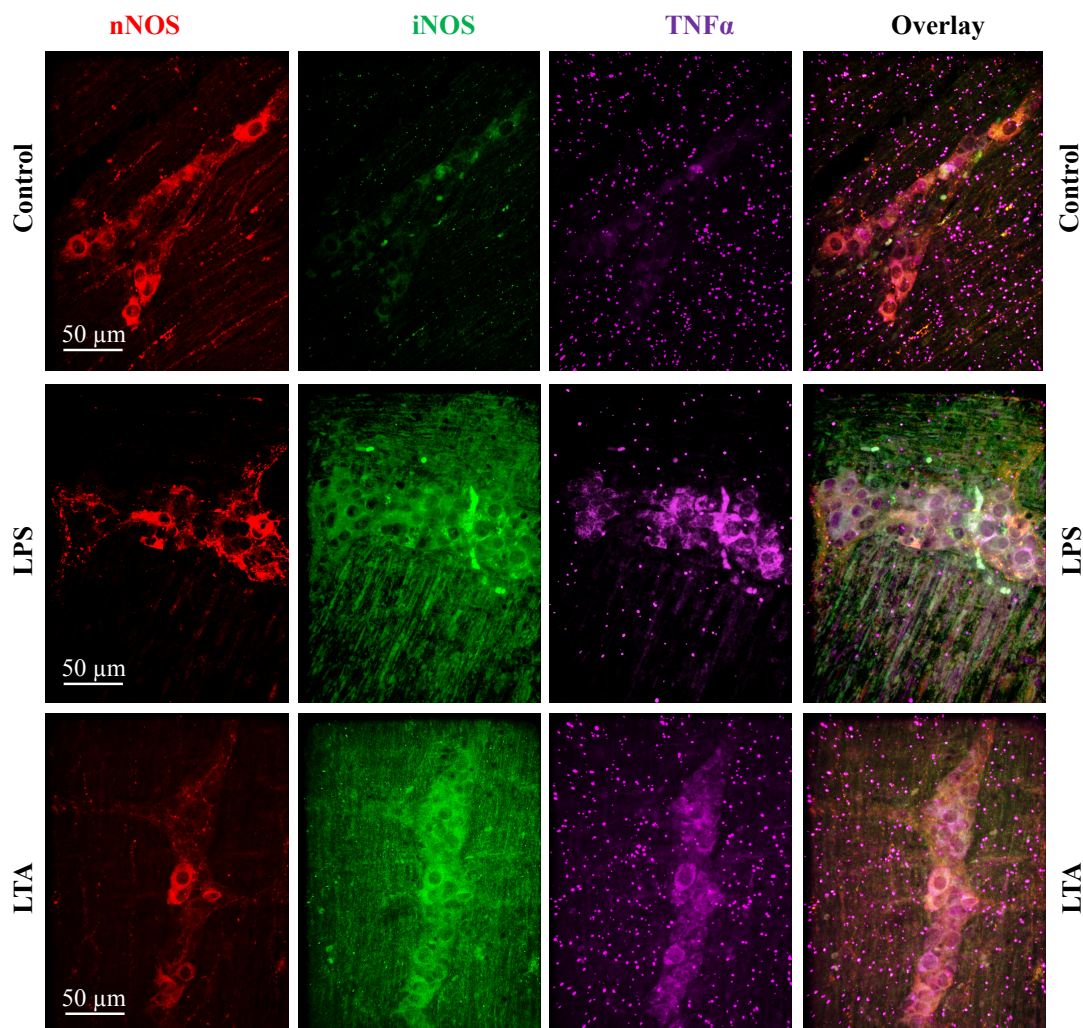


Figure 4-7 LTA treatment caused nitrosative stress and induced the production of TNF α .

Images to demonstrate qualitative analysis of inducible nitric oxide synthase (iNOS, green) and TNF α immunoreactivity (purple) in nNOS neurons (red) in control, LPS and LTA treated samples, after 12 hours. Similar to LPS treatment, LTA treatment increased the number of neurons expressing TNF α , and increased the number of neurons expressing iNOS compared to control samples.

Discussion

The goals of this study were to: a) determine whether the gut microbiota plays an essential role in the development of HFD-induced enteric neuropathy and b) determine the role of gut microbiota derived LTA and SCFAs on enteric neuropathy and dysmotility. Our results demonstrate that GF mice fed a HFD do not develop the enteric neuropathy observed in CR mice fed HFD suggesting that gut microbiota is required for the development of enteric neuropathy. The data presented herein also demonstrates that HFD caused gut microbial alterations in CR mice, characterized by higher abundance of Gram-positive Firmicutes bacteria in cecum. Furthermore, Gram-positive bacterial LTA, like Gram-negative bacterial LPS, induced enteric neuropathy, oxidative stress and TNF α -mediated inflammation, but did not affect duodenal muscle contractions. 30mM concentrations of the major SCFAs produced as a result of gut bacterial fermentation (acetate, propionate, butyrate) did not damage myenteric neurons or inhibit duodenal muscle contractions. This is the first study, to our knowledge, to establish an association between the increase of Gram-positive gut bacteria caused by HFD ingestion and the development of enteric neuropathy through LTA.

The main finding from this study is that the gut microbiota is required for the development of HFD-induced enteric neuropathy including injury to nitrergic myenteric neurons. We report for the first time that HFD ingestion does not affect the total number of neurons and the number of nitrergic neurons in the myenteric plexus of GF mouse duodenum, which is in contrast to findings in CR mice^{3,9,12}. The HFD-induced reductions in the total number of neurons and the number of nitrergic myenteric neurons in duodenal myenteric plexus of CR mice observed in this study correspond with previous observations utilizing HFD of different compositions ranging from 45% to 72% caloric intake from fat^{3,9,12}. There are three potential explanations for the observed differences between GF and CR HFD mice that support the involvement of gut microbiota in causing enteric neuropathy. The first explanation is that HFD induced changes to the gut microbiota are involved in the development of enteric neuropathy likely through endotoxemia. This view is supported by previous studies showing that LPS is increased in the bloodstream of mice and humans fed the high fat diet^{34,20,37} and that LPS acts synergistically with dietary saturated fat (palmitate) to cause enteric neuropathy in diabetic mice^{3,4}. Our results also strongly support this view as we have found that both LPS and LTA damages myenteric neurons. Second, it has been shown that hyperglycemia and hyperlipidemia are involved in causing enteric neuropathy in CR mice^{38,39}. Interestingly, GF HFD mice do not develop hyperlipidemia, hyperglycemia or obesity after 8 weeks^{40,41} however they develop diabetic conditions upon receiving gut microbiota transplants from diabetic patients^{40,41} which further highlights the important role of the microbiota in the pathophysiology of diabetic conditions including enteric neuropathy. Finally, new studies show that HFD-induced damage to ENS neurons can occur in the

absence of hyperglycemia^{9,42}, which suggests that other factors, including microbial factors, play a key role in causing enteric neuropathy associated with HFD ingestion and T2D.

Another important finding of our study is the observation that LTA causes HFD-induced and T2D enteric neuropathy. The majority of previous studies linking gut microbiota alterations to enteric neuropathy have focused on LPS, which is derived from Gram-negative bacteria^{3,4}. However, like several other studies in HFD mouse models and in diabetic humans^{9,14}, the current study found HFD-induced alterations of microbiota in cecum was characterized by the increased abundance of Firmicutes (Gram-positive) and decreased abundance of Bacteroidetes (Gram-negative) bacteria. These increases in Gram-positive bacteria correlate with the increase in Gram-positive gut bacteria in the bloodstream of T2D patients¹⁵. Gram-positive bacteria are distinguished from Gram-negative bacteria by the absence of an outer cell membrane⁴³, and an inner cellular membrane composed of LTA and peptidoglycan instead of LPS⁴³. Therefore, an increase in Gram-positive bacteria in the cecum of CR mice fed HFD led us to hypothesize that Gram-positive LTA induces enteric neuropathy associated with oxidative- stress and TNF α mediated neuroinflammation. In testing this idea, we have established that like LPS, LTA induces damage to ENS neurons, particularly nitrergic myenteric neurons, likely through oxidative stress and inflammation. It has been shown that LTA damages cerebellar granule neurons by activating glial cells to release pro-inflammatory cytokines (TNF α , IL-1 β and IL-6), which damage neurons via oxidative-nitrosative stress and caspase activation¹⁷. LTA is a TLR2 agonist that induces oxidative and nitrosative stress through a similar pathway as LPS^{16,44}, mainly by activating myd88, NF-kB and Nrf2¹⁶. LPS acts via TLR4 to damage nitrergic myenteric neurons via oxidative-nitrosative stress and inflammation^{3,4}. Therefore, it is likely that these mechanisms were involved in the observed LPS and LTA-induced activation of inflammation, increased oxidative stress and damage to nitrergic myenteric neurons in myenteric ganglia. Collectively, our results support the need for determining the levels of components of Gram-positive bacteria, including peptidoglycan and LTA in the blood stream of HFD mouse models and T2D patients. Our study also signifies the need for elucidating the involvement of enteric glia in LTA-induced enteric neuropathy and analyzing the cellular mechanisms by which LTA damages ENS neurons in future studies.

The short chain fatty acids (SCFAs) acetate, propionate and butyrate appear to have no role in HFD induced damage to nitrergic myenteric neurons and impaired duodenal contractions. We have previously shown that HFD causes loss of nitrergic myenteric neurons and impairs duodenal contractions in conventionally raised male and female mice^{9,12}. Other studies have demonstrated that HFD ingestion in a rat model of T2D and alterations of the gut microbiota in diabetic humans is

associated with lower fermentative bacteria and impaired production of the major SCFAs acetate, propionate and butyrate^{11,45-47}. The concentrations of all three fatty acids are also reduced by HFD ingestion in humans¹⁰. At the 30mM concentration used in this study, acetate, propionate and butyrate did not affect duodenal muscle contractions and the number of nitrergic myenteric neurons. These concentrations were selected because a previous study had determined that 30mM concentrations affected colonic motility *ex vivo*, and because we considered 30mM to be representative of the lower SCFA concentrations found in the gut of diabetic subjects⁴⁸. These findings suggest that low concentrations of these SCFAs do not cause neuropathy or impair intestinal motility by disrupting muscle contractions. Effects of SCFAs on nitrergic myenteric neurons have not been evaluated thoroughly, warranting future studies with different concentrations and combinations of SCFAs.

This study found that the intact gut microbiota is required for the development of the optimal number of all neurons and nitrergic neurons in the myenteric plexus of mice. GF mice fed SCD had lower myenteric neuronal densities and a lower proportion of nitrergic neurons in the duodenum compared to CR mice fed SCD. Our results support previous findings that GF mice have fewer myenteric neurons and the conclusion that the gut microbiota is needed for a healthy development of the ENS^{49,50}. However, in contrast with our study in duodenum, other studies reported an increased proportion of nNOS neurons in the jejunum and ileum of GF mice fed SCD. These differences are likely due to regional differences in the gut.

In conclusion, our data strongly supports the hypothesis that gut microbiota alterations likely cause enteric neuropathy through LPS- and LTA-induced mechanisms. Additional studies are needed to identify the specific mechanisms of LTA-induced neuropathy including the involvement of enteric glial cells.

Literature Cited

1. Yarandi, S. S. & Srinivasan, S. Diabetic gastrointestinal motility disorders and the role of enteric nervous system: current status and future directions. *Neurogastroenterol. Motil.* **26**, 611–24 (2014).
2. Feldman, M. & Schiller, L. R. Disorders of gastrointestinal motility associated with diabetes mellitus. *Ann. Intern. Med.* **98**, 378–84 (1983).
3. Reichardt, F. *et al.* Western diet induces colonic nitrenergic myenteric neuropathy and dysmotility in mice via saturated fatty acid- and lipopolysaccharide-induced TLR4 signalling. *J. Physiol.* **595**, 1831–1846 (2017).
4. Anitha, M. *et al.* Intestinal Dysbiosis Contributes to the Delayed Gastrointestinal Transit in High-Fat Diet Fed Mice. *Cell. Mol. Gastroenterol. Hepatol.* **2**, 328–339 (2016).
5. Nyavor, Y. E. A. & Balemba, O. B. Diet-induced dysmotility and neuropathy in the gut precedes endotoxaemia and metabolic syndrome: the chicken and the egg revisited. *J. Physiol.* **595**, 1441–1442 (2017).
6. Kashyap, P. C. *et al.* Complex interactions among diet, gastrointestinal transit, and gut microbiota in humanized mice. *Gastroenterology* **144**, 967–77 (2013).
7. Van Hul, M. *et al.* Reduced obesity, diabetes, and steatosis upon cinnamon and grape pomace are associated with changes in gut microbiota and markers of gut barrier. *Am. J. Physiol. Metab.* **314**, E334–E352 (2018).
8. Everard, A. *et al.* Microbiome of prebiotic-treated mice reveals novel targets involved in host response during obesity. *ISME J.* **8**, 2116–2130 (2014).
9. Nyavor, Y. *et al.* Intestinal nerve cell injury occurs prior to insulin resistance in female mice ingesting a high-fat diet. *Cell Tissue Res.* **376**, 325–340 (2019).
10. Amar, J. *et al.* Energy intake is associated with endotoxemia in apparently healthy men. *Am. J. Clin. Nutr.* **87**, 1219–1223 (2008).
11. Jakobsdottir, G., Xu, J., Molin, G., Ahrné, S. & Nyman, M. High-Fat Diet Reduces the Formation of Butyrate, but Increases Succinate, Inflammation, Liver Fat and Cholesterol in Rats, while Dietary Fibre Counteracts These Effects. *PLoS One* **8**, e80476 (2013).

12. Stenkamp-Strahm, C. M., Kappmeyer, A. J., Schmalz, J. T., Gericke, M. & Balemba, O. High-fat diet ingestion correlates with neuropathy in the duodenum myenteric plexus of obese mice with symptoms of type 2 diabetes. *Cell Tissue Res.* **354**, 381–94 (2013).
13. Winzell, M. S. & Ahren, B. The High-Fat Diet-Fed Mouse: A Model for Studying Mechanisms and Treatment of Impaired Glucose Tolerance and Type 2 Diabetes. *Diabetes* **53**, S215–S219 (2004).
14. Larsen, N. *et al.* Gut Microbiota in Human Adults with Type 2 Diabetes Differs from Non-Diabetic Adults. *PLoS One* **5**, e9085 (2010).
15. Sato, J. *et al.* Gut Dysbiosis and Detection of “Live Gut Bacteria” in Blood of Japanese Patients With Type 2 Diabetes. *Diabetes Care* **37**, 2343–2350 (2014).
16. Schwandner, R., Dziarski, R., Wesche, H., Rothe, M. & Kirschning, C. J. Peptidoglycan- and Lipoteichoic Acid-induced Cell Activation Is Mediated by Toll-like Receptor 2. *J. Biol. Chem.* **274**, 17406–17409 (1999).
17. Kinsner, A. *et al.* Inflammatory neurodegeneration induced by lipoteichoic acid from *Staphylococcus aureus* is mediated by glia activation, nitrosative and oxidative stress, and caspase activation. *J. Neurochem.* **95**, 1132–1143 (2005).
18. Neher, J. J. & Brown, G. C. Neurodegeneration in models of Gram-positive bacterial infections of the central nervous system. *Biochem. Soc. Trans.* **35**, 1166–1167 (2007).
19. Tang, C.-H., Hsu, C.-J., Yang, W.-H. & Fong, Y.-C. Lipoteichoic acid enhances IL-6 production in human synovial fibroblasts via TLR2 receptor, PKC δ and c-Src dependent pathways. *Biochem. Pharmacol.* **79**, 1648–1657 (2010).
20. Jayashree, B. *et al.* Increased circulatory levels of lipopolysaccharide (LPS) and zonulin signify novel biomarkers of proinflammation in patients with type 2 diabetes. *Mol. Cell. Biochem.* **388**, 203–210 (2014).
21. Walker, A. W., Duncan, S. H., McWilliam Leitch, E. C., Child, M. W. & Flint, H. J. pH and Peptide Supply Can Radically Alter Bacterial Populations and Short-Chain Fatty Acid Ratios within Microbial Communities from the Human Colon. *Appl. Environ. Microbiol.* **71**, 3692–3700 (2005).
22. Lin, H. V *et al.* Butyrate and propionate protect against diet-induced obesity and regulate gut hormones via free fatty acid receptor 3-independent mechanisms. *PLoS One* **7**, e35240 (2012).

23. Huuskonen, J., Suuronen, T., Nuutinen, T., Kyrylenko, S. & Salminen, A. Regulation of microglial inflammatory response by sodium butyrate and short-chain fatty acids. *Br. J. Pharmacol.* **141**, 874–80 (2004).
24. Soret, R. *et al.* Short-Chain Fatty Acids Regulate the Enteric Neurons and Control Gastrointestinal Motility in Rats. *Gastroenterology* **138**, 1772-1782.e4 (2010).
25. Nyavor, Y., Brands, C., Cox, K. K., Starks, K. & Balemba, O. B. 552 High Fat Diet-Microbiota-Host Interactions Result in the Production of Substances That Cause Intestinal Dysmotility and Enteric Neuropathy in Type Two Diabetic Mice. *Gastroenterology* **150**, S116–S117 (2016).
26. Caesar, R., Tremaroli, V., Kovatcheva-Datchary, P., Cani, P. D. & Bäckhed, F. Crosstalk between Gut Microbiota and Dietary Lipids Aggravates WAT Inflammation through TLR Signaling. *Cell Metab.* **22**, 658–668 (2015).
27. Soares, A., Beraldi, E. J., Ferreira, P. E. B., Bazotte, R. B. & Buttow, N. C. Intestinal and neuronal myenteric adaptations in the small intestine induced by a high-fat diet in mice. *BMC Gastroenterol.* **15**, 3 (2015).
28. Yuan, S., Cohen, D. B., Ravel, J., Abdo, Z. & Forney, L. J. Evaluation of methods for the extraction and purification of DNA from the human microbiome. *PLoS One* **7**, e33865 (2012).
29. Ravel, J. *et al.* Vaginal microbiome of reproductive-age women. *Proc. Natl. Acad. Sci. U. S. A.* **108 Suppl**, 4680–7 (2011).
30. Stenkamp-Strahm, C. M. *et al.* Prolonged high fat diet ingestion, obesity, and type 2 diabetes symptoms correlate with phenotypic plasticity in myenteric neurons and nerve damage in the mouse duodenum. *Cell Tissue Res.* **361**, 411–426 (2015).
31. Benov, L., Szejnberg, L. & Fridovich, I. Critical evaluation of the use of hydroethidine as a measure of superoxide anion radical. *Free Radic. Biol. Med.* **25**, 826–831 (1998).
32. Brown, I. A. M., McClain, J. L., Watson, R. E., Patel, B. A. & Gulbransen, B. D. Enteric Glia Mediate Neuron Death in Colitis Through Purinergic Pathways That Require Connexin-43 and Nitric Oxide. *Cell. Mol. Gastroenterol. Hepatol.* **2**, 77–91 (2016).
33. Hurst, N. R., Kendig, D. M., Murthy, K. S. & Grider, J. R. The short chain fatty acids, butyrate and propionate, have differential effects on the motility of the guinea pig colon. *Neurogastroenterol. Motil.* **26**, 1586–96 (2014).

34. Cani, P. D. *et al.* Changes in gut microbiota control metabolic endotoxemia-induced inflammation in high-fat diet-induced obesity and diabetes in mice. *Diabetes* **57**, 1470–81 (2008).
35. Brown, I. A. M. & Gulbransen, B. D. The antioxidant glutathione protects against enteric neuron death in situ, but its depletion is protective during colitis. *Am. J. Physiol. Liver Physiol.* **314**, G39–G52 (2018).
36. Lei, B. *et al.* Anti-Inflammatory Effects of Progesterone in Lipopolysaccharide-Stimulated BV-2 Microglia. *PLoS One* **9**, e103969 (2014).
37. Guo, S., Al-Sadi, R., Said, H. M. & Ma, T. Y. Lipopolysaccharide Causes an Increase in Intestinal Tight Junction Permeability in Vitro and in Vivo by Inducing Enterocyte Membrane Expression and Localization of TLR-4 and CD14. *Am. J. Pathol.* **182**, 375–387 (2013).
38. Nezami, B. G. *et al.* MicroRNA 375 Mediates Palmitate-Induced Enteric Neuronal Damage and High-Fat Diet-Induced Delayed Intestinal Transit in Mice. *Gastroenterology* **146**, 473-483.e3 (2014).
39. Anitha, M. *et al.* GDNF rescues hyperglycemia-induced diabetic enteric neuropathy through activation of the PI3K/Akt pathway. *J. Clin. Invest.* **116**, 344–356 (2006).
40. Bäckhed, F., Manchester, J. K., Semenkovich, C. F. & Gordon, J. I. Mechanisms underlying the resistance to diet-induced obesity in germ-free mice. *Proc. Natl. Acad. Sci.* **104**, 979–984 (2007).
41. Rabot, S. *et al.* Germ-free C57BL/6J mice are resistant to high-fat-diet-induced insulin resistance and have altered cholesterol metabolism. *FASEB J.* **24**, 4948–4959 (2010).
42. Rivera, L. R. *et al.* Damage to enteric neurons occurs in mice that develop fatty liver disease but not diabetes in response to a high-fat diet. *Neurogastroenterol. Motil.* **26**, 1188–99 (2014).
43. Silhavy, T. J., Kahne, D. & Walker, S. The Bacterial Cell Envelope. *Cold Spring Harb. Perspect. Biol.* **2**, a000414–a000414 (2010).
44. Long, E. M., Millen, B., Kubes, P. & Robbins, S. M. Lipoteichoic Acid Induces Unique Inflammatory Responses when Compared to Other Toll-Like Receptor 2 Ligands. *PLoS One* **4**, e5601 (2009).
45. Vrieze, A. *et al.* Transfer of Intestinal Microbiota From Lean Donors Increases Insulin Sensitivity in Individuals With Metabolic Syndrome. *Gastroenterology* **143**, 913-916.e7 (2012).

46. Qin, J. *et al.* A metagenome-wide association study of gut microbiota in type 2 diabetes. *Nature* **490**, 55–60 (2012).
47. Udayappan, S. D., Hartstra, A. V., Dallinga-Thie, G. M. & Nieuwdorp, M. Intestinal microbiota and faecal transplantation as treatment modality for insulin resistance and type 2 diabetes mellitus. *Clin. Exp. Immunol.* **177**, 24–29 (2014).
48. Puddu, A., Sanguineti, R., Montecucco, F. & Viviani, G. L. Evidence for the Gut Microbiota Short-Chain Fatty Acids as Key Pathophysiological Molecules Improving Diabetes. *Mediators Inflamm.* **2014**, 1–9 (2014).
49. Collins, J., Borojevic, R., Verdu, E. F., Huizinga, J. D. & Ratcliffe, E. M. Intestinal microbiota influence the early postnatal development of the enteric nervous system. *Neurogastroenterol. Motil.* **26**, 98–107 (2014).
50. De Vadder, F. *et al.* Gut microbiota regulates maturation of the adult enteric nervous system via enteric serotonin networks. *Proc. Natl. Acad. Sci.* **115**, 6458–6463 (2018).

Chapter 5: Conclusion

The studies conducted in this dissertation contributed new knowledge towards a better understanding of the role diet-microbiota-host interactions play in the development of enteric neuropathy and dysmotility in a high fat diet mouse model of type 2 diabetes.

In Chapter 2, we showed that unlike conventionally raised male mice, conventionally raised female mice did not develop obesity or type 2 diabetes conditions after 8 weeks of high fat diet ingestion. This led us to establish that gut microbiota alterations, enteric neuropathy, impaired neuromuscular transmission and dysmotility develops before hyperglycemia and insulin resistance in conventionally raised female mice fed a high fat diet. We also demonstrated that enteric neuropathy and dysmotility correlated with high fat diet induced gut microbiota alterations.

Studies in Chapter 3 led to the discovery that there are unknown toxic molecules (substances) in luminal contents from the large intestine of conventionally raised high fat fed mice that cause enteric neuropathy and dysmotility in isolated intestinal segments. These substances also damaged smooth muscle and impaired neuromuscular transmission. We also showed that these molecules could be isolated using solid phase extraction.



In Chapter 4, we made the new discovery that an intact gut microbiota is required for the development of enteric neuropathy. We also showed that in conventionally raised mice, enteric neuropathy is associated with alterations of the microbiota in cecum, which was characterized by increased abundance of Gram positive bacteria in high fat fed conventionally raised mice. Finally, we discovered for the first time that lipoteichoic acid from gram-positive bacteria could induce enteric neuropathy through oxidative stress and inflammation.

These studies provided novel contributions to the body of scientific literature regarding the development of diabetic enteric neuropathy and dysmotility. They further support the idea that enteric neuropathy and dysmotility develop before diabetic symptoms, and play a role in the early disease stages during the development of T2D. They also highlight a new idea that there are neurotoxic and antimotility molecules, likely derived from diet-microbiota-host interactions, in the gut of diabetic mice and humans. Our results strongly implicate these molecules as key triggers of HFD and diabetes dysmotility before obesity and insulin resistance. It is important that these molecules be identified in order to identify potential new targets of treatment and biomarkers for gastrointestinal disease in type two diabetes patients. The final new idea coming out of this dissertation points to the important previously unidentified role of lipoteichoic acid in the development of enteric neuropathy.

Overall, these studies have contributed new knowledge that supports the need for the broader investigation of neurotoxic and antimotility molecules from gut contents with potential for triggering dysmotility in early stages of disease development before the development of clear symptoms of T2D. The outcome could significantly contribute towards the development of biomarkers for diagnosis of GI neuropathy and dysmotility prior to T2D. This could identify novel targets for therapies that can improve the quality of life of T2D patients.

Appendix A- Supplementary Table 2-1

Modified DIO 70% Kcal Fat Diet w/ 2% Additional Corn Oil 5SSV

DESCRIPTION	NUTRITIONAL PROFILE ¹	
Modification of TestDiet® DIO Basal 70% Kcal from Fat Purified Diet (58H0) with 2% Additional Corn Oil (8.87% Total Corn Oil). Dyed Green.		
Storage conditions are particularly critical to TestDiet® products, due to the absence of antioxidants or preservative agents. To provide maximum protection against possible changes during storage, store in a dry, cool location. Storage under refrigeration (2° C) is recommended. Maximum shelf life is six months. (If long term studies are involved, storing the diet at -20° C or colder may prolong shelf life.) Be certain to keep in air tight containers.		
Product Forms Available*	Catalog #	
Meal	1813733	
<i>*Other Forms Available On Re</i>		
INGREDIENTS (%)		
Lard	36.7980	
Casein - Vitamin Free	28.8560	
Corn Oil	8.8705	
Dextrin	7.7682	
RP Mineral Mix #10 (adds 1.29% fiber)	6.8705	
Sucrose	3.4353	
RP Vitamin Mix (adds 1.94% sucrose)	2.7482	
Powdered Cellulose	2.0612	
Inulin	2.0612	
Choline Chloride	0.2748	
DL-Methionine	0.2061	
Green Dye	0.0500	
	Protein, %	25.6
	Arginine, %	1.01
	Histidine, %	0.74
	Isoleucine, %	1.38
	Leucine, %	2.50
	Lysine, %	2.10
	Methionine, %	0.95
	Cystine, %	0.11
	Phenylalanine, %	1.38
	Tyrosine, %	1.46
	Threonine, %	1.12
	Tryptophan, %	0.32
	Valine, %	1.65
	Alanine, %	0.80
	Aspartic Acid, %	1.86
	Glutamic Acid, %	5.89
	Glycine, %	0.56
	Proline, %	3.40
	Serine, %	1.59
	Taurine, %	0.00
	Fat, %	45.7
	Cholesterol, ppm	350
	Linoleic Acid, %	8.61
	Linolenic Acid, %	0.24
	Arachidonic Acid, %	0.07
	Omega-3 Fatty Acids, %	0.24
	Total Saturated Fatty A	16.47
	Total Monounsaturated	17.64
	Fatty Acids, %	
	Polyunsaturated Fatty Acids, %	8.92
	Fiber (max), %	5.9
	Carbohydrates, %	13.9
	Energy (kcal/g) ²	5.67
	From:	kcal %
	Protein	1.024 18.0
	Fat (ether extract)	4.110 72.2
	Carbohydrates	0.555 9.8
	Minerals	
	Calcium, %	0.83
	Phosphorus, %	0.78
	Phosphorus (available), %	0.78
	Potassium, %	0.55
	Magnesium, %	0.09
	Sodium, %	0.30
	Chloride, %	0.36
	Fluorine, ppm	6.8
	Iron, ppm	87
	Zinc, ppm	38
	Manganese, ppm	89
	Copper, ppm	20.6
	Cobalt, ppm	4.4
	Iodine, ppm	0.79
	Chromium, ppm	4.2
	Molybdenum, ppm	1.12
	Selenium, ppm	0.41
	Vitamins	
	Vitamin A, IU/g	30.4
	Vitamin D-3 (added), IU/g	3.0
	Vitamin E, IU/kg	68.8
	Vitamin K (as menadione), ppm	14.29
	Thiamin Hydrochloride, ppm	28.4
	Riboflavin, ppm	28.5
	Niacin, ppm	124
	Pantothenic Acid, ppm	78
	Folic Acid, ppm	5.7
	Pyridoxine, ppm	22.7
	Biotin, ppm	0.6
	Vitamin B-12, mcg/kg	33
	Choline Chloride, ppm	1,924
	Ascorbic Acid, ppm	0.0
	1. Based on the latest ingredient analysis information. Since nutrient composition of natural ingredients varies, analysis will differ accordingly. Nutrients expressed as percent of ration on an As-Fed basis except where otherwise indicated.	
	2. Energy (kcal/gm) - Sum of decimal fractions of protein, fat and carbohydrate x 4,9,4 kcal/gm respectively.	
FEEDING DIRECTIONS		
Feed ad libitum. Plenty of fresh, clean water should be available at all times.		
CAUTION:		
Perishable - store properly upon receipt. For laboratory animal use only; NOT for human consumption.		
6/3/2009		
		
	 www.testdiet.com	

Appendix B- Supplementary Table 2-2

	Duodenal velocity		HFD Effect on Abundance
	p value	r squared	
Allobaculum	0.0022	-0.9978	Increased
Anaerobacter	0.0546	0.9454	Reduced
Anaerophaga	0.0436	0.9564	Reduced
Anaerorhabdus	0.0105	0.9895	Reduced
Atopobacter	0.0256	0.9744	Reduced
Bifidobacterium	0.0118	0.9882	Reduced
Butyrivibrio	0.0101	0.9899	Reduced
Clostridium.sensu.stricto	0.0477	0.9523	Reduced
Coprobacillus	0.0140	0.9860	Reduced
Gordonibacter	0.0376	0.9624	Reduced
Hallella	0.0383	0.9617	Reduced
Lactobacillus	0.0334	0.9666	Reduced
Meniscus	0.0364	0.9636	Reduced
Oscillibacter	0.0537	0.9463	Reduced
Paludibacter	0.0165	0.9835	Reduced
Parabacteroides	0.0021	-0.9979	Increased
Paralactobacillus	0.0162	0.9838	Reduced
Paraprevotella	0.0103	0.9897	Reduced
Parasutterella	0.0412	0.9588	Reduced

Pilibacter	0.0027	-0.9973	Increased
Tannerella	0.0464	0.9536	Reduced
TM7_genera_incertae_sedis	0.0497	0.9503	Reduced
Xylanibacter	0.0210	0.9790	Reduced

Appendix C- Supplementary Table 2-3

	Colon Velocity		HFD Effect on Abundance
	p value	r squared	
<i>Acetivibrio</i>	0.0157	0.9843	Reduced
<i>Anaerophaga</i>	0.0005	0.9995	Reduced
<i>Anaerorhabdus</i>	0.0258	0.9742	Reduced
<i>Atopobacter</i>	0.0186	0.9814	Reduced
<i>Barnesiella</i>	0.0069	0.9931	Reduced
<i>Bifidobacterium</i>	0.0433	0.9567	Reduced
<i>Butyricimonas</i>	0.0301	0.9699	Reduced
<i>Butyrivibrio</i>	0.0396	0.9604	Reduced
<i>Coprobacillus</i>	0.0431	0.9569	Reduced
<i>Hallella</i>	0.0004	0.9996	Reduced
<i>Lachnobacterium</i>	0.0186	0.9814	Reduced
<i>Oscillibacter</i>	0.0573	0.9427	Reduced
<i>Paludibacter</i>	0.0172	0.9828	Reduced
<i>Parabacteroides</i>	0.0565	-0.9435	Increased
<i>Paralactobacillus</i>	0.0081	0.9919	Reduced

<i>Paraprevotella</i>	0.0552	0.9448	Reduced
<i>Roseburia</i>	0.0462	0.9538	Reduced
<i>Ruminococcus</i>	0.0284	0.9716	Reduced
<i>Sarcina</i>	0.0019	0.9981	Reduced
<i>Tannerella</i>	0.0002	0.9998	Reduced
<i>Xylanibacter</i>	0.0106	0.9894	Reduced

Appendix D- Supplementary Table 2-4

	Duodenum nNOS		HFD Effect on Abundance
	p value	r squared	
<i>Allobaculum</i>	0.0430	-0.9570	Increased
<i>Anaerobacter</i>	0.0243	0.9757	Reduced
<i>Anaeroplasma</i>	0.0057	0.9943	Reduced
<i>Anaerovorax</i>	0.0007	0.9993	Reduced
<i>Bifidobacterium</i>	0.0472	0.9528	Reduced
<i>Butyrivibrio</i>	0.0511	0.9489	Reduced
<i>Catonella</i>	0.0010	0.9990	Reduced
<i>Clostridium.sensu.stricto</i>	0.0218	0.9782	Reduced
<i>Coprobacillus</i>	0.0478	0.9522	Reduced
<i>Lactobacillus</i>	0.0077	0.9923	Reduced
<i>Meniscus</i>	0.0172	0.9828	Reduced
<i>Paraprevotella</i>	0.0363	0.9637	Reduced
<i>Parasutterella</i>	0.0310	0.9690	Reduced
<i>Pilibacter</i>	0.0409	-0.9591	Increased
<i>Streptophyta</i>	0.0307	0.9693	Reduced

<i>TM7_genera_incertae_sedis</i>	0.0586	0.9414	Reduced
<i>Turicibacter</i>	0.0590	0.9410	Reduced

Appendix E- Supplementary Table 2-5

		Colon nNOS	
	p value	r squared	HFD Effect on Abundance
<i>Allobaculum</i>	0.0439	-0.9561	Increased
<i>Anaerobacter</i>	0.0289	0.9711	Reduced
<i>Anaerophaga</i>	0.0208	0.9792	Reduced
<i>Anaerorhabdus</i>	0.0104	0.9896	Reduced
<i>Atopobacter</i>	0.0026	0.9974	Reduced
<i>Bifidobacterium</i>	0.0132	0.9868	Reduced
<i>Butyrivibrio</i>	0.0133	0.9867	Reduced
<i>Clostridium.sensu.stricto</i>	0.0282	0.9718	Reduced
<i>Coprobacillus</i>	0.0114	0.9886	Reduced
<i>Hallella</i>	0.0257	0.9743	Reduced
<i>Lactobacillus</i>	0.0480	0.9520	Reduced
<i>Lactococcus</i>	0.0198	-0.9802	Increased
<i>Meniscus</i>	0.0302	0.9698	Reduced
<i>Paludibacter</i>	0.0071	0.9929	Reduced
<i>Paralactobacillus</i>	0.0193	0.9807	Reduced

<i>Paraprevotella</i>	0.0208	0.9792	Reduced
<i>Parasutterella</i>	0.0181	0.9819	Reduced
<i>Pilibacter</i>	0.0431	-0.9569	Increased
<i>Sarcina</i>	0.0416	0.9584	Reduced
<i>Tannerella</i>	0.0315	0.9685	Reduced
<i>Xylanibacter</i>	0.0080	0.9920	Reduced

Appendix F- Supplementary Table 2-6

	Duodenal velocity		Colon Velocity	
	p value	Pearson's r	p value	Pearson's r
Duodenum nNOS	0.0642	0.9358	N/A	N/A
Colon nNOS	N/A	N/A	0.0277	0.973
Duodenal velocity	N/A	N/A	0.0465	0.953

Appendix G- Supplementary Table 2-7

	SCD-M	HFD-M	SCD-F	HFD-F
<i>Allobaculum</i>	9.1899	71.8223	8.8504	85.5914
<i>Barnesiella</i>	9.1960	0.2041	5.0555	0.6045
<i>Bifidobacterium</i>	9.0787	0.0153	9.0068	0.0254
<i>Clostridium.sensu.stricto</i>	10.2478	0.0233	12.6283	1.2479
<i>Enterorhabdus</i>	1.6832	2.4180	1.7065	0.4763
<i>Hallella</i>	5.5171	0.0071	3.7255	0.2659
<i>Lachnospiracea_incertae_sedis</i>	0.5917	6.6283	0.4638	0.3487
<i>Lactobacillus</i>	34.2739	6.3136	42.5157	4.4987
<i>Turicibacter</i>	3.1487	0.0149	4.8437	1.3549
OTHER				
	SCD-M	HFD-M	SCD-F	HFD-F
<i>Akkermansia</i>	0.5909	0.8970	0.0000	0.0382
<i>Anaerovorax</i>	0.2055	0.0547	0.3039	0.0183
<i>Bacteroides</i>	0.4445	0.1126	0.4458	0.3081
<i>Enterococcus</i>	0.6400	0.6212	0.6167	0.3871
<i>Erysipelotrichaceae_incertae_sedis</i>	0.7949	0.0358	0.2105	0.0436
<i>Gordonibacter</i>	0.8789	0.3653	0.7017	0.0208
<i>Marvinbryantia</i>	0.6645	0.0695	0.0955	0.0248
<i>Oscillibacter</i>	0.3717	0.1748	0.2694	0.0969
<i>TM7_genera_incertae_sedis</i>	0.6151	0.4021	0.6856	0.1966
<i>Alistipes</i>	1.1677	0.0557	0.1839	0.0732
<i>Anaerobacter</i>	1.3421	0.0026	1.6689	0.2063

<i>Butyrivibrio</i>	1.0129	0.0332	0.9851	0.0251
<i>Clostridium.XIVa</i>	0.9797	1.7108	0.1815	0.2797
<i>Flavonifractor</i>	0.5142	1.1510	0.3130	0.3432
<i>Pseudoflavonifractor</i>	1.3657	1.0182	0.6686	0.5042
<i>Ruminococcus</i>	1.1781	0.0020	0.4940	0.0090
<i>Lactococcus</i>	0.0107	2.5613	0.0097	1.5570

Appendix H- Copyright Release for Chapter 2

6/14/2019

RightsLink Printable License

SPRINGER NATURE LICENSE TERMS AND CONDITIONS

Jun 14, 2019

This Agreement between Yvonne Nyavor ("You") and Springer Nature ("Springer Nature") consists of your license details and the terms and conditions provided by Springer Nature and Copyright Clearance Center.

License Number	4607790566263
License date	Jun 14, 2019
Licensed Content Publisher	Springer Nature
Licensed Content Publication	Cell and Tissue Research
Licensed Content Title	Intestinal nerve cell injury occurs prior to insulin resistance in female mice ingesting a high-fat diet
Licensed Content Author	Yvonne Nyavor, Rachel Estill, Hannah Edwards et al
Licensed Content Date	Jan 1, 2019
Licensed Content Volume	376
Licensed Content Issue	3
Type of Use	Thesis/Dissertation
Requestor type	academic/university or research institute
Format	print and electronic
Portion	full article/chapter
Will you be translating?	no
Circulation/distribution	<501
Author of this Springer Nature content	yes
Title	Interactions between a high fat diet, the gut microbiota and host in enteric neuropathy and dysmotility
Institution name	University of Idaho
Expected presentation date	Jul 2019
Requestor Location	Yvonne Nyavor 875 Campus Dr MS 3051 MOSCOW, ID 83844 United States Attn: Yvonne Nyavor
Total	0.00 USD
Terms and Conditions	

**Springer Nature Terms and Conditions for RightsLink Permissions
Springer Nature Customer Service Centre GmbH (the Licensor)**
hereby grants you a non-exclusive, world-wide licence to reproduce the material and for the purpose and requirements specified in the attached

6/14/2019

RightsLink Printable License

copy of your order form, and for no other use, subject to the conditions below:

1. The Licensor warrants that it has, to the best of its knowledge, the rights to license reuse of this material. However, you should ensure that the material you are requesting is original to the Licensor and does not carry the copyright of another entity (as credited in the published version).

If the credit line on any part of the material you have requested indicates that it was reprinted or adapted with permission from another source, then you should also seek permission from that source to reuse the material.

2. Where **print only** permission has been granted for a fee, separate permission must be obtained for any additional electronic re-use.
3. Permission granted **free of charge** for material in print is also usually granted for any electronic version of that work, provided that the material is incidental to your work as a whole and that the electronic version is essentially equivalent to, or substitutes for, the print version.
4. A licence for 'post on a website' is valid for 12 months from the licence date. This licence does not cover use of full text articles on websites.
5. Where '**reuse in a dissertation/thesis**' has been selected the following terms apply: Print rights of the final author's accepted manuscript (for clarity, NOT the published version) for up to 100 copies, electronic rights for use only on a personal website or institutional repository as defined by the Sherpa guideline (www.sherpa.ac.uk/romeo/).
6. Permission granted for books and journals is granted for the lifetime of the first edition and does not apply to second and subsequent editions (except where the first edition permission was granted free of charge or for signatories to the STM Permissions Guidelines <http://www.stm-assoc.org/copyright-legal-affairs/permissions/permissions-guidelines/>), and does not apply for editions in other languages unless additional translation rights have been granted separately in the licence.
7. Rights for additional components such as custom editions and derivatives require additional permission and may be subject to an additional fee. Please apply to Journalpermissions@springernature.com/bookpermissions@springernature.com for these rights.
8. The Licensor's permission must be acknowledged next to the licensed material in print. In electronic form, this acknowledgement must be visible at the same time as the figures/tables/illustrations or abstract, and must be hyperlinked to the journal/book's homepage. Our required acknowledgement format is in the Appendix below.
9. Use of the material for incidental promotional use, minor editing privileges (this does not include cropping, adapting, omitting material or any other changes that affect the meaning, intention or moral rights of the author) and copies for the disabled are permitted under this licence.
10. Minor adaptations of single figures (changes of format, colour and style) do not require the Licensor's approval. However, the adaptation should be credited as shown in Appendix below.

Appendix — Acknowledgements:

For Journal Content:

Reprinted by permission from [the Licensor]: [Journal Publisher
(e.g. Nature/Springer/Palgrave)] [JOURNAL NAME]

6/14/2019

RightsLink Printable License

[REFERENCE CITATION] (Article name, Author(s) Name),
[COPYRIGHT] (year of publication)

For Advance Online Publication papers:

Reprinted by permission from **[the Licensor]**: **[Journal Publisher]**
 (e.g. Nature/Springer/Palgrave) **[JOURNAL NAME]**
[REFERENCE CITATION] (Article name, Author(s) Name),
[COPYRIGHT] (year of publication), advance online publication,
 day month year (doi: 10.1038/sj.[JOURNAL ACRONYM].)

For Adaptations/Translations:

Adapted/Translated by permission from **[the Licensor]**: **[Journal Publisher]**
 (e.g. Nature/Springer/Palgrave) **[JOURNAL NAME]**
[REFERENCE CITATION] (Article name, Author(s) Name),
[COPYRIGHT] (year of publication)

Note: For any republication from the British Journal of Cancer, the following credit line style applies:

Reprinted/adapted/translated by permission from **[the Licensor]**: on behalf of Cancer Research UK: : **[Journal Publisher]** (e.g. Nature/Springer/Palgrave) **[JOURNAL NAME]** **[REFERENCE CITATION]** (Article name, Author(s) Name), **[COPYRIGHT]** (year of publication)

For Advance Online Publication papers:

Reprinted by permission from The **[the Licensor]**: on behalf of Cancer Research UK: **[Journal Publisher]** (e.g. Nature/Springer/Palgrave) **[JOURNAL NAME]** **[REFERENCE CITATION]** (Article name, Author(s) Name), **[COPYRIGHT]** (year of publication), advance online publication, day month year (doi: 10.1038/sj.[JOURNAL ACRONYM].)

For Book content:

Reprinted/adapted by permission from **[the Licensor]**: **[Book Publisher]** (e.g. Palgrave Macmillan, Springer etc) **[Book Title]** by **[Book author(s)]** **[COPYRIGHT]** (year of publication)

Other Conditions:

Version 1.1

Questions? customercare@copyright.com or +1-855-239-3415 (toll free in the US) or +1-978-646-2777.

Appendix I- IACUC Approvals to conduct animal experiments

 **University of Idaho**
Office of Research Assurances
Institutional Animal Care and Use Committee
875 Perimeter Drive, MS 3010
Moscow, ID 83844-3010
Phone: 208-885-6162
Fax: 208-885-6014
Email: iacuc@uidaho.edu


Date: July 02, 2019
To: Onesmo B Balemba
From: University of Idaho Institutional Animal Care and Use Committee
Re: Protocol IACUC-2018-18 *Diet-gut microbiota-host interactions and diabetic gastrointestinal neuropathy and dysmotility*

Your requested amendment of the animal care and use protocol listed above was reviewed and approved by the Institutional Animal Care and Use Committee on 07/01/2019.

This amendment request, 005566, was submitted for review on: 06/25/2019 07:53:29 PM PDT
The original approval date for this protocol was: 04/17/2018
This approval will remain in effect until: 06/30/2020
The protocol may be continued by annual updates until: 04/16/2021

Currently approved internal personnel on this protocol are: Balemba, Onesmo B

Federal laws and guidelines require that institutional animal care and use committees review ongoing projects annually. For the first two years after initial approval of the protocol you will be asked to submit an annual update form describing any changes in procedures or personnel. The committee may, at its discretion, extend approval for the project in yearly increments until the third anniversary of the original approval of the project. At that time, the protocol must be replaced by an entirely new submission.



Craig McGowan, IACUC Chair

University of Idaho
Institutional Animal Care and Use Committee

Date: July 25, 2018
To: Onesmo B Balemba
From: University of Idaho
Institutional Animal Care and Use Committee
Re: Protocol IACUC-2018-18 *Diet-gut microbiota-host interactions and diabetic gastrointestinal neuropathy and dysmotility*

Your requested amendment of the animal care and use protocol listed above was reviewed and approved by the Institutional Animal Care and Use Committee on 07/24/2018.

This amendment request was submitted for review on: 06/21/2018 08:41:35 AM PDT
The original approval date for this protocol was: 04/17/2018
This approval will remain in effect until: 07/23/2019
The protocol may be continued by annual updates until: 04/16/2021

Federal laws and guidelines require that institutional animal care and use committees review ongoing projects annually. For the first two years after initial approval of the protocol you will be asked to submit an annual update form describing any changes in procedures or personnel. The committee may, at its discretion, extend approval for the project in yearly increments until the third anniversary of the original approval of the project. At that time, the protocol must be replaced by an entirely new submission.



Craig McGowan, IACUC Chair

University of Idaho
Institutional Animal Care and Use Committee

Date: December 14, 2018
To: Dr. Peter Fuerst
From: University of Idaho
Institutional Animal Care and Use Committee
Re: Approval of personnel amendment request for Protocol
IACUC-2015-50 *Role of Cell Adhesion Molecules in Neural Patterning*

Your personnel amendment request, 004182, submitted on 10/31/2018 05:43:03 AM PDT to the animal care and use protocol listed above was administratively reviewed and approved by the Institutional Animal Care and Use Committee on 12/14/2018.

The original approval date for this protocol was: 05/24/2016
This protocol approval will remain in effect until: 05/24/2019
The protocol may be continued by annual updates until: 05/24/2019

Currently approved internal personnel on this protocol are: Balemba, Onesmo B; Camerino, Michael; Clemons, Mellisa, B.S. Biology; Fuerst, Peter; Hansen, Ethan; Richardson, Benjamin, PhD

Federal laws and guidelines require that institutional animal care and use committees review ongoing projects annually. For the first two years after initial approval of the protocol you will be asked to submit an annual update form describing any changes in procedures or personnel. The committee may, at its discretion, extend approval for the project in yearly increments until the third anniversary of the original approval of the project. At that time, the protocol must be replaced by an entirely new submission.



Craig McGowan, IACUC Chair

University of Idaho
Institutional Animal Care and Use Committee

Date: April 17, 2018
To: Onesmo B Balemba
From: University of Idaho
Institutional Animal Care and Use Committee
Re: IACUC-2018-18 *Diet-gut microbiota-host interactions and diabetic gastrointestinal neuropathy and dysmotility*

Your animal care and use protocol for the project shown above was reviewed and approved by the Institutional Animal Care and Use Committee on 04/17/2018.

The original approval date for this protocol is: 04/17/2018
This approval will remain in effect until: 04/16/2019
The protocol may be continued by annual updates until: 04/16/2021

Federal laws and guidelines require that institutional animal care and use committees review ongoing projects annually. For the first two years after initial approval of the protocol you will be asked to submit an annual update form describing any changes in procedures or personnel. The committee may, at its discretion, extend approval for the project in yearly increments until the third anniversary of the original approval of the project. At that time, the protocol must be replaced by an entirely new submission.



Craig McGowan, IACUC Chair

University of Idaho
Institutional Animal Care and Use Committee

Date: November 06, 2018
To: Dr. Peter Fuerst
From: University of Idaho
Institutional Animal Care and Use Committee
Re: Approval of personnel amendment request for Protocol
IACUC-2015-50 *Role of Cell Adhesion Molecules in Neural Patterning*

Your personnel amendment request, 004181, submitted on 10/31/2018 05:40:18 AM PDT to the animal care and use protocol listed above was administratively reviewed and approved by the Institutional Animal Care and Use Committee on 11/06/2018.

The original approval date for this protocol was: 05/24/2016
This protocol approval will remain in effect until: 05/24/2019
The protocol may be continued by annual updates until: 05/24/2019

Currently approved internal personnel on this protocol are: Balemba, Onesmo B; Clemons, Mellisa; Fuerst, Peter; Hansen, Ethan; Richardson, Benjamin

Federal laws and guidelines require that institutional animal care and use committees review ongoing projects annually. For the first two years after initial approval of the protocol you will be asked to submit an annual update form describing any changes in procedures or personnel. The committee may, at its discretion, extend approval for the project in yearly increments until the third anniversary of the original approval of the project. At that time, the protocol must be replaced by an entirely new submission.



Craig McGowan, IACUC Chair

University of Idaho
Institutional Animal Care and Use Committee

Date: September 05, 2018
To: Peter Fuerst
From: University of Idaho
Institutional Animal Care and Use Committee
Re: Protocol IACUC-2015-50 *Role of Cell*
Adhesion Molecules in Neural Patterning

Your requested amendment of the animal care and use protocol listed above was reviewed and approved by the Institutional Animal Care and Use Committee on 09/05/2018.

This amendment request, 003746, was submitted for review on: 08/26/2018 02:09:40 PM PDT
The original approval date for this protocol was: 05/24/2016
This approval will remain in effect until: 05/24/2019
The protocol may be continued by annual updates until: 05/24/2019

Federal laws and guidelines require that institutional animal care and use committees review ongoing projects annually. For the first two years after initial approval of the protocol you will be asked to submit an annual update form describing any changes in procedures or personnel. The committee may, at its discretion, extend approval for the project in yearly increments until the third anniversary of the original approval of the project. At that time, the protocol must be replaced by an entirely new submission.



Craig McGowan, IACUC Chair

University of Idaho
Institutional Animal Care and Use Committee

Date: August 21, 2018
To: Dr. Peter Fuerst
From: University of Idaho
Institutional Animal Care and Use Committee
Re: Approval of personnel amendment request for Protocol
IACUC-2015-50 *Role of Cell Adhesion Molecules in Neural Patterning*

Your personnel amendment request, 003745, submitted on 08/08/2018 09:59:09 AM PDT to the animal care and use protocol listed above was administratively reviewed and approved by the Institutional Animal Care and Use Committee on 08/21/2018.

The original approval date for this protocol was: 05/24/2016
This protocol approval will remain in effect until: 05/24/2019
The protocol may be continued by annual updates until: 05/24/2019

Currently approved internal personnel on this protocol are: Balemba, Onesmo B; Fuerst, Peter; Hansen, Ethan; Richardson, Benjamin

Federal laws and guidelines require that institutional animal care and use committees review ongoing projects annually. For the first two years after initial approval of the protocol you will be asked to submit an annual update form describing any changes in procedures or personnel. The committee may, at its discretion, extend approval for the project in yearly increments until the third anniversary of the original approval of the project. At that time, the protocol must be replaced by an entirely new submission.



Craig McGowan, IACUC Chair

University of Idaho
Institutional Animal Care and Use Committee

Date: August 21, 2018
To: Peter Fuerst
From: University of Idaho
Institutional Animal Care and Use Committee
Re: Protocol IACUC-2015-50 *Role of Cell*
Adhesion Molecules in Neural Patterning

Your requested amendment of the animal care and use protocol listed above was reviewed and approved by the Institutional Animal Care and Use Committee on 08/21/2018.

This amendment request, 003747, was submitted for review on: 08/08/2018 10:10:10 AM PDT
The original approval date for this protocol was: 05/24/2016
This approval will remain in effect until: 05/24/2019
The protocol may be continued by annual updates until: 05/24/2019

Federal laws and guidelines require that institutional animal care and use committees review ongoing projects annually. For the first two years after initial approval of the protocol you will be asked to submit an annual update form describing any changes in procedures or personnel. The committee may, at its discretion, extend approval for the project in yearly increments until the third anniversary of the original approval of the project. At that time, the protocol must be replaced by an entirely new submission.



Craig McGowan, IACUC Chair

University of Idaho
Institutional Animal Care and Use Committee

Date: January 18, 2018
To: Onesmo B Balemba
From: University of Idaho
Institutional Animal Care and Use Committee
Re: Protocol IACUC-2015-13 *High fat diet-induced enteric nervous system damage in obesity and type two diabetes mellitus, and novel combination dietary therapies to mitigate it.*

Your requested renewal of the animal care and use protocol listed above was reviewed and approved by the Institutional Animal Care and Use Committee on 01/18/2018.

This renewal was originally submitted for review on: 12/23/2017 09:46:45 AM PST
The original approval date for this protocol was: 04/17/2015
This approval will remain in effect until: 04/17/2018
The protocol may be continued by annual updates until: 04/17/2018

Federal laws and guidelines require that institutional animal care and use committees review ongoing projects annually. For the first two years after initial approval of the protocol you will be asked to submit an annual update form describing any changes in procedures or personnel. The committee may, at its discretion, extend approval for the project in yearly increments until the third anniversary of the original approval of the project. At that time, the protocol must be replaced by an entirely new submission.



Craig McGowan, IACUC Chair

University of Idaho
Institutional Animal Care and Use Committee

Date: August 06, 2018
To: Peter Fuerst
From: University of Idaho
Institutional Animal Care and Use Committee
Re: Protocol IACUC-2015-50 *Role of Cell Adhesion Molecules in Neural Patterning*

Your requested amendment of the animal care and use protocol listed above was reviewed and approved by the Institutional Animal Care and Use Committee, through Veterinary Verification and Consultation review on 08/06/2018.

This amendment request was submitted for review on: 07/17/2018 09:30:50 AM PDT
The original approval date for this protocol was: 05/24/2016
This approval will remain in effect until: 05/24/2019
The protocol may be continued by annual updates until: 05/24/2019

Federal laws and guidelines require that institutional animal care and use committees review ongoing projects annually. For the first two years after initial approval of the protocol you will be asked to submit an annual update form describing any changes in procedures or personnel. The committee may, at its discretion, extend approval for the project in yearly increments until the third anniversary of the original approval of the project. At that time, the protocol must be replaced by an entirely new submission.



Craig McGowan, IACUC Chair

University of Idaho
Institutional Animal Care and Use Committee

Date: January 18, 2018
To: Onesmo B Balemba
From: University of Idaho
Institutional Animal Care and Use Committee
Re: Protocol IACUC-2015-13 *High fat diet-induced enteric nervous system damage in obesity and type two diabetes mellitus, and novel combination dietary therapies to mitigate it.*

Your requested renewal of the animal care and use protocol listed above was reviewed and approved by the Institutional Animal Care and Use Committee on 01/18/2018.

This renewal was originally submitted for review on: 12/23/2017 09:46:45 AM PST
The original approval date for this protocol was: 04/17/2015
This approval will remain in effect until: 04/17/2018
The protocol may be continued by annual updates until: 04/17/2018

Federal laws and guidelines require that institutional animal care and use committees review ongoing projects annually. For the first two years after initial approval of the protocol you will be asked to submit an annual update form describing any changes in procedures or personnel. The committee may, at its discretion, extend approval for the project in yearly increments until the third anniversary of the original approval of the project. At that time, the protocol must be replaced by an entirely new submission.



Craig McGowan, IACUC Chair

From: UI Animal Care and Use Committee <iacuc@uidaho.edu>
Sent: Wednesday, February 03, 2016 9:17 AM
To: Balemba, Onesmo (obalemba@uidaho.edu) <obalemba@uidaho.edu>
Subject: IACUC Protocol Renewal: 2015-13 - High fat diet-induced enteric nervous system damage in obesity and type two diabetes mellitus, and novel combination dietary therapies to mitigate it.

**University of Idaho
Institutional Animal Care and Use Committee
Annual Protocol Review**

Date: Wednesday, February 3, 2016
To: Onesmo B. Balemba
From: University of Idaho
Institutional Animal Care and Use Committee
Re: Protocol 2015-13
High fat diet-induced enteric nervous system damage in obesity and type two diabetes mellitus, and novel combination dietary therapies to mitigate it.

Original Approval:	4/17/2015	Annual Expiration:	4/17/2016	3 Year Expiration:	4/17/2018
---------------------------	-----------	---------------------------	-----------	---------------------------	-----------

Federal laws and guidelines require that institutional animal care and use committees review ongoing projects annually. This brief renewal application will provide the basis for an annual review for projects that have not changed or may have only minor modifications from year to year. A new protocol must be submitted for new projects, major changes in existing protocols, and for all protocols every three years.

1) Please indicate the present status of your project by checking one of the statements below:

- This project is no longer active, please withdraw.
- This project is pending/active and there have been no changes in procedures with respect to animal use or personnel.
- This project is active and there have been changes in the personnel or experimental procedures. (Describe any such changes below.)

2) Please provide a description of any changes in procedures with respect to animal care and use since your protocol was originally approved. Attach additional pages if necessary.

3) List all changes in personnel involved in your project:

Add	Delete	Name	Department	Email	Training & Experience
<hr/>					

Signature: _____ Date: _____
</div>

Send this completed form to iacuc@uidaho.edu or IACUC, Office of Research Assurances, University of Idaho, Moscow, Idaho 83844-3010. **You must immediately cease all live animal activities described under this protocol on or before the renewal date of this protocol, 4/17/2016, unless it is reviewed and approved by the Institutional Animal Care and Use Committee prior to this date.** If you have any questions, please contact the Office of Research Assurances at (208) 885-6162.

3/18/2016

Print: A00001668 - A00001668-00

Date: Friday, March 18, 2016 12:23:28 PM

General Information

Title of Project:
High fat diet-induced enteric nervous system damage and dysmotility in obesity and type 2 diabetes

Intention:
Experimental Research

Indicate Mayo Foundation location(s) where the protocol will be conducted:
Rochester

Species:
Mice

Principal Investigator:
Purna Kashyap

Housing

Check all facilities where the animals will be housed:
Building
Medical Sciences Building

Will live animals be taken out of the animal facility to laboratory or non-clinical areas? Yes No

Will procedures involving animals be performed in clinical areas supporting patients? Yes No

Will this study be conducted in accordance with 21CFR part 58, Good Laboratory Practice for Nonclinical Laboratory Studies? Please note these are usually pre-clinical studies and additional institutional approvals will be required before this protocol can be activated. Yes No

Personnel Information

Mayo Personnel involved with animals:

Name	Role	Phone	Email	Teach	Con FD Sub Reqd	Filed	Training	Anes	Intra	Surg	Post	Euth
Purna Kashyap	PI	(77)4-0839	yes	no	yes	yes	Dr. Kashyap has years of extensive experience working with Germ free (GF) animals and in depth knowledge on handling procedures. He manages GF facility and has also several active IACUC protocols. He will also guide and supervises the project.	no	no	no	no	no
Yogesh Bhattarai	PRF		yes	no	yes	no	Yogesh has experience in dealing with germ-free animals and has undergone several trainings on animal handling procedures. He also has experince in developing an IACUC protocol.	no	no	no	no	yes
Lisa Till	RT	(77)4-2116	yes	no	no	no	Lisa has experience in dealing with germ-free animals and has undergone training on animal handling procedures.	no	no	no	no	yes
Charles Salmonson	RTN	(77)4-2116	yes	no	yes	no	Has extensive experience in dealing with germ-free animals and has undergone several trainings on animal handling procedures.	no	no	no	no	yes

Other Personnel Information

List all personnel who will not perform animal procedures, but who will need clerical access to this IACUC protocol information:

Last	First	Role	Phone	Notifications	Controlled Sub	FD
------	-------	------	-------	---------------	----------------	----

3/18/2016

Print: A00001668 - A00001668-00

There are no items to display

Personnel that are not affiliated with the Mayo Clinic but who will be working with animals:

Name	Affiliation	Email	Reason for Participation	Experience
There are no items to display				

Funding Information**Check all that apply and complete subsequent fields as appropriate:** **New/Renewal/Existing: Extramural Grant Funding (NIH, AHA, etc.)** **Intramural Funding** **PAU Funding**PAU Number:
94332Activity Number (if known):
94332016 **Commercial/Industry Funding or Equipment****Abstract****Provide a scientific abstract that summarizes the overall goals and specific objectives of the proposed work. Do NOT describe specific experimental or procedural details here:**

Dietary factors, bacterial metabolites and antigens as well as host factors play critical roles in the pathogenesis of obesity and type two diabetes mellitus (T2D). The composition of the gut microbial community changes in response to different diets and gut motility patterns. It is increasingly becoming evident that bacterial metabolites and antigens signal to the enteric nervous system (ENS) and can alter neurochemical coding, neurotransmitter release and neurotransmission and hence, inhibit gut motility. Bacterial metabolites such as short chain fatty acids, bacterial antigens (e.g. polysaccharides) and fatty acids such as palmitic acid could inflict or predispose the ENS to injuries. The roles of these and other molecules present in the intestinal lumen in dysmotility and the pathobiology of ENS nerve cell damage (neuropathy) in obesity and T2D are poorly understood. Our preliminary data show that supernatants from ileocecal (bowel) luminal contents from mice fed a high fat (HF) diet inhibit motility in duodenum of mice fed a standard chow (SC) diet and intestinal muscle contractions ex vivo. We want to expand this study further and test the effects of ileocaecal contents on bowel movement and secretion. We postulate that the supernatants contains anti-motility molecules. These molecules are associated with increased specific members of the microbiota since filtering bacterial cells from the antimotility supernatant reduces its effectiveness by about 5-10% (Nyavor et al., unpublished). In addition, we postulate that HF diet-induced alterations to the ileocecal microbial community results in the production of molecules that disrupt bowel motility and secretion. The antimotility substances inflict apoptotic damage or induce functional changes (plasticity) to inhibitory neurons in myenteric plexus, the nerve cells, which mainly regulate gut motility by causing a relaxation of smooth muscle. Our goal is to use supernatants from germ free (GF) mice to test the hypothesis that the production of antimotility substances require microbiota and is independent of host genetics.

Non-Scientific Description**In non-technical, everyday language that a high-school student would understand, explain how the proposed project will benefit human or animal health, the advancement of knowledge, or the good of society:**

The ultimate goal of the project is to identify molecules that inhibit intestinal motility. Pilot data obtained in previous experiments show that supernatants from luminal contents collected from the ileum and the cecum from mice fed a HF diet for 8 weeks slow down contractions and intestinal motility when introduced intraluminally into isolated, duodenal or jejunal segments obtained from healthy mice. We also know that the supernatants inhibit muscle contractions in cultured muscle preparations from mouse intestine. In addition, pilot data suggests that ileocecal supernatants cause neuronal death, including the inhibitory motor neurons. These findings together suggests that the supernatant contains molecules (presently unknown) that cause nerve injuries, dysmotility and disruption in secretion in HF diabetic mice. Likely, these molecules occur in diabetic humans. The identification of the molecules will enable us study their presence in T2D humans, it could reveal new biomarkers of obesity and type 2 diabetes, and also shed light on new ways to treat HF diet induced GI motility disorders. In order to reveal such biomarkers, it is essential to understand if the molecules in ileocecal supernatants are either produced from gut microorganisms (microbiota), from the diet or from the host (mice) itself. The planned experiments using ileocecal supernatants from germ free mice fed a standard diet and a HF diet will therefore be instrumental to help solve this puzzle and confirm whether these molecules are produced by microbiota or HF diet and if production of these molecules are influenced by host genetics.

Species General Information**Species:**
Mice

3/18/2016

Print: A00001668 - A00001668-00

Other Details:				
Strain/Breed/Type	Other Details	Age	Weight Sex	Justification
C57BL6	These mice are germ free.	6-11	Male	Although preliminary studies have showed no differences between sexes, some studies show that estrogen increases basal NO production, which might increase variability in our study. Therefore we will be using only males in our study.
Swiss Webster	These mice are germ free.	6-11 weeks	N/A Male	Although preliminary studies have showed no differences between sexes, some studies show that estrogen increases basal NO production, which might increase variability in our study. Therefore we will be using only males in our study.

Alternatives

This section of the protocol is to verify that a literature search was performed to determine if alternatives exist and to determine whether the protocol unnecessarily duplicates previous research.

When searching for alternatives consider the 3Rs of W.M.S. Russell and R.L. Burch in their book *The Principles of Humane Experimental Technique*. The 3Rs are: **reduction, refinement and replacement**.

Specify all key words and concepts important in the development of the search strategy e.g., general area of study, proposed animal species, systems or anatomy involved, drugs or compounds used, methods and procedures -- particularly alternatives to procedures causing pain or distress. "Animal model" should always be included as one of the key words. Procedures that cause more than momentary pain (e.g. thoracotomy, vascular cutdown) should be included. The species chosen for the protocol (e.g. canine & dog) should be included.

Animal model, Mouse, Microbiota, diet, host, antimotility molecules/substances, short chain fatty acids, palmitate, motility, neuropathy, neuroplasticity, constipation.

I have determined, by means of the following sources, searches, or methods, that alternatives to the procedures which may cause animal pain or distress proposed in this protocol are not available and that this protocol does not unnecessarily duplicate previous experiments:

PUBMED

"Other" source, search or method:

Years covered by this search (e.g. 2001-2015):

2002-2016

Most recent date on which the search was performed (Must be within 6 months) :

3/11/2016

Were any potential alternatives found when performing the search? Yes No

Species Justification

Select criteria explaining the appropriateness of the animal model (check all that apply):

Systemic interactions are needed

No in-vitro options available

Other (specify)

*** Specify "Other" rationale criteria:**

- A) Similarity to human biology
- B) Genetic model available
- C) Best model to work with
- D) Germ free state available

Procedures

Check all procedures to be performed:

- Behavior Studies/Testing
- Breeding
- Food and Water Restriction

3/18/2016

Print: A00001668 - A00001668-00

- Genotyping Pigs
- Genotyping Rodents or Fish
- Hypo/Hyperthermia
- Immunization
- Organ System Failure or Dysfunction will be Experimentally Induced
- Paralysis Experimentally Induced
- Prolonged Physical Restraint or Restriction of Movement with Mechanical Devices
- Radiation Exposure/Imaging
- Rodent Identification
- Sepsis
- Special Housing and Husbandry**
- Specimens (tissue and/or body fluids) will be collected from live animals
- Substances/Agents will be administered to live animals
- Surgery-Survival (Single or Multiple)
- Surgery-Terminal Non-Survival
- Tumor Growth/Inoculation with Biological Products
- Other: study procedure not described/listed

Special Housing and Husbandry

This section is required because you indicated special housing and husbandry.

Medicated Water Yes No

Special Diet Yes No

List diet:

Vendor: TestDiet

Name of diet: Modified 70% Kcal Fat Diet w/ 2% additional corn oil

Diet contents : 71% kcal from fat, 17.8% protein, 11.0% carbohydrate

List person(s) feeding the diet (*include pager/phone number(s)*):

Yogesh Bhattarai, ph (77)4- 0871 ,127 (13557); Charles Salmonson, Ph (77)4-2116 127(00587)

Where will the special diet be stored?

Medsci 4-10H

Metabolic Cages Yes No

Experimental devices added to caging (e.g. running wheels) Yes No

Other Yes No

Non-Mayo Animal Work

Will live animal work be conducted as part of this protocol at facilities or institutions outside of Mayo prior to the animals arriving at Mayo? Yes No

Will live animal work be conducted as part of this protocol at facilities or institutions outside of Mayo at any time after the animals have been assigned to a Mayo protocol? Yes No

Biosafety

If agents such as the following will be used in this protocol, click the "Add" button and provide details of each agent/organism below:

- Recombinant DNA molecules
- Cell lines using viral vector technology
- Biological toxins (Diphtheria, Pertussis, etc.)
- Bacteria, virus, protozoan or fungus infectious to other animals or humans

Agent	Level	Route	Infectious	Maintained	Room	Room After
-------	-------	-------	------------	------------	------	------------

3/18/2016

Print: A00001668 - A00001668-00

There are no items to display

Are any of the following agents being used on this protocol? Yes No

- Herpes Simples Virus -1 (HSV-1)
- Methicillin Resistant S. aureus (MRSA)
- Vaccinia Virus (VACV or VV)
- Vancomycin-Resistant Enterococcus (VRE)
- Enterovirus 71 (EV71)

Chemical Safety

Will a chemical that is hazardous, toxic, mutagenic or carcinogenic be used? Yes No

Study Design and Timeline

You have selected the following procedures:

Special Housing and Husbandry

Study Design & Timeline:

Germ free mice will be weaned by the end of three weeks. One group of mice will be fed a standard chow diet while the other will be fed High fat diet until 8 weeks. At the end of 8 weeks, mice will be euthanized. Mouse cecal contents, blood serum and distal colon will be collected after euthanasia.

Mice	Diet (Duration 8 weeks)
Group 1	Standard chow diet
Group 2	High fat diet

Numbers Justification

This section is required because you indicated Experimental Research as an intention.

Ensuring proper justification of animals requested is a critical charge of the IACUC. Please provide adequate statistical justification for the animal numbers requested.

- Justify the number of animals required for the 3-year duration of the IACUC protocol.
- Each group size and the total number of animals must be justified.
- The total number of animals requested must be justified on the basis of the experimental design.

Please use the categories below as a guide.

Check all that apply and provide the requested information:

Hypothesis driven research

List numbers in each group Total (Sum of numbers needed for all groups):

To estimate the optimal sample size of mice for these experiments, we used the pilot data from motility assay and ussing studies and statistical power analysis. We considered an alpha of 5% corresponding to a 95% confidence interval. Using this information, we determined that using 5 mice per diet group would allow us to reach statistical significance ($\alpha=0.05$) with the power of 99.8%. Therefore, we will use a minimum of 5 mice per experimental group.

For Control diet fed Group: 24 mice

Breakdown :

3/18/2016

Print: A00001668 - A00001668-00

Part 1: For Blood collection, Cecal content collection, Distal colon tissue sample collection for IHC and gene expression = 5 mice/group (Note: Blood, Cecal contents and distal colon tissue sample will be collected from same mice)

Part 2: For permeability studies using Ussing chamber=5 mice/group

Total Germ free mice needed for Control diet fed Group: **(5 mice (Part 1)+ 5 mice (Part 2)+ 20% failure rate) *2 (two mice strains C57BL6 and swiss webster) = 24 Mice**

Total Germ Free mice needed for High Fat fed group: **24 mice**

Breakdown :

Part 1: For Blood collection, Cecal content collection, Distal colon tissue sample collection for IHC and gene expression = 5 mice/group

Part 2: For permeability studies using Ussing chamber=5 mice/group

Total Germ free mice needed for High fat diet fed Group: **(5 mice (Part 1)+ 5 mice (Part 2)+ 20% failure rate) *2 mice strains (C57BL6 and Swiss webster) = 24 Mice**

Total mice for group 1 and 2 = 24+24 = 48 Mice

The procedures are technically difficult and extra animals will be needed to replace failures of the experiment

Give an estimate of the failure rate and number of replacement animals needed to maintain group size. (Number per group and total)

Since Ussing chamber experiments and blood extraction are technically difficult and based on our other preliminary studies we anticipate the failure rate to be 20%. We have therefore asked for 4 extra mice (2 of Swiss webster and 2 of C57BL6 mice) from each group to maintain our group size.

- The experiment is a feasibility study to develop or learn a new procedure**
- The experiment is a pre-clinical study (e.g. device testing, therapeutic intervention testing)**
- The experiment requires a specific amount of tissue or number of cells for work in vitro**
- Other experimental design or justification**

Animal Numbers

Provide total number of animals required for this protocol (include any animal numbers calculated in the breeding procedure section): 48

Will any animals experience procedures that will cause significant pain, (more than just momentary) or distress for which anesthetics, analgesics and/or tranquilizers will be withheld? Yes No

Complications

Describe the most commonly recognized complications or side effects of the specific drug, device and/or procedures that the animals may experience as a result of these experiments.

Although various earlier studies have utilized high fat diet consumption in mice models, no adverse effect has been reported in association with eight weeks of high fat diet consumption. In some cases however, diabetic neuropathy, retinopathy and respiratory depression may occur.

How often will the animal be observed to detect complications or side effects?

These mice will be monitored closely everyday for any signs of discomfort and/or other complications

3/18/2016

Print: A00001668 - A00001668-00

Describe how each complication or side effect will be reduced or alleviated.

If an animals exhibit signs of labored breathing, lethargy, self induced trauma they will be euthanized by CO2. Furthermore, some mice might experience difficulty ambulating or reaching for food/water due to weight gain. In such cases mice will be euthanized by CO2.

Humane Endpoints

Early removal (before the planned experimental endpoint) of an animal from the study must occur based on humane endpoints.

List the specific clinical or behavioral signs that indicate a humane endpoint. When these signs are observed, animals must be removed from studies and euthanized. NOTE: Death is not an acceptable end point. Every effort to recognize endpoints predictive of death so that animals can be humanely euthanized prior to death must be made to avoid death as an endpoint.

Note: The following are institutional policy endpoints that must be observed for all studies:

- Weight loss greater than or equal to 20% of body weight
- Inability to ambulate
- Inability to reach food and/or water
- Tumors greater than or equal to 10% body weight
- Tumors that have ulcerated
- A body condition score of 1 or less using the IACUC approved scoring system

Provide additional humane endpoints not already listed above that will be observed:

If an animals exhibit signs of labored breathing, lethargy, self induced trauma and other general signs of pain or distress such has hunched posture or bleeding from the anus, erratic behavior, excessive attempts to turn around or struggling mice will be euthanized.

Exemption Request for Mice

This protocol requires the following exemption(s) to IACUC policies and/or the Guide for the Care and Use of Laboratory Animals (check all that apply):

- Exemption from Standard Housing Density/Weaning Time (e.g. >1 litter/cage or other increase in cage density, pups kept with mother > 28 days of age)**
- Exemption from Social Housing**
- Exemption from Environmental Enrichment**
- Exemption from Standard Cage Change Frequency**
- Exemption from Standard Environmental Conditions (e.g. cage size/type, temperature, humidity, light level or cycle)**
- Exemption from the Use of Pharmaceutical Grade Compounds (Include all non-pharmaceutical substances administered to animals)**
- Exemption from Humane Endpoint**
- Other**
- * Describe the exemption request. Be specific.
- This protocol requests exemption to the Guide for the Care and use of Laboratory Animals based on standard operating procedure for germ free facility. Exemptions are a part of standard operating procedure for the facility that have been reviewed and approved by the IACUC.
- No exemptions requested for this protocol**

3/18/2016

Print: A00001668 - A00001668-00

Euthanasia/Final Disposition of Animals

At the end of the experiment/study, the animals will be (Select all that apply):

Transferred to another protocol Yes No

Euthanized via Chemical Overdose (*CO₂, pentobarbital, isoflurane, etc.*) Yes No

Agent	Other	Route	Other	Group(s)	2nd Method	Other
Carbon Dioxide		Inhalation		Group 1 and Group 2	Cervical Dislocation	

Euthanized via Physical Method (*cervical dislocation, decapitation, exsanguination, etc.*) Yes No

Study Staff Member Information

Name	Purna Kashyap	Department	Gastroenterology
Role	PI	Work phone	(77)4-0839
After Hours Phone		Work e-mail	kashyap.purna@mayo.edu

Should this individual receive email communication regarding this protocol? Yes No

Responsibilities

Will this individual:

Administer Anesthesia? Yes No

Perform intra-operative/procedural monitoring while the animal is anesthetized? Yes No

Perform Surgery? Yes No

Be involved in the post-operative care, if applicable? Yes No

Perform euthanasia (*e.g. cervical dislocation, exsanguination, CO₂, pentobarbital overdose*)? Yes No

Operate imaging equipment? Yes No

Operate irradiation equipment? Yes No

Handle radionuclides? Yes No

Provide the on-site instruction and supervision if training/teaching protocol? Yes No

Controlled Substances

Is this individual authorized to order or handle controlled substances? Yes No

Financial Disclosure

Does this individual need to provide disclosure information? Yes No

Training/Qualifications

The Department of Comparative Medicine (DCM) offers hands on training sessions in animal handling and standard procedures. Contact DCM to schedule a training session, if applicable.

Description of experience and qualifications specific to this protocol and the procedures and species involved:

Dr. Kashyap has years of extensive experience working with Germ free (GF) animals and in depth knowledge on handling procedures. He manages GF facility and has also several active IACUC protocols. He will also guide and supervises the project.

Training Completed:

Course	Name	Completion Date	Status	Months Valid
--------	------	-----------------	--------	--------------

3/18/2016

Print: A00001668 - A00001668-00

500209IAC000A1 (Animal Researchers) IACUC: The Care and Use of Animals in Research at Mayo Clinic	8/15/2013	COURSE-COMplete	36
500209IAC000AA Animal Allergen	8/20/2014	COURSE-COMplete	36

The date shown is the date the individual listed on this protocol has completed the IACUC training module(s) required for this protocol. Training modules need to be renewed three years from the date shown. If the date shown is past the three-year time point, modules can be completed here: <http://intranet.mayo.edu/charlie/research-education/education-and-training/animal-research/>

Study Staff Member Information

Name Yogesh Bhattarai
Role PRF
After Hours Phone

Department RS-Gastroenterology
Work phone
Work e-mail bhattarai.yogesh@mayo.edu

Should this individual receive email communication regarding this protocol? Yes No

Responsibilities

Will this individual:

Administer Anesthesia? Yes No

Perform intra-operative/procedural monitoring while the animal is anesthetized? Yes No

Perform Surgery? Yes No

Be involved in the post-operative care, if applicable? Yes No

Perform euthanasia (e.g. cervical dislocation, exsanguination, CO₂, pentobarbital overdose)? Yes No

Operate imaging equipment? Yes No

Operate irradiation equipment? Yes No

Handle radionuclides? Yes No

Provide the on-site instruction and supervision if training/teaching protocol? Yes No

Controlled Substances

Is this individual authorized to order or handle controlled substances? Yes No

Financial Disclosure

Does this individual need to provide disclosure information? Yes No

Training/Qualifications

The Department of Comparative Medicine (DCM) offers hands on training sessions in animal handling and standard procedures. Contact DCM to schedule a training session, if applicable.

Description of experience and qualifications specific to this protocol and the procedures and species involved:

Yogesh has experience in dealing with germ-free animals and has undergone several trainings on animal handling procedures. He also has experience in developing an IACUC protocol.

Training Completed:

Course	Name	Completion Date	Status	Months Valid
500209IAC000A1 (Animal Researchers) IACUC: The Care and Use of Animals in Research at Mayo Clinic		6/1/2015	COURSE-COMplete	36
500209IAC000AA Animal Allergen		6/25/2015	COURSE-COMplete	36

The date shown is the date the individual listed on this protocol has completed the IACUC training module(s) required for this

3/18/2016

Print: A00001668 - A00001668-00

protocol. Training modules need to be renewed three years from the date shown. If the date shown is past the three-year time point, modules can be completed here: <http://intranet.mayo.edu/charlie/research-education/education-and-training/animal-research/>

Study Staff Member Information

Name Lisa Till
Role RT
Department RS-Research Services
After Hours Phone
Work phone (77)4-2116
Work e-mail till.lisa@mayo.edu

Should this individual receive email communication regarding this protocol? Yes No

Responsibilities

Will this individual:

Administer Anesthesia? Yes No

Perform intra-operative/procedural monitoring while the animal is anesthetized? Yes No

Perform Surgery? Yes No

Be involved in the post-operative care, if applicable? Yes No

Perform euthanasia (e.g. cervical dislocation, exsanguination, CO₂, pentobarbital overdose)? Yes No

Operate imaging equipment? Yes No

Operate irradiation equipment? Yes No

Handle radionuclides? Yes No

Provide the on-site instruction and supervision if training/teaching protocol? Yes No

Controlled Substances

Is this individual authorized to order or handle controlled substances? Yes No

Financial Disclosure

Does this individual need to provide disclosure information? Yes No

Training/Qualifications

The Department of Comparative Medicine (DCM) offers hands on training sessions in animal handling and standard procedures. Contact DCM to schedule a training session, if applicable.

Description of experience and qualifications specific to this protocol and the procedures and species involved:

Lisa has experience in dealing with germ-free animals and has undergone training on animal handling procedures.

Training Completed:

Course	Name	Completion Date	Status	Months Valid
500209IAC000AA	Animal Allergen	6/23/2014	COURSE-COMplete	36
500209IAC000A1	(Animal Researchers) IACUC: The Care and Use of Animals in Research at Mayo Clinic	5/1/2015	COURSE-COMplete	36

The date shown is the date the individual listed on this protocol has completed the IACUC training module(s) required for this protocol. Training modules need to be renewed three years from the date shown. If the date shown is past the three-year time point, modules can be completed here: <http://intranet.mayo.edu/charlie/research-education/education-and-training/animal-research/>

Study Staff Member Information

3/18/2016

Print: A00001668 - A00001668-00

Name Charles Salmonson
Role RTN
Department RS-Research Services
After Hours Phone
Work phone (77)4-2116
Work e-mail salmonson.charles@mayo.edu

Should this individual receive email communication regarding this protocol? Yes No

Responsibilities

Will this individual:

Administer Anesthesia? Yes No

Perform intra-operative/procedural monitoring while the animal is anesthetized? Yes No

Perform Surgery? Yes No

Be involved in the post-operative care, if applicable? Yes No

Perform euthanasia (e.g. cervical dislocation, exsanguination, CO₂, pentobarbital overdose)? Yes No

Operate imaging equipment? Yes No

Operate irradiation equipment? Yes No

Handle radionuclides? Yes No

Provide the on-site instruction and supervision if training/teaching protocol? Yes No

Controlled Substances

Is this individual authorized to order or handle controlled substances? Yes No

Financial Disclosure

Does this individual need to provide disclosure information? Yes No

Training/Qualifications

The Department of Comparative Medicine (DCM) offers hands on training sessions in animal handling and standard procedures. Contact DCM to schedule a training session, if applicable.

Description of experience and qualifications specific to this protocol and the procedures and species involved:

Has extensive experience in dealing with germ-free animals and has undergone several trainings on animal handling procedures.

Training Completed:

Course	Name	Completion Date	Status	Months Valid
500209IAC000A1	(Animal Researchers) IACUC: The Care and Use of Animals in Research at Mayo Clinic	1/4/2016	COURSE-COMplete	36
500209IAC000AA	Animal Allergen	7/11/2014	COURSE-COMplete	36

The date shown is the date the individual listed on this protocol has completed the IACUC training module(s) required for this protocol. Training modules need to be renewed three years from the date shown. If the date shown is past the three-year time point, modules can be completed here: <http://intranet.mayo.edu/charlie/research-education/education-and-training/animal-research/>

Euthanasia - Chemical Method

Agent: Carbon Dioxide Specify "Other" Agent:

Route: Inhalation Other Route:

Personnel: Member

3/18/2016

Print: A00001668 - A00001668-00

Yogesh Bhattarai

Charles Salmonson

Lisa Till

Group(s)/Animals euthanized by this method:

Group 1 and Group 2

Secondary method to confirm euthanasia: Explain "Other" Method:

Cervical Dislocation